Mercury Open Water Final Report for Compliance with the Delta Mercury Control Program

Chapter 3. Yolo Bypass -Technical Studies

Submitted by the Open Water Mercury Technical Workgroup

Aug 31, 2020

Pacific Northwest
NATIONAL LABORATORY
Proudly Operated by Battelle *Since 1965*

USGS
science for a changing world

The Open Water Mercury Technical Workgroup

California Department of Water Resources
Division of Environmental Sciences
Carol DiGiorgio
David Bosworth

San Jose State University
Moss Landing Marine Laboratory
Wesley Heim,
Mark Stephenson (ret.)

Pacific Northwest National Laboratory
Marine Sciences Laboratory
Gary Gill, (ret.)

United States Geological Survey
California Science Center
David Schoellhamer.
Paul A. Work,

Acknowledgements

The Department of Water Resources (DWR) would like to acknowledge the hard work by our field and analytical staff who helped collect and analyze water samples associated with the Mass Balance studies. In addition to Carol DiGiorgio and David Bosworth, field staff included Petra Lee, Julianna Manning, Sonia Miller, Jasmine Hamiliton, Patrick Scott, Elaine Jeu, Alice Tung, Tyler Salman, Todd Percival, Pasha Kashkooli, Otome Lindsey, and Joaquin Garza. We also thank DWR's Municipal Water Quality Program, including Steve San Julian, Arin Conner, Mark Bettencourt, Travis Brown and Jeremy DelCid for their help and use of space to conduct mesocosm experiments at Bryte Yard. Analytical staff included chemists at Bryte Laboratory, Marine Pollution Studies Laboratory which is an affiliate of Moss Landing Marine Laboratories, and Pacific Northwest National Laboratory. We would like to thank the analytical Staff at Moss Landing Marine Labs who contributed to the study by the analysis of TSS, MeHg and Hg, especially Amy Byington, Adam Newman and Autumn Bonnema. Brianna Machucha helped with the laboratory study in VegSens 2018. Staff at Department of Fish and Wildlife helped in field work and access to the Yolo Wildlife Area including Jeff Stoddard, Joe Hobbs, and Chris Rocco. Mike Brock helped with the field work and provided helpful land use information.

Contents

List of Figures

List of Tables

List of Acronyms and Abbreviations

BMP	Best Management Practice
CVRWQCB	Central Valley Regional Water Quality Control Board
CCSB	Cache Creek Settling Basin
Conc.	Concentration
Delta	Sacramento-San Joaquin Delta
D-MCM	Dynamic Mercury Cycling Model
DOC	Dissolved Organic Carbon
DMCP	Delta Mercury Control Program (DMCP)
DWR	(California) Department of Water Resources
EPA	Environmental Protection Agency
fHg	Filter-passing Mercury
fMeHg	Filter-passing Methylmercury
GIS	Geographic Information System
Hg	Mercury
KLRC	Knights Landing Ridge Cut
MeHg	Methylmercury
pHg	Particulate Mercury
pMeHg	Particulate Methylmercury
POC	Particulate Organic Carbon
tHg	Total Mercury (in sediment)
TOC	Total Organic Carbon
TSS	Total Suspended Solids
uHg	An unfiltered (aqueous) mercury (sample)
uMeHg	An unfiltered (aqueous) methylmercury (sample)
VSS	Volatile Suspended Solids
WY	Water Year(s)

Introduction - Technical Field Studies

The Delta Mercury Control Program (DMCP) requires the (California) Department of Water Resources (DWR) to reduce methylmercury (MeHg) open water sediment flux from areas out of compliance in the Delta and Yolo Bypass (See Chapter 1). A mercury mass balance biogeochemical modeling approach was approved to evaluate how hydrodynamic and other changes to the water flow system might impact open water sediment fluxes. At the time of the workplan's approval, mercury cycling and transport in the Yolo Bypass was not well understood, therefore technical studies were designed to provide critical input data to the Yolo Bypass Dynamic Mercury Cycling Model (D-MCM). The originally approved workplan relied upon large-scale, field-based studies to provide information for the model. However, the proposed studies had feasibility and funding constraints. Therefore, DWR discussed, and received approval from the (California) Central Valley Regional Water Quality Control Board (CVRWQCB) staff, to instead conduct laboratory and mesocosm studies to provide necessary information on mercury behavior with which to develop the mercury model for the Yolo Bypass.

The objective of this chapter is to summarize and provide key findings of interest to management and policy makers from the studies listed in Table 3-1**Error! Reference source not found.**. Stand-alone chapters for each of the laboratory and field studies are published in four Technical Appendices. In-depth details on study design, methodology as well as in-depth analysis of results can be found in the individual technical appendices. Data including QC, have been provided to staff of the CVRWQB. DWR staff are also working on publishing data to the Environmental Data Initiative (EDI) data portal.

Table 3-1 List of Summarized Open Water Yolo Bypass Technical Studies

Study	Description	Research Team[1]	Technical Appendix
Yolo Bypass Mass Balance Study	Information used to parameterize the mercury model. This study expands on previous CALFED investigations by determining MeHg in filtered and particulate fractions as well as extending sampling below Liberty Island.	DWR	B
Sediment-water Flux Study	Addressed Hg and MeHg fluxes from sediments of different land uses.	MLML	C
Gust Chamber Erosion Study	Addressed soil erosion of different land uses under different flow velocities.	USGS	D
Vegetation Senescence Study	Addressed possible vegetation impacts associated with the largest actively managed land use and investigated possible BMPs.	DWR MLML	E and E1

[1]DWR = California Department of Water Resources; MLML = Moss Landing Marine Laboratories; USGS = United States Geological Survey

Background

The Yolo Bypass

The Yolo Bypass is a 3-mile wide, 40 mile-long, 59,000-acre flood conveyance system that diverts flood waters from the Sacramento River around the City of Sacramento (Figure 3-1**Error! Reference source not found.**). The Yolo Bypass floods in roughly 7 out of 10 years with inundation occurring roughly between October and April. When completely flooded, the Yolo Bypass covers an area equal to about one-third the size of San Francisco and San Pablo Bays (Natural Resources Defense Council,https://www.nrdc.org/experts/monty-schmitt/building-rivers-yolo-bypass-hiding-plain-sight) and

can carry up to four times the flow of the Sacramento River's main channel during large floods (Suddeth Grimm and Lund, 2016). When fully inundated, the wetted area of the Sacramento-San Joaquin Delta system approximately doubles. The project design capacity is 343,000 cfs (DWR, https://water.ca.gov/LegacyFiles/newsroom/docs/WeirsReliefStructures.pdf, accessed 11/25/19).

The main input to the Yolo Bypass is at the 2-mile wide Fremont weir where water passively flows into the Yolo Bypass when the Sacramento river reaches 32 feet stage height (NAVD88 datum) or approximately 60,000 cfs. Additional tributaries into the Yolo Bypass include the Knight's Landing Ridge Cut (KLRC), the Cache Creek Overflow weir and low flow channel for the Cache Creek Settling Basin (CCSB), Willow Slough and Putah Creek (Figure 3-1). Depending on flood flows, the flood gates of the Sacramento weir can also be opened. In January 2017, a period captured by some of our studies, the Sacramento weir gates were opened for the first time in eleven years. The dominant hydrological feature at the southern end of the Yolo Bypass is Liberty Island, a 5,300-acre parcel of open water and wetland habitat that is tidally-influenced (fresh water) except during large floods in the Yolo Bypass. Just north of Liberty Island is the feature referred to as the Stairsteps drainage canals (Figure 3-1).

The use of the Yolo Bypass as a floodplain cannot be compromised, however, several spring-fall agricultural uses are compatible with maintaining the Yolo Bypass as an unimpeded floodplain. The Yolo Bypass is farmed, irrigated, left unmanaged, disked, mowed and grazed by cattle. Figure 3-2 shows the top land uses and their boundary cells used in the D-MCM model. Many technical studies in this chapter involved the Yolo Wildlife Area. The Yolo Wildlife Area is located within the Yolo Bypass and is managed by the California Department of Fish and Wildlife with the intent of restoring and managing a variety of wildlife habitats in the Yolo Bypass (Figure 3-1).

Figure 3-1 Yolo Bypass Schematic Map

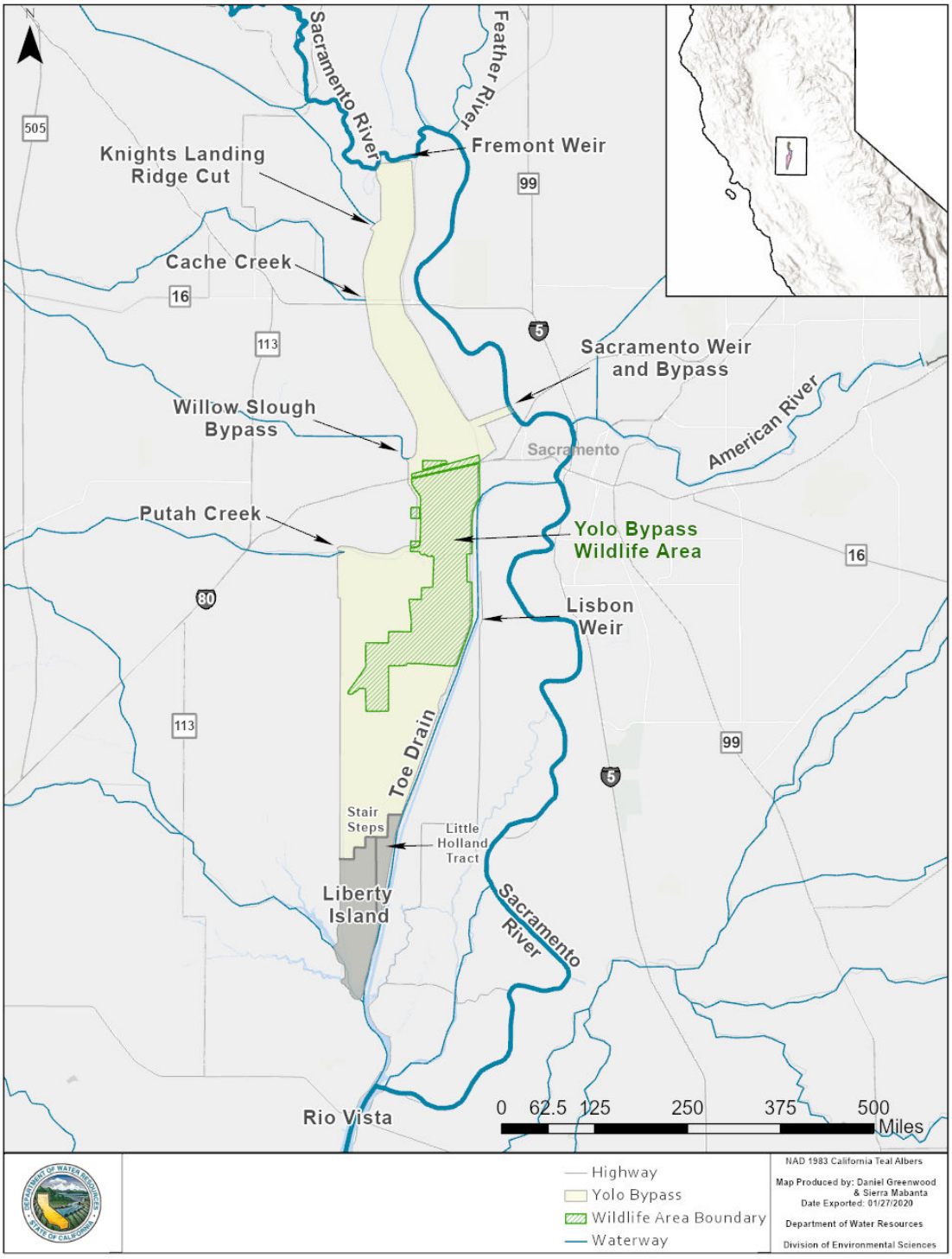

Figure 3-2 Land Uses in the Yolo Bypass as Delineated in the Yolo Bypass Dynamic Cycling Model.

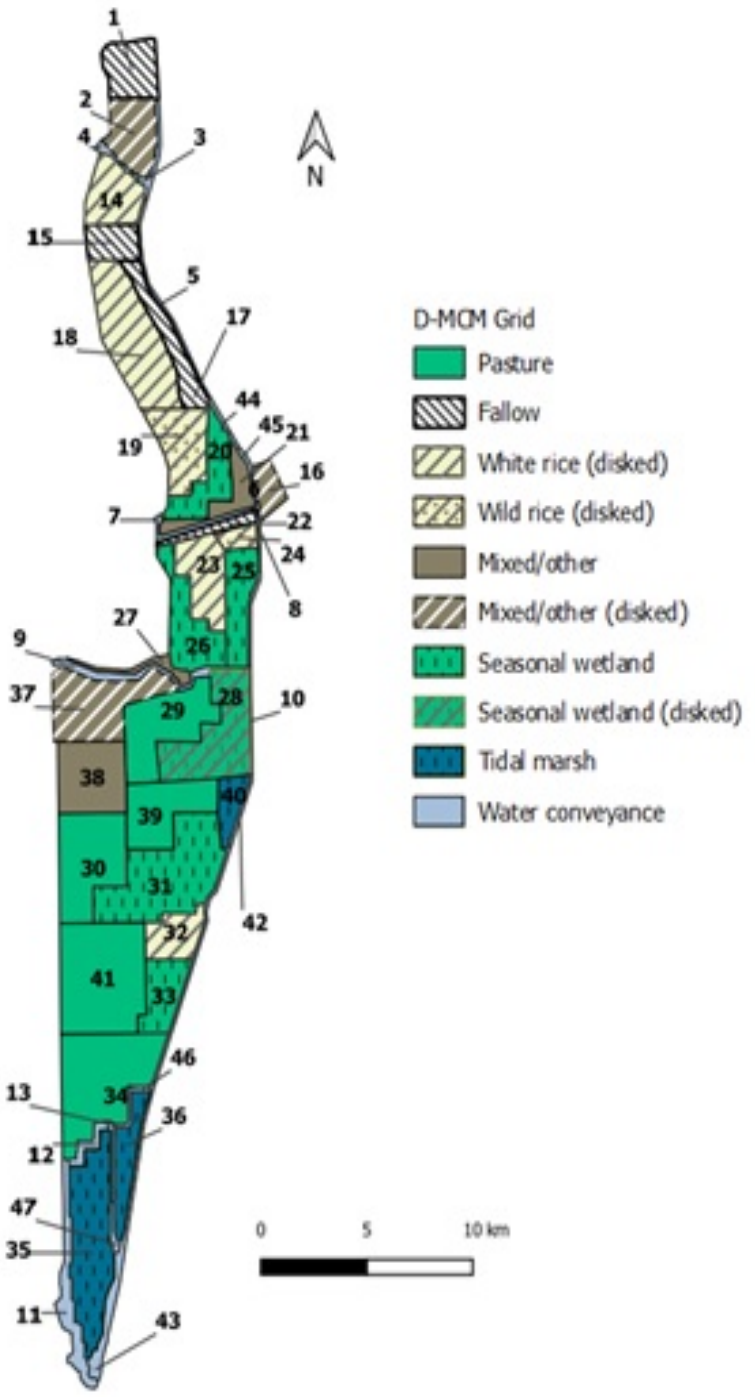

Cell #	Land use
1	Fallow
2	Mixed/other
3	Water
4	Water
5	Water
6	Water
7	Water
8	Water
9	Water
10	Water
11	Water
12	Water
13	Water
14	White rice
15	Fallow
16	Mixed/other
17	Fallow
18	White rice
19	Wild rice
20	Wetland
21	Mixed/other
22	Fallow
23	White rice
24	Wild rice
25	Wetland
26	Wetland
27	Mixed/other
28	Wetland
29	Pasture
30	Pasture
31	Wetland
32	White rice
33	Wetland
34	Pasture
35	Tidal marsh
36	Tidal marsh
37	Mixed/other
38	Mixed/other
39	Pasture
40	Tidal marsh
41	Pasture
42	Water
43	Water
44	Water
45	Water
46	Water
47	Water

Program Goals

The main goal of this work was to provide critical information for model development. Toward this end, many of the report's technical studies evaluated needed parameters for different land uses and were not necessarily studies evaluating open water MeHg contributions as defined in the DMCP. Except for the Vegetation Senescence (VegSens) studies, field studies were used to provide data for the model and were not hypothesis driven, however, they did provide useful insights beyond providing data for the model. The technical studies significantly expanded on the earlier CALFED work and also allowed for an evaluation of Best Management Practices (BMP). The DMCP and additional work conducted for CALFED primarily looked at mercury and methylmercury in unfiltered samples (uHg and uMeHg, respectively). This current work expanded on this to include measurements of Hg and MeHg in filtered samples (fHg and fMeHg, respectively)[1] and estimates of Hg and MeHg in the particulate fraction (pHg and pMeHg, respectively). Understanding the patterns associated with individual fractions provides information on which fractions to target in future control studies. Additionally, the Yolo Bypass Mass Balance Study included sample collection below Liberty Island in addition to the inputs and exports at the Stairsteps. Collecting samples below Liberty Island provided a better estimate of the total loads exiting the Yolo Bypass into the Delta. Previous work had not included this lower reach.

Foe and others, (2008) documented that the Yolo Bypass, under large flood events, was a net internal producer of uMeHg. Understanding the source(s) of this internal production is a critical first step in assessing future BMP approaches. The sediment-water flux experiments provided flux values for the model, but also provided rough estimates of whether open water sediments could account for observed Yolo Bypass in-situ production. The VegSens studies looked at pasture vegetation inundated by floodwaters as another possible internal source of MeHg to the Yolo Bypass. Pasture was evaluated as this was the largest land use in the land use map developed for the Yolo Bypass model. This is a new source that has never been assessed. The vegetation studies were also designed to examine BMP's for pastureland to minimize in-situ production of MeHg and introduction into flood waters.

The following sections provide summaries of key highlights from the individual technical appendices.

[1] In this document, the term filtered or filter-passing mercury (fHg) and methylmercury (fMeHg) refers to the mercury or methylmercury passing through a 0.45-micron filter

Mass Balance Study - Import and Export Loads from the Yolo Bypass

Workplan Objectives

Objectives for the mass balance study were to: 1) quantify input, output, and net loads of Hg, MeHg (total filtered and particulate), and suspended particles (TSS) during periods of time when the Bypass is flooded; and 2) investigate the possible sources that contribute to within-Bypass production of MeHg during floods by evaluating filtered vs. particulate loads and correlations with ancillary parameters. A third objective of this study, not originally proposed in the Workplan, was to quantify the contribution of Liberty Island to the Hg and MeHg loads of the Yolo Bypass. The data from this study was also used to parameterize and validate the D-MCM developed by consultants to DWR. As discussed below, we were unable to pursue workplan objectives to compare mini-flood events to larger flood events. A mini-flood event was defined when flows in Knights Landing Ridge Cut, Cache Creek and/or Putah Creek are greater than the carrying capacity of their channels, resulting in local flooding, but no spillage over the Fremont weir. A major flood event was defined by the Sacramento River overtopping the Fremont Weir resulting in wide-scale flooding of the Yolo Bypass for days, weeks or months. As discussed in Technical Appendix A, safety concerns precluded collecting enough east-west transects across the Yolo Bypass to allow examination of the banded water mass contributions occurring in the flooded Yolo Bypass. Any changes associated with the original Workplan were discussed and approved by the Central Valley Regional Water Quality Control Board.

Sampling Locations

Water sampling locations from the major input and export sites are shown in Figure 3-3. Input samples were collected at Fremont Weir, Sacramento Weir (when it was open), the Knights Landing Ridge Cut (KLRC), Cache Creek Settling Basin (CCSB), and Putah Creek. Output samples were collected along the drainage canal known as the “Stairsteps” (Toe Drain, Liberty Cut, and Shag Slough). The stairsteps drainage canal is located immediately above Liberty Island. Additionally, during 8 sampling events in 2017 when an adequate volume of water was exiting the Yolo Bypass, samples were also collected from Cache and Miner Sloughs which are located downstream of Liberty Island. Sampling Cache and Miner Sloughs allowed us to divide the Yolo Bypass into upper and lower reaches. The upper reach encompasses the area receiving drainages from the inlets to the outlet at the stairsteps drainage canals which covers about two-thirds of the length of the Bypass. The lower reach encompasses the area from the stairsteps to below Liberty Island which is dominated by Liberty Island. Details on sample locations, sample dates, and other logistics are given in Technical Appendix B.

Figure 3-3 Mass Balance Study Sampling Locations in the Yolo Bypass

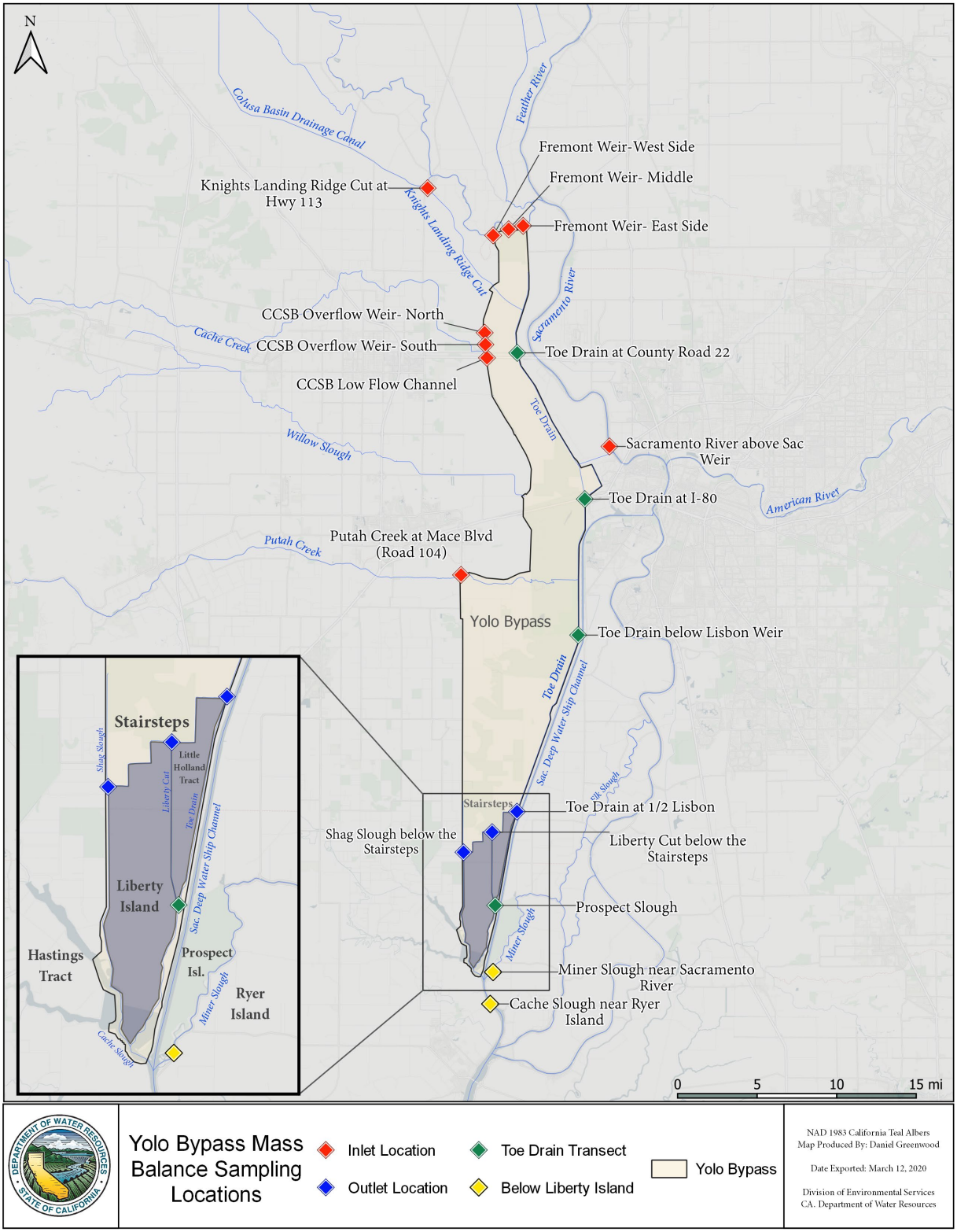

Mercury and Water Quality Parameters

Water samples were collected at the inlet and outlet locations and analyzed for several constituents, including uHg, fHg, uMeHg, fMeH, TSS, and organic carbon (TOC, DOC). The Environmental Protection Agency's (EPA) Method 1669 "clean hands-dirty hands" was used when collecting samples and while processing and filtering samples in the laboratory (EPA, 1995). Particulate Hg (pHg) and particulate MeHg (pMeHg), as well as particulate organic carbon (POC), were determined as the difference between their respective unfiltered and filtered values. All inlet locations, except for Putah Creek had nearby flow monitoring gages. Outlet sites on the Stairsteps lack flow gaging stations, therefore, after evaluating a modeling approach, outlet flows were estimated as the sum of the inlet flows.

Tributary Input Sources and Export of Methyl Mercury to the Delta

Water Balances

Over the course of the study, the state of California experienced a severe drought in Water Years (WYs) 2013-2016 classified as either dry, critical, or below normal (CDEC, http://cdec.water.ca.gov/reportapp/javareports?name=WSIHIST, accessed September 2019) and the Governor of California declared a drought state of emergency in 2014. The lack of flooding events resulted in the sampling of only one mini-flood event in 2014 and one flooding event in 2016. In contrast, WY 2017 was the second wettest year in a 122-year record and mass balance sampling occurred on nine occasions from January 2017 through April 2017 covering the full extent of the flooding season. Based on weather constraints, collection efforts were unable to collect enough samples to meaningfully compare mass balance differences between mini-flood and major flooding events. Therefore, mass balance insights summarized in this chapter are confined to the nine sampling events associated with WY 2017 (October 1, 2016-Sept. 30, 2017).

Intensive sampling of one of the wettest years on record provided the opportunity to evaluate a sustained flooding season when most of the uMeHg from the Yolo Bypass is transported to the Delta (Foe and others, 2008). Inputs consisted of the sum of Fremont Weir, Sacramento Weir, CCSB, KLRC and Putah Creek. Outputs consisted of the sum of the stations at the Stairsteps. Water balance calculations indicated that most of the water volume entering and leaving the Yolo Bypass was accounted for. The balance between inlet and outlet volumes was close to 100% for the overall 2017 flood event (see Technical Appendix B).

When spilling, the Fremont weir was the largest contributor of water to the Yolo Bypass accounting for an average of 75% of tributary inflows, followed by the Sacramento weir at 14%. The CCSB was a relatively small contributor to the overall water balance, providing on average 5% of the water volume entering the Yolo Bypass. Water balances were nearly identical between the nine-sampling events and the entire flood season (Figure 3-4). Other tributaries were also minor contributors to the total inflow. It is important to note that the sampling was designed to target periods of peak flow at the Fremont weir, which meant that samples collected at other inlets did not always correspond to peak flow periods. For example, Figure 3-5 shows the hydrographs for the Fremont Weir and CCSB and the point in the hydrograph when samples were collected. For flashier systems, like the CCSB, their load contributions may have been underestimated with this sampling scheme. On the one occasion when the Fremont weir was not overtopping (March 15, 2017), the CCSB became the dominant source (55%) of water into the Yolo Bypass (Figure 3-6), but this event was the smallest event overall.

Figure 3-4 Average Input Water Balances in Percent for the A) 2017 Sampling Events and B) Season Total from 1/9/17 to 5/4/17

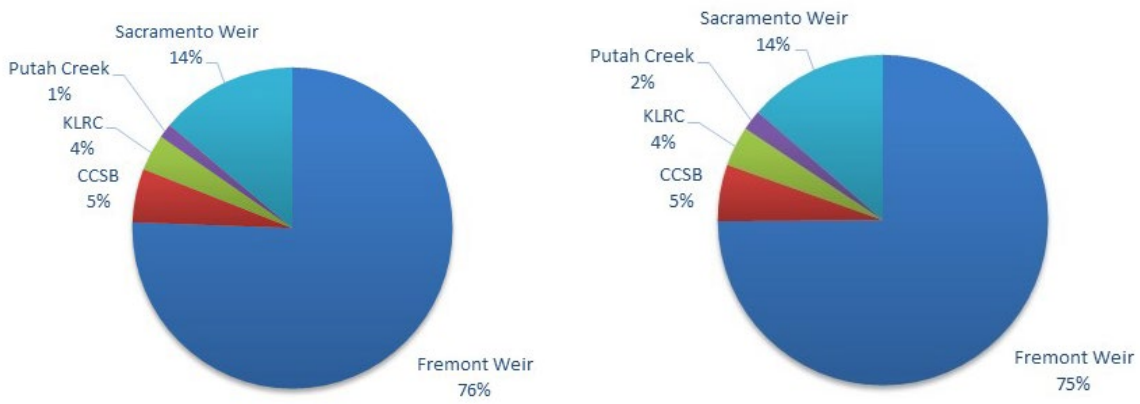

Figure Note: KLRC = Knights Landing Ridge Cut; CCSB = Cache Creek Settling

Figure 3-5 Daily Average Flow from the Cache Creek Settling Basin and the Fremont Weir January 2017 to April 2017

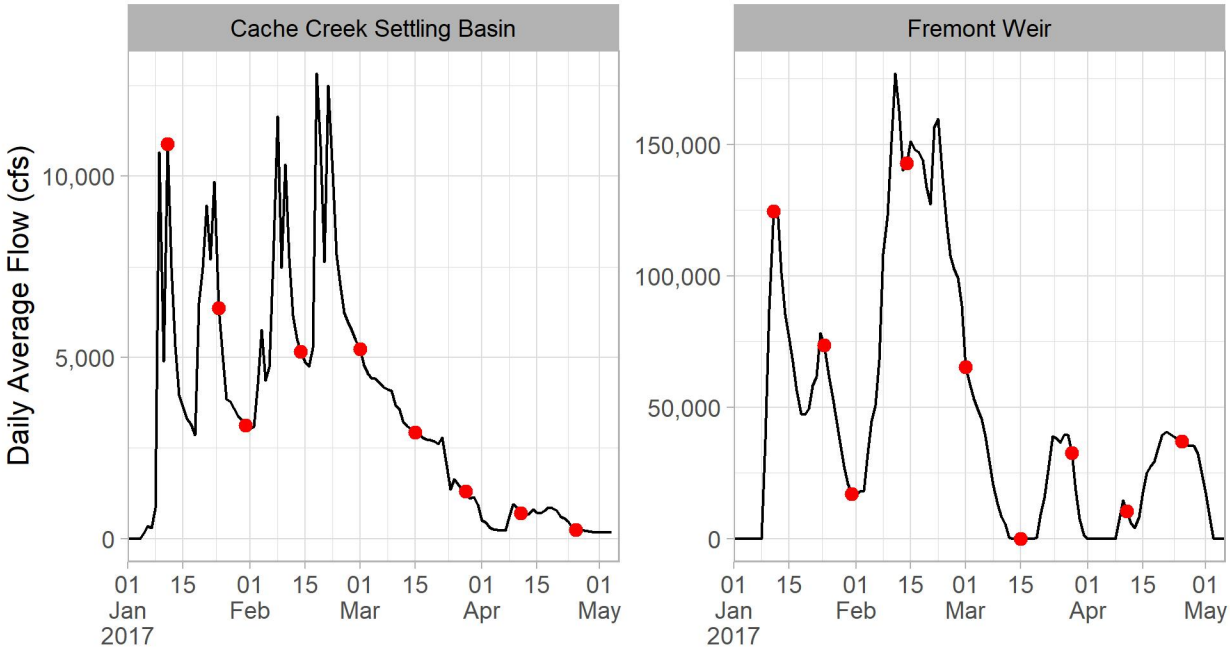

Figure Note: Sampling events shown in red

Figure 3-6 Proportion of Water Inputs to Total Inflow by Tributary and Date

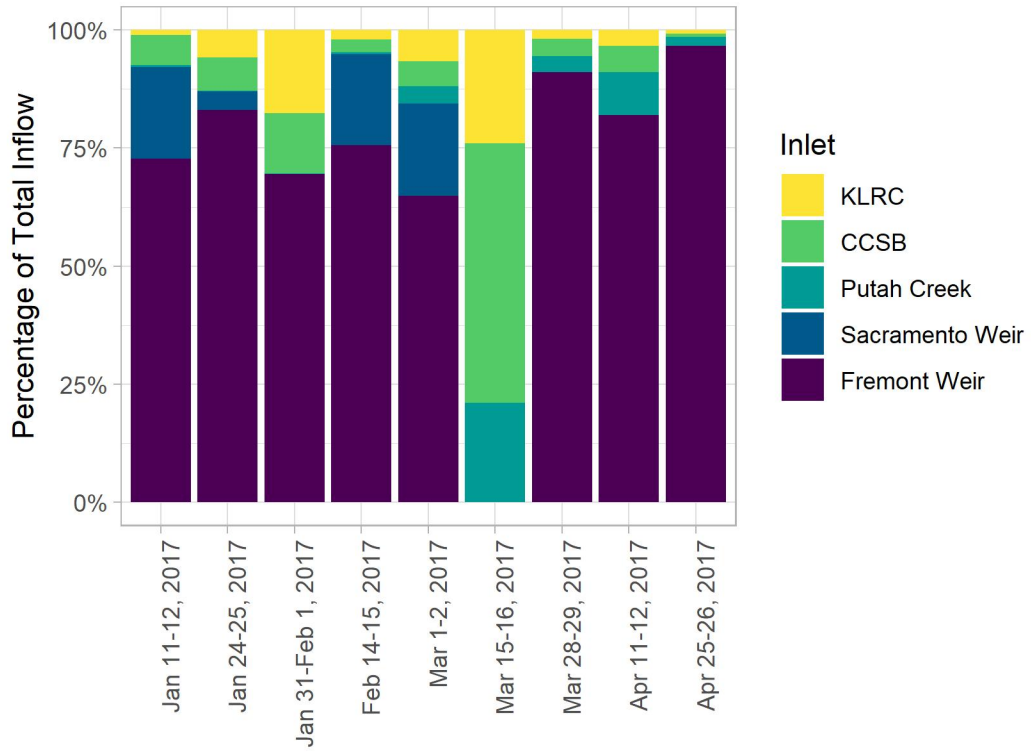

Methylmercury Concentrations in the Upper Yolo Bypass

Tributary concentrations of uMeHg varied spatially and across a broad range of tributary inflows. Concentrations of uMeHg in inlet tributaries ranged over almost an order of magnitude, from a low of 0.058 ± 0.008 ng/L at the Fremont Weir sites to a high of 0.515 ng/L at CCSB, both occurring on the last sampling event on 4/25/2017 (Table 3-2). The Cache Creek Settling Basin (CCSB) and the Knights Landing Ridge Cut (KLRC) exhibited the highest average concentrations of uMeHg (0.23 ± 0.12 and 0.242 ± 0.122 ng/L, respectively), and the Fremont Weir site had the lowest average uMeHg concentration (0.090 ± 0.028 ng/L) for the nine sampling events in 2017. In general, uMeHg values varied the least across all sampling events at the Fremont Weir and Sacramento Weir sites (Coefficient of Variation = 31% and 24%, respectively) and varied the most at the CCSB and KLRC, both of which had a coefficient of variation of 50%. Concentrations of tributary fMeHg and pMeHg each varied by an order of magnitude. The highest average fMeHg concentration occurred at KLRC, while the lowest average occurred at Fremont Weir (Table 3-3). For pMeHg, the highest average pMeHg was from the CCSB, while the lowest was from the Fremont Weir (Table 3-4). In terms of partitioning of uMeHg into particulate and filter passing fractions, partitioning occurred over a narrow range amongst the tributaries. CCSB had the highest percentage of pMeHg (65 ± 4.6 %) and KLRC had the lowest percentage of pMeHg (49 ± 16%) (data not shown, see Technical Appendix B).

Table 3-2. **Summary of Tributary Inputs of uMeHg Concentrations (ng/L) for Nine Sampling Events to the Upper Yolo Bypass for Water Year 2017**

Sampling Date	Fremont Weir	CCSB	Putah Creek	Sacramento Weir	KLRC
1/11/2017	0.146 ± 0.033	0.217	0.316	0.159	0.124
1/24/2017	0.098 ± 0.007	0.168	0.105	0.114	0.188
1/31/2017	0.065 ± 0.003	0.12	0.115		0.211
2/14/2017	0.11 ± 0.03	0.222	0.131	0.094	0.399
3/1/2017	0.083	0.162	0.158	0.156	0.276
3/15/2017		0.179	0.162		0.477
3/28/2017	0.081	0.210	0.161		0.189
4/11/2017	0.082 ± 0.002	0.318	0.137		0.119
4/25/2017	0.058 ± 0.008	0.515	0.127		0.198
Average (all dates)	***0.090 ± 0.028***	***0.23 ± 0.12***	***0.157 ± 0.063***	***0.13 ± 0.03***	**0.242 ± 0.122**
CV (all dates)	***31%***	***50%***	***40.2%***	***24%***	**50.4%**

Table Notes: CCSB = Cache Creek Settling Basin. KLRC = Knights Landing Ridge Cut. Fremont Weir concentration data represent the average of three collection sites: the east side, west side, and middle sampling stations. A standard deviation is given for the Fremont collections when all three sites were sampled. MeHg concentration data were excluded if the value of the filter-passing fraction was greater that the unfiltered value, which was the case for the Fremont Weir east location on 3/1/2017 and 3/28/2017. The CCSB data represent the average of two sampling sites, the north and south weirs, except for the 3/28/2017 and 4/11/2017 sampling dates which also include the low-flow channel, and the 4/25/2017 sampling date which is the average of the south weir and low-flow channel sampling sites. Particulate MeHg (pMeHg) concentrations were determined by difference (pMeHg = uMeHg – fMeHg).

First Flush Effect for Tributary Inflow Concentrations

A first flush effect with uMeHg is clearly evident during the first sampling event on January 11th for the Fremont Weir and Putah Creek sampling sites, driven primarily by an enhanced pMeHg concentration (Tables 3-2 through 3-4). The uMeHg concentration on the first sampling event at Fremont Weir (0.146 ± 0.033 ng/L) is higher than all the other sampling events, and 60% higher than the average concentration for all sampling events at the Fremont Weir (0.090 ± 0.028). Similarly, the uMeHg concentration on the first sampling event at Putah Creek (0.316 ng/L) is higher than all the other sampling events and was two-fold higher than the average for all 9 sampling events (0.157 ± 0.063 ng/L). The other sampling sites did not show a clear first flush effect with uMeHg or pMeHg. Interestingly, there was a reverse trend at CCSB, where uMeHg concentrations continually rose in the last three sampling events, cumulating in the highest uMeHg concentration being observed in the last sampling event (0.515 ng/L), which was double the average concentration for the entire flood event (0.23 ± 0.12 ng/L). The rise in uMeHg at the end of the flood event at CCSB were driven by increases in both fMeHg and pMeHg concentrations (Tables 3-3 and 3-4).

Table 3-3. **Summary of Tributary Inputs of fMeHg Concentrations (ng/L) for Nine Sampling Events to the Upper Yolo Bypass for Water Year 2017**

Sampling Date	Fremont Weir	CCSB	Putah Creek	Sacramento Weir	KLRC
1/11/2017	0.044 ± 0.009	0.082	0.042	0.042	0.054
1/24/2017	0.037 ± 0.003	0.058	0.044	0.057	0.102
1/31/2017	0.023 ± 0.002	0.040	0.049		0.130
2/14/2017	0.038 ± 0.003	0.074	0.058	0.029	0.246
3/1/2017	0.030	0.042	0.050	0.060	0.169
3/15/2017		0.060	0.060		0.172
3/28/2017	0.037	0.060	0.049		0.089
4/11/2017	0.037 ± 0.003	0.130	0.056		0.087
4/25/2017	0.023 ± 0.001	0.182	0.062		0.039
Average (all dates)	***0.034 ± 0.007***	***0.081 ± 0.047***	***0.052 ± 0.007***	***0.047 ± 0.014***	***0.12 ± 0.07***
CV (all dates)	***22%***	***57%***	***14%***	***31%***	***54%***

Table Notes: CCSB = Cache Creek Settling Basin. KLRC = Knights Landing Ridge Cut. Fremont Weir concentration data represent the average of three collection sites: the east side, west side, and middle sampling stations. A standard deviation is given for the Fremont collections when all three sites were sampled. MeHg concentration data were excluded if the value of the filter-passing fraction was greater that the unfiltered value, which was the case for the Fremont Weir east location on 3/1/2017 and 3/28/2017. The CCSB data represent the average of two sampling sites, the north and south weirs, except for the 3/28/2017 and 4/11/2017 sampling dates which also include the low-flow channel, and the 4/25/2017 sampling date which is the average of the south weir and low-flow channel sampling sites. Particulate MeHg (pMeHg) concentrations were determined by difference (pMeHg = uMeHg – fMeHg).

Table 3-4. **Summary of Tributary Inputs of pMeHg Concentrations (ng/L) for Nine Sampling Events to the Upper Yolo Bypass for Water Year 2017**

Sampling Date	Fremont Weir	CCSB	Putah Creek	Sacramento Weir	KLRC
1/11/2017	0.10 ± 0.03	0.135	0.274	0.117	0.070
1/24/2017	0.061 ± 0.008	0.11	0.061	0.057	0.086
1/31/2017	0.041 ± 0.003	0.085	0.066		0.081
2/14/2017	0.070 ± 0.029	0.15	0.073	0.065	0.153
3/1/2017	0.053	0.12	0.108	0.096	0.107
3/15/2017		0.12	0.102		0.305
3/28/2017	0.044	0.150	0.112		0.100
4/11/2017	0.045 ± 0.003	0.188	0.081		0.032
4/25/2017	0.035 ± 0.009	0.332	0.065		0.159
Average (all dates)	***0.056 ± 0.022***	***0.15 ± 0.07***	***0.10 ± 0.07***	***0.084 ± 0.028***	***0.12 ± 0.08***
CV (all dates)	***38%***	***47%***	***63%***	***33%***	***65%***

Table Notes: CCSB = Cache Creek Settling Basin. KLRC = Knights Landing Ridge Cut. Fremont Weir concentration data represent the average of three collection sites: the east side, west side, and middle sampling stations. A standard deviation is given for the Fremont collections when all three sites were sampled. MeHg concentration data were excluded if the value of the filter-passing fraction was greater that the unfiltered value, which was the case for the Fremont Weir east location on 3/1/2017 and 3/28/2017. The CCSB data represent the average of two sampling sites, the north and south weirs, except for the 3/28/2017 and 4/11/2017 sampling dates which also include the low-flow channel, and the 4/25/2017 sampling date which is the average of the south weir and low-flow channel sampling sites. Particulate MeHg (pMeHg) concentrations were determined by difference (pMeHg = uMeHg – fMeHg).

Variability in MeHg Concentrations with Inflow

Figure 3-7 shows how uMeHg, pMeHg, and fMeHg varied as a function of tributary flow for the Fremont Weir and the CCSB. For the Fremont Weir, all the forms of MeHg increased in concentration with increasing flow, while for the CCSB, the concentrations were much higher at very low tributary inflows. For the CCSB, there was no significant relationship between flow and concentration. Because the Fremont Weir accounts for approximately 75% of the hydrologic inflow (Figure 3-4), it has a dominant impact on MeHg concentrations in the Yolo Bypass. This increase in MeHg concentrations with flow in the Fremont Weir tributary input has important impacts on loads to the upper Yolo Bypass. It means that increases in load with hydrologic flow are driven not only by delivery of more water, but also by increases in MeHg concentrations as flow increases.

Figure 3-7 Variation in MeHg Concentrations as a Function of Tributary Inflow for the Fremont Weir and Cache Creek Settling Basin

Unfiltered MeHg **Filtered MeHg** **Particulate MeHg**

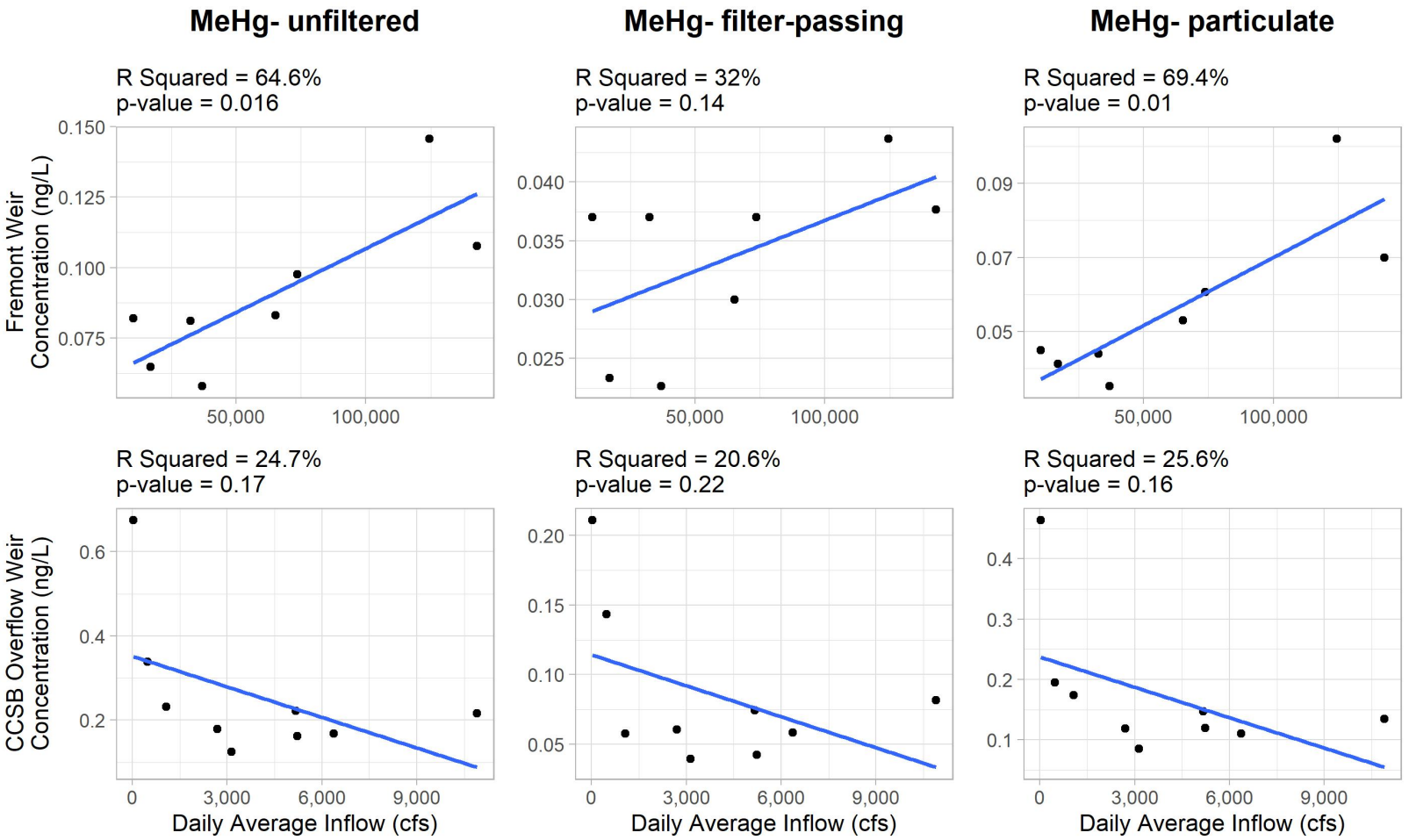

Internal Production or Loss of Mercury, Methylmercury and Several Biogeochemical Parameters in the Upper Yolo Bypass

Changes in concentrations of several parameters were evaluated as water traversed from north to south down the Yolo Bypass. Table 3-5 lists a comparison of the percentage increase of Hg and MeHg with several biogeochemical parameters between the tributary input at the Fremont Weir and an average of the Half-Lisbon and Liberty Cut export sites for the 2017 flood event. The data in Table 3-5 represent only those sampling events where the specific conductance at the export was within 15% of the specific conductance for the Fremont Weir input water. The average specific conductance for the west side tributaries (437 µS/cm) is considerably higher than the average for the Fremont Weir (123 µS/cm), allowing a clear distinction between east side from west side tributary sources at the export sites. The export site at Shag Slough was not used in this comparison because its specific conductance was similar to the specific conductance for west side water sources most of the time.

Table 3-5 **Comparison of the Percentage Increase of Hg and MeHg with Several Biogoechemical Parameters between the Fremont Weir Tributary Input and Export at Liberty Island**

Parameter (units)	Average Concentration at Fremont Weir	Average Export Concentration	% Increase in Export Concentration
Specific Conductance (µS/cm)	118	118	0.3%
Chloride (mg/L)	2.8	3.1	11%
uHg (ng/L)	13.2	14	5.9%
fHg (ng/L)	2.1	2.2	4.1%
pHg (ng/L)	11.1	11.8	6.3%
uMeHg (ng/L)	0.096	0.171	79%
fMeHg (ng/L)	0.035	0.066	91%
pMeHg (ng/L)	0.061	0.105	72%
TOC (mg/L)	2.3	2.3	-0.1%
DOC (mg/L)	1.8	1.9	9.3%
TSS (mg/L)	95	52	-45%
MeHg, solid phase (ng/g)	0.77	2.53	229%
TOC/TSS (proportion organic)	0.027	0.052	94%

Table Notes: TSS = Total Suspended Solids. TOC = Total Organic Carbon. DOC = Dissolved Organic Carbon. The average concentrations only include sampling events when the specific conductance value of the export was within 15% of the specific conductance observed at the Fremont Weir. The average export concentration was the average for collections obtained at Half-Lisbon and Liberty Cut, and the average concentration at Fremont Weir was the average of three collection sites: the east side, west side, and middle sampling stations.

This comparison suggests that there were significant increases in all forms of MeHg (uMeHg, fMeHg and pMeHg) during passage of flood waters through the upper Yolo Bypass, with only minor increases (4-6%) in the (inorganic) Hg forms (uHg, fHg, and pHg). The major MeHg form that showed increases was solid phase MeHg (i.e. MeHg on particles), which increased more than two-fold between the Fremont Weir input and export. The comparison also suggests that there is a substantial internal loss (45%) of Total Suspended Solids (TSS) and only minor or no changes in TOC or DOC. Note also that particles at the export site were far more organic rich (94%) than that for the Fremont Weir input, as evidenced by the

TOC/TSS ratio which describes the proportion of the solids that were organic in nature. This analysis strongly supports the contention that there is a substantial internal production of MeHg in the upper Yolo Bypass which enhances MeHg concentrations in overlying flood waters as it progresses from input to exit through the upper Yolo Bypass. As discussed in the Vegetation Senescence section of this report, one potential source for this enhancement is pastureland vegetation which releases its MeHg content both in dissolved and particulate phases.

Mass Balances - Mercury, Total Suspended Solids, and Organic Carbon

Tributary Input Loads

Tributary loads exhibited a first flush pattern for all forms of Hg, MeHg, and organic carbon, as well as TSS (Figure 3-8). The first sampling event occurred a few days after the Yolo Bypass first began flooding. In subsequent sampling events, loads generally fell by half or more for all parameters except MeHg, lending support to the first flush idea. MeHg loads were equally high on the February 14th sampling event which had the highest sample event flows. As discussed previously, there was a strong positive relationship between flow and uMeHg concentrations at the Fremont Weir.

Fremont Weir was the largest contributor of water to the Yolo Bypass and, on average, of the eight sampling events when the Fremont Weir was spilling it was the largest contributor of uHg (73%), uMeHg (68%), and TSS (80%) to the Yolo Bypass (Figure 3-9). Similarly, when the Sacramento Weir was spilling, it was the second largest water volume contributor to the Yolo Bypass, and was generally the second largest contributor of uMeHg loads. When open, the Sacramento Weir provided averages of 19% of the total inflow to the Bypass, and 28, 21, and 18% of the total input load of uHg, uMeHg, and TSS, respectively. While the gates of the Sacramento Weir are rarely open, this emphasizes that it can be an important source.

When compared to the Fremont Weir, the CCSB and KLRC were relatively small inputs of MeHg to the Yolo Bypass. Both the CCSB and KLRC contributed an average of 10% of the uMeHg input load when the Fremont Weir was spilling in 2017. However, when the Fremont Weir was not spilling, the CCSB generally became the second largest contributor of uHg. Overall, the CCSB contributed an average of 570 g/day of uHg during the 2017 flood. Excluding the one sampling event when the Fremont weir was not overtopping, the largest Hg and TSS loads from the CCSB were on the first two sampling events of the 2017 flood, which may be due to a first-flush effect. The CCSB contributed about 25% of the uHg and pHg input loads while it was about 7% of the total inflow during these first two sampling events. The CCSB contributed a much smaller percentage of the Hg input load to the Yolo Bypass after about 5 weeks into the 2017 flood which continued throughout the duration of the flood (except for when the Fremont Weir was not spilling on March 15th). Interestingly, the KLRC had a consistently higher percentage of the total mercury in the methylmercury fraction (MeHg/Hg ratios) than the other inputs (see Technical Appendix B). These higher ratios at KLRC suggest that the land use management and or habitat type associated with this site was more effective at converting inorganic Hg to MeHg.

Figure 3-8 Total Input Loads by Event for Hg, MeHg, Organic Carbon and TSS

Figure 3-9 Proportion of Individual Tributary Loads to the Total Input Load

Regardless of the sampling event or the tributary, the pHg fraction strongly dominated all input Hg loads while input loads for MeHg, tended to be more evenly distributed between the particulate and filtered fractions (Figures 3-10 and 3-11). This relationship held regardless of the sampling event. KLRC generally showed the highest fraction of fMeHg and CCSB the highest fraction of pMeHg. Overall, 87% and 64% of the total inlet loads of Hg and MeHg, respectively, were in the particulate fraction during the 2017 flood.

Figure 3-10 Percentage of Filtered and Particulate uHg Fractions by Sampling Event for Inlet Tributaries into the Yolo Bypass

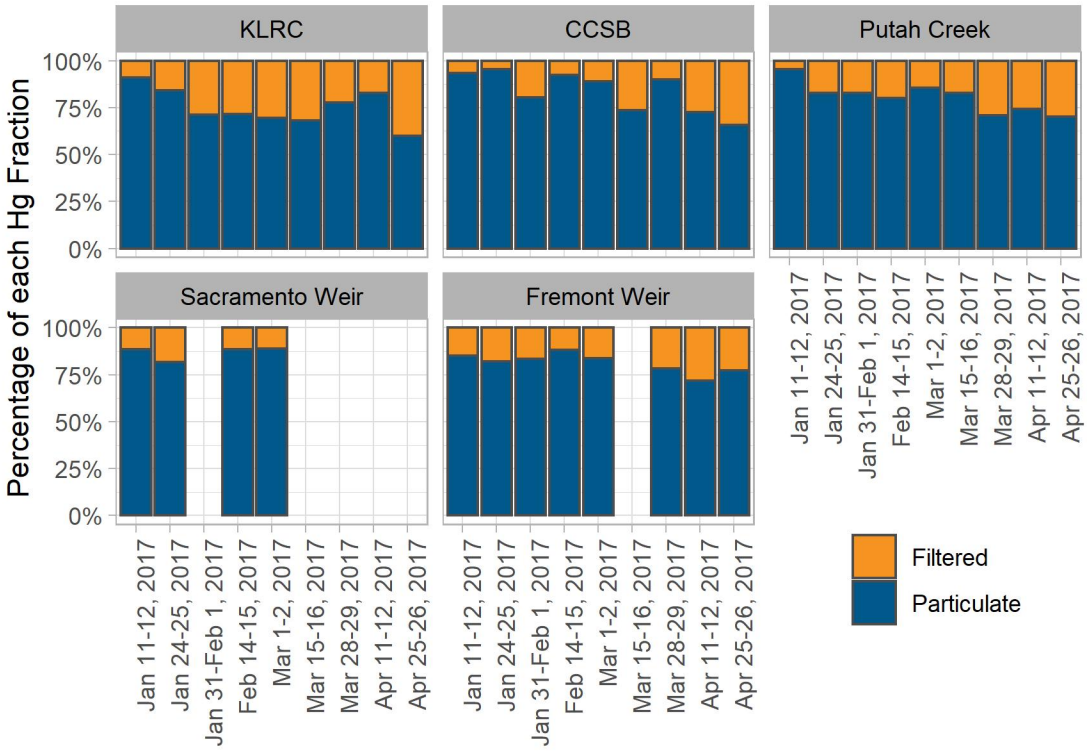

Figure 3-11 Percentage of Filtered and Particulate uMeHg Fractions by Sampling Event for Inlet Tributaries into the Yolo Bypass

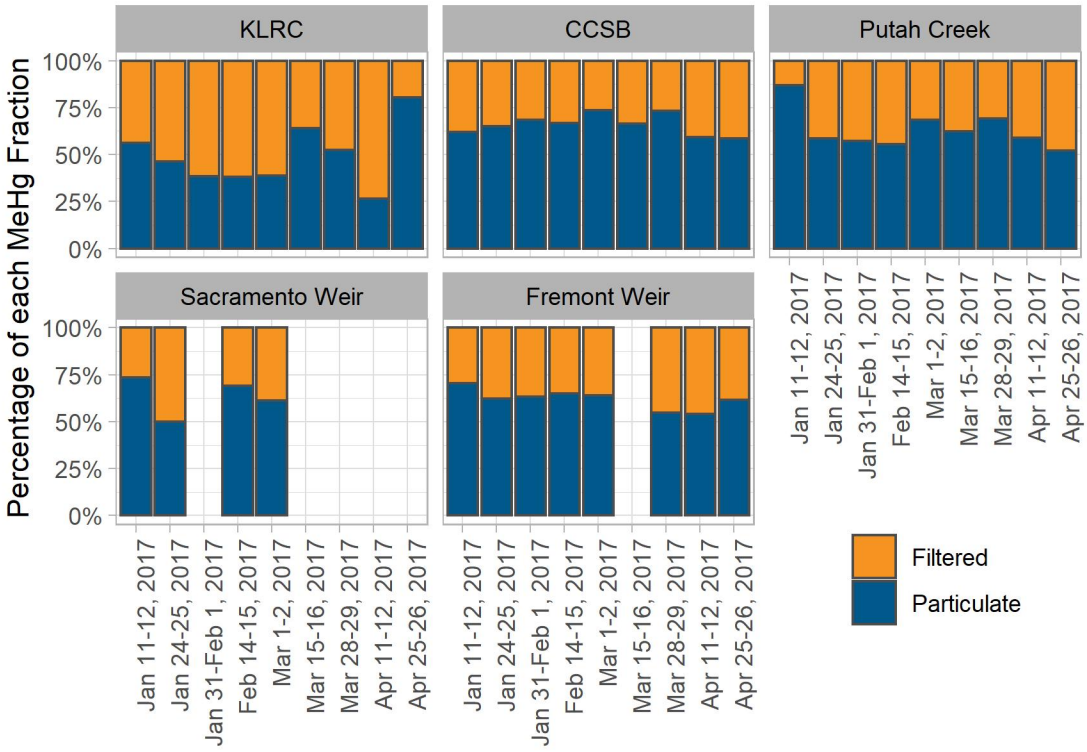

Average seasonal loads for uHg and uMeHg for tributaries into the Yolo Bypass for water year 2017 are shown below in Table 3-6. Detailed flows, and load associated with these calculations are presented in Technical Appendix B. The particulate fraction again strongly dominated uHg inflows while pMeHg, generally made up a little more than half of the uMeHg fraction. Note that the high level of uncertainty associated with these averages is due to the large changes in flows across the 9 sampling events and not the concentrations (see for example Tables 3-2 through 3-4). As illustrated in Figure 3-5, tributary input flows could vary by several orders of magnitude. For example, across the nine sampling events, total input flows varied between 5,338 cfs (March 15, 2017) to 188,700 cfs (February 14, 2017). These large variations translated to large variations in total input flows. Large changes in flow between sampling events resulted in large changes in loads. Thus, the uncertainty calculations associated with average loads for all sampling events in this document reflects the variation between large seasonal flow differences, and not uncertainties associated with individual sampling event estimates of loads.

Table 3-6 **Average uHg and uMeHg loads by tributary entering the Yolo Bypass**

Inlet location	uHg load (g/day)	uMeHg load (g/day)
Fremont Weir	2,100 ± 2,700 (81%)	14 ± 16 (62%)
Sacramento Weir	694 ± 1,070 (87%)	3.3 ± 4.9 (64%)
Cache Creek Settling Basin	570 ± 1,200 (84%)	1.9 ± 1.7 (66%)
Knight's Landing Ridge Cut	59 ± 65 (75%)	1.72 ± 1.61 (49%)
Putah Creek	40 ± 66 (81%)	0.421 ± 0.426 (63%)
Total	3,500 ± 4,800 (81%)	22 ± 23 (61%)

Table Note: Loads are the average calculated from nine sampling events collected from January 2017 through April 2017. Loads are in g/day ± 1 standard deviation. Numbers in parentheses are the percentage of the total load in the particulate form.

Net Export Loads

As discussed earlier, the sampling design allowed the division of the Yolo Bypass into an upper and lower reach. This approach provided a more accurate picture of the net exports to the Delta and was the first time that the influence of Liberty Island on total exports was examined. The upper reach encompasses the area receiving drainages from the inlets to the outlet at the Stairsteps drainage canals which covers about two-thirds of the length of the Yolo Bypass. The lower reach encompasses the area from the stairsteps to below Liberty Island which allowed us to isolate the effects of Liberty Island (see figure 3-3). Net loads associated with the upper reach were calculated by subtracting the sum of the tributary inlet loads from the stairstep outlet loads. Net loads associated with both reaches were calculated similarly by subtracting the sum of the tributary inlet loads from the loads below Liberty Island.

Upper Reach

Total exports from the upper reach showed a strong first flush phenomenon for uHg, all organic carbon fractions (DOC, POC and TOC), and to a lesser extent, TSS (Figure 3-12). Export loads of all forms of MeHg also showed a first flush phenomenon. Additionally, export loads associated with each form of MeHg were similar in both the first event and the February 14 event.

Figure 3-12 Export Loads by Date for the Upper Reach of the Yolo Bypass

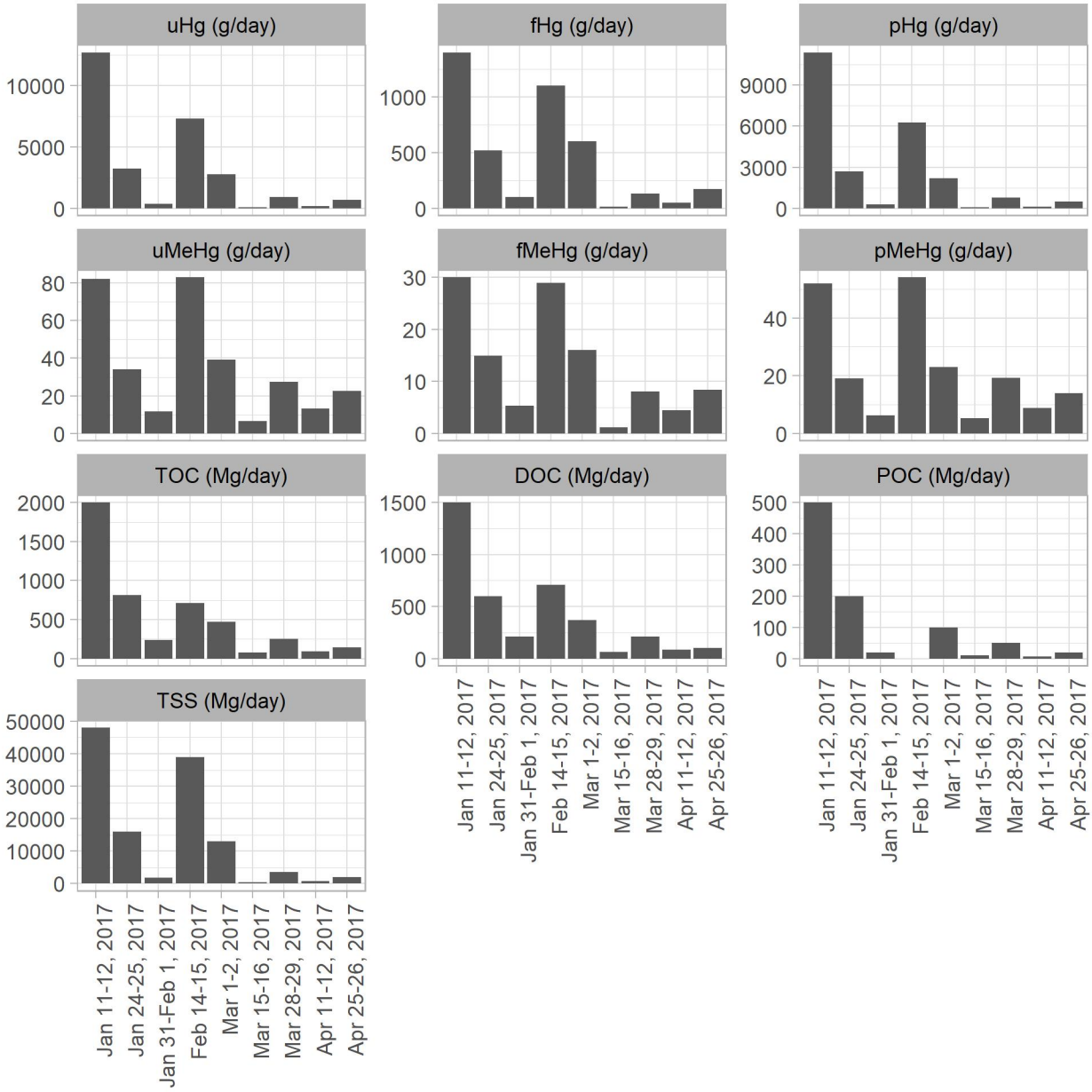

On average, the upper reach of the Yolo Bypass was a net sink for all fractions of Hg and a net source for all fractions of MeHg (Table 3-7). The net load of uHg deposited in the upper reach of the Yolo Bypass was predominately in the particulate form (~99%), while approximately 60% of the net uMeHg load was in the particulate form (Table 3-7). While the upper reach was a net sink for TSS and TOC, it was a net source of DOC.

Internal MeHg production in the upper reach of the Yolo Bypass resulted in a substantial increase in uMeHg loads exiting the Stairsteps. On average, 36 ± 29 g/day was exported from the upper reach of the Yolo Bypass. Of this, on average, 22 ± 23 g/day or 61% came from tributary inputs while, on average, internal production added an additional 14 ± 8.1 or 39%.

As with input loads, high levels of uncertainty reflect the large changes in flow used to calculate loads and are not indicative of the variability associated with the sampling of a single location or event. Calculations of the uncertainty associated with load measurements provides a means to evaluate the strength of mass balance calculations that indicate a reach is a net source or sink for a parameter. It should be noted that the net loads of all fractions of Hg within the entire Bypass had percent differences less than their measurement uncertainty of 11% making them inconclusive (Table 3-7). The percent difference of a net load quantifies the proportion of the load produced or retained within the system in relation to the load entering the system. Percent differences should be greater than the measurement uncertainty of the load values for their associated net loads to be conclusive.

.

Table 3-7 **Average Loads ± 1 std. dev. and Percent Differences for Hg Species (g/day) and other Water Quality Parameters (Mg/day) Entering and Leaving the Yolo Bypass for 9 Sampling Events in WY 2017**

Parameter	Input Load	Output Load (at Stairsteps)	Output Load (Below Liberty Island	Net Load-Upper Reach (Stairsteps - Input)	Percent Difference Upper Reach	Net Load Lower Reach (Below Liberty Island - Stairsteps)	Percent Difference Lower Reach	Net Load-Entire Bypass	Percent Difference Entire Yolo Bypass
uHg	3,500 ± 4,800	3,100 ± 4,300	3,700 ± 5,200	-320 ± 530	-9.2%	190 ± 810	5.5%	-170 ± 550	-4.3%
fHg	500 ± 600	450 ± 490	520 ± 580	-8 ± 100	-1.7%	26 ± 110	5.2%	20 ± 100	3.3%
pHg	3,000 ± 4,200	2,700 ± 3,800	3,200 ± 4,600	-320 ± 480	-11%	160 ± 690	5.2%	-200 ± 490	-6.0%
uMeHg	22 ± 23	36 ± 29	42 ± 41	14 ± 8.1	63%	3.7 ± 12	10%	18 ± 19	75%
fMeHg	7.7 ± 7.3	13 ± 10	17 ± 13	5.4 ± 3.4	70%	2.9 ± 4.1	21%	8.6 ± 6.9	101%
pMeHg	14 ± 16	22 ± 19	25 ± 29	8.6 ± 6.0	62%	0.49 ± 12	2.0%	9.3 ± 14	60%
TOC	500 ± 700	540 ± 620	670 ± 780	-4 ± 60	-0.7%	83 ± 160	14%	70 ± 100	12%
DOC	400 ± 500	400 ± 400	500 ± 500	10 ± 60	2.3%	30 ± 70	6.7%	40 ± 40	8.3%
POC	100 ± 200	100 ± 200	200 ± 300	-20 ± 50	-17%	40 ± 100	33%	10 ± 70	10%
TSS	20,000 ± 30,000	14,000 ± 18,000	20,000 ± 28,000	-7,000 ± 10,000	-34%	4,200 ± 10,000	27%	-3,600 ± 3,200	-15%

Table Note: Net loads at the Stairstep sampling sites plus the net loads below Liberty Island do not sum to the net loads exported from the Yolo Bypass because no samples were collected below Liberty Island on the April 11, 2017 sampling event.

All values are reported to appropriate significant digits. Average load calculations may not sum exactly based on individual event loads being either negative or positive and the use of significant figures.

Positive net load values represent net internal production and negative values represent loss within the segment. The percent differences of the net loads for the Upper Reach and Entire Yolo Bypass were calculated by dividing the average net loads by their associated average inlet loads. The percent differences of the net loads for the Liberty Island Reach were calculated by dividing the average net loads by their associated average outlet load measured at the Stairsteps location. Calculations for the Liberty Island Reach and the Entire Yolo Bypass exclude the April 11, 2017 sampling event because samples were not collected below Liberty Island during this event. Therefore, the net loads from the Upper and Liberty Island Reaches do not sum to the net loads exported from the Entire Yolo Bypass.

The partitioning between the filter-passing and particulate net MeHg loads from the upper reach changed through the course of the 2017 flood event. Net fMeHg loads were greater than the net pMeHg loads during the first two sampling events in 2017 (Figure 3-13, suggesting that diffusion of fMeHg from sediment porewater was the more influential source of MeHg at the start of the flood. The particulate fraction became the larger contributor to the net MeHg loads during the remaining seven sampling events in 2017 covering the last 3 months of the flood (Figure 3-13). Moreover, the MeHg concentration on solids, which provides an estimate of the amount of MeHg bound to the suspended sediment, increased at the three Stairsteps locations during the last four sampling events in 2017 (Figure 3-14). This hints that suspended organic and inorganic particles enriched with MeHg became the more important source of MeHg during the latter half of the flood. Additionally, as shown in Figure 3-15, the upper reach transitioned from a net sink to more of a net source of Volatile Suspended Solids (VSS) during the last three months of the flood. A measurement of VSS provides an estimate of the amount of organic material suspended in the water. Together, this suite of evidence points to an organic source for this end of season pMeHg.

Figure 3-13 Net Internal Production of Filter-Passing and Particulate Methylmercury within the Upper Reach for Sampling Events in 2017

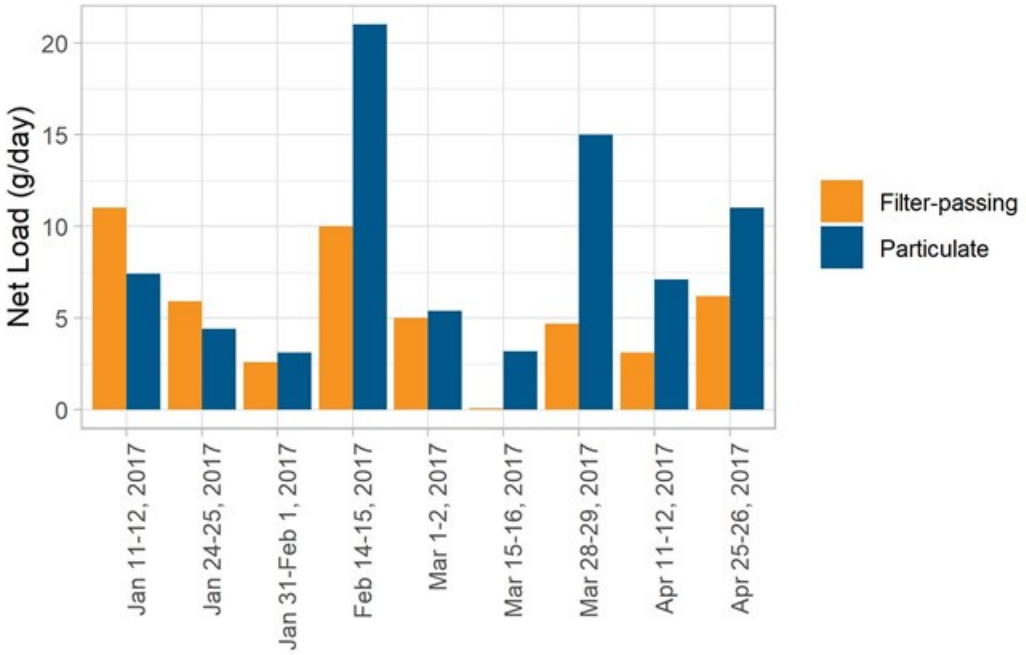

Figure 3-14 Methylmercury Concentrations on Solids at the Three Stairsteps Locations for Sampling Events in 2017

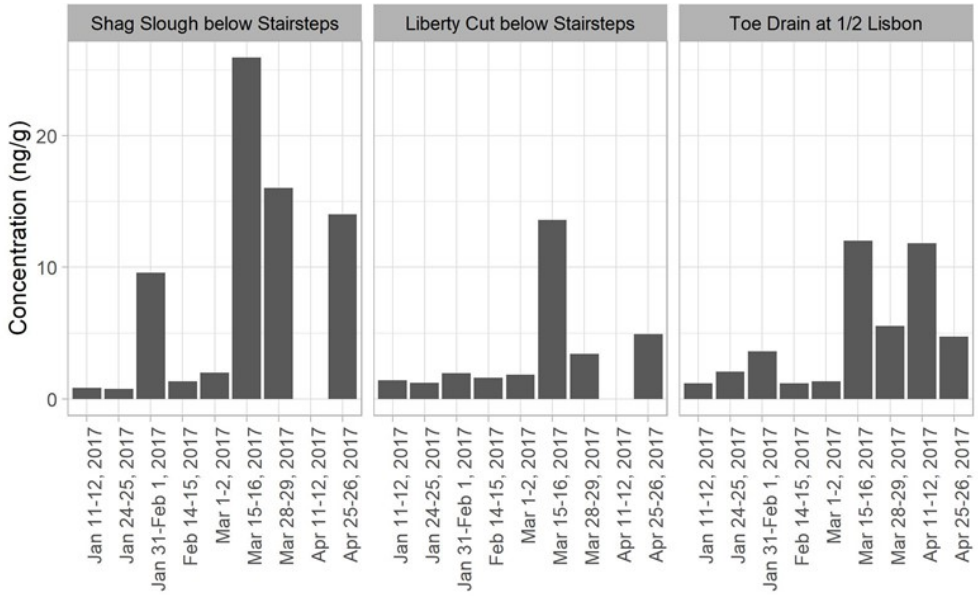

Figure 3-15 Net loads of Volatile Suspended Solids Within the Upper Reach for Sampling Events in 2017

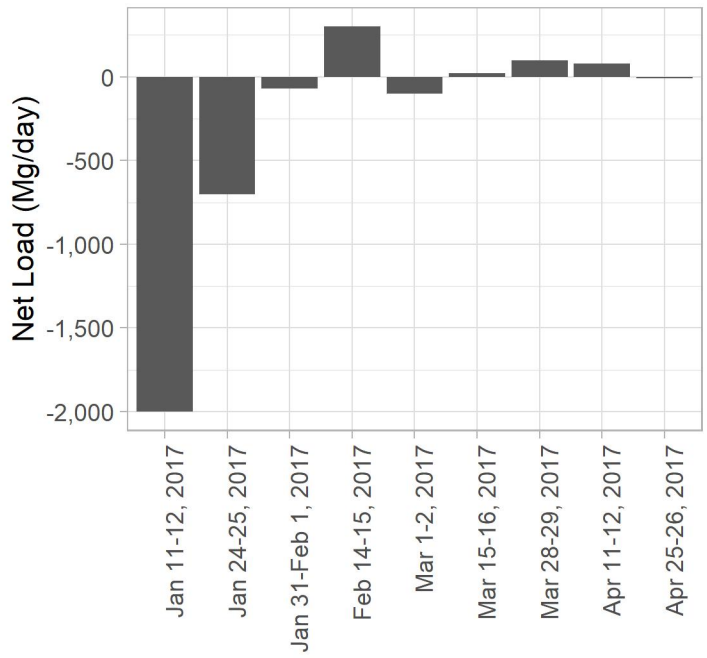

Figure Note: Negative values indicate a net sink. Positive values indicate a net source.

Net internal production of MeHg within the Yolo Bypass significantly increased as inflows increased particularly with fMeHg and uMeHg. The strongest positive correlation was observed with fMeHg within the upper reach where Yolo Bypass inflow explained 84% of the variation in the internal production of fMeHg (Figure 3-16). In contrast, total inflow to the Bypass did not have a significant effect on the internal production of pMeHg within the upper reach (R^2 = 24%, p = 0.18). The strong positive relationship between inflow and the net internal production of fMeHg suggests that diffusion of fMeHg from sediment porewater is the process most affected by increasing inflow and inundated land.

Foe and others (2008) also documented a significant increase in net uMeHg production in the upper reach of the Yolo Bypass, however, the net internal MeHg relationship developed from our mass balance study was lower than that developed by Foe and others (2008) (Figure 3-17). Several lines of evidence suggest that the relationship developed by the two studies cannot be compared directly, and that similarities as well as differences exist. First, the four highest flows in WY 2017 occurred when the gates to the Sacramento Weir were open. Sacramento weir gates were not open in the Foe and others (2008) study. Second, in this study, the entire winter flood event, from January to April, was sampled, however, Foe and others (2008), collected samples exclusively in the spring from the beginning of March to the end of May. This difference in the timing of sample collection could be important since the spring months tend to have warmer water temperatures, which can increase mercury methylation rates. Third, the 2006 and 2017 sampling events had very different hydrographs. The Yolo Bypass flooded extensively twice during the 2006 wet season: from the end of December 2005 to the middle of February 2006, and from the beginning of March to the beginning of May 2006. In contrast, the 2017 flood consisted of one extended flood event from the beginning of January to the beginning of May 2017. These differences may have impacted Mg cycling. The two studies showed similar relationships between net internal MeHg production with flow once the four data points associated with the highest flows of the Sacramento Weir contributions are removed. Similarly, the two sampling events from WYs 2014 and 2016 of this study fall along the originally developed regression line calculated by Foe and others (2008).

Based on information provided in Table 3-7 Figure 3-18 provides a conceptual mass balance model for uMeHg loads for the Upper Reach of the Yolo Bypass for the nine sampling events in WY 2017.

Figure 3-16 Relationship between Net Internal Loads (Source or Sink) of Mercury (Filtered, Particulate and Total), Methyl Mercury (Filtered, Particulate and Total), and Total Suspended Solids to Total Water Inflow for the Upper Reach in the Yolo Bypass for Sampling Events in 2017

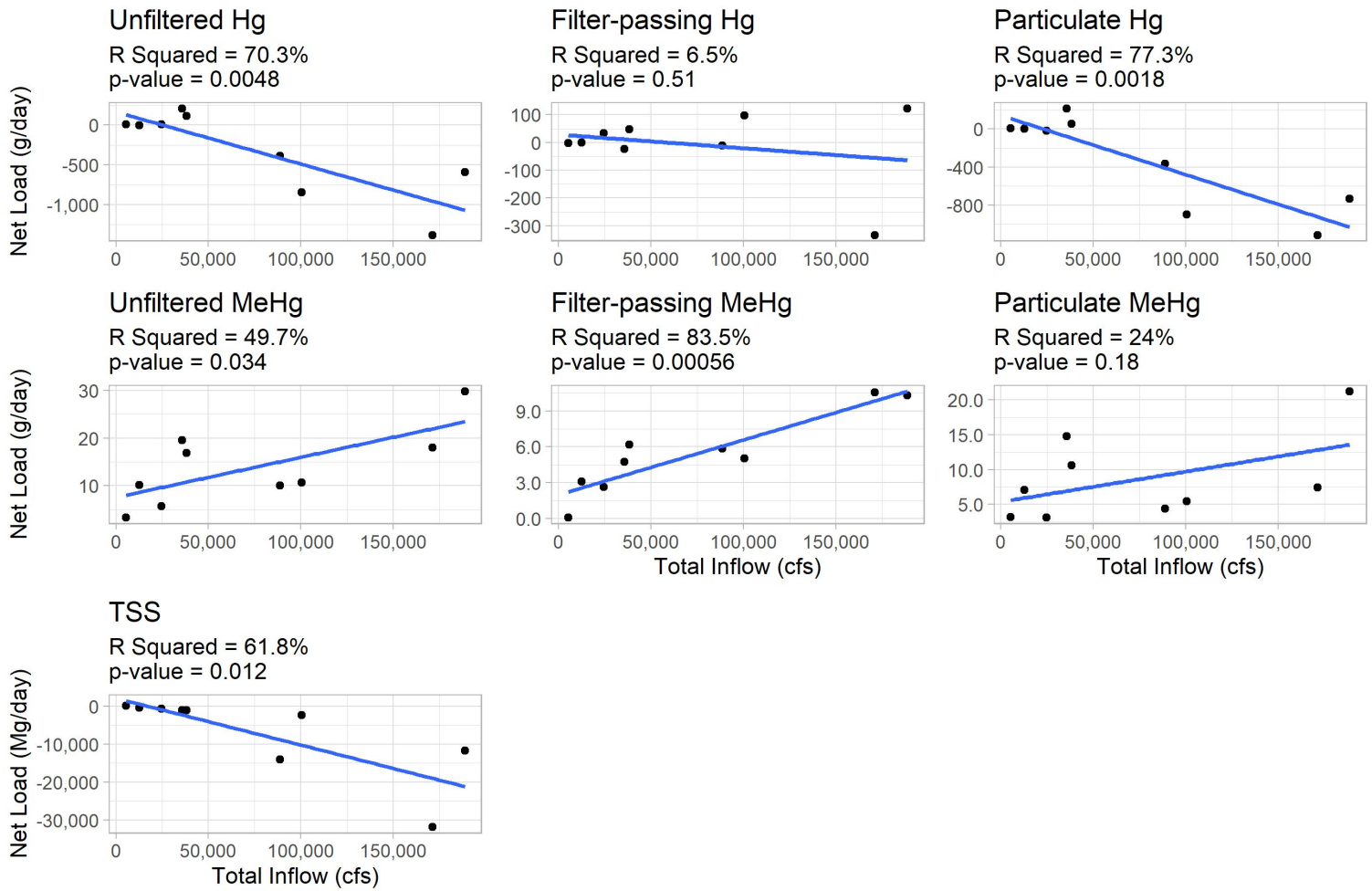

Figure 3-17 Comparison between Total Tributary Inflow and MeHg Loads Exported for Samples Collected in 2006 by Foe and others, (2008) and this Study (Water Years 2014, 2016 and 2017)

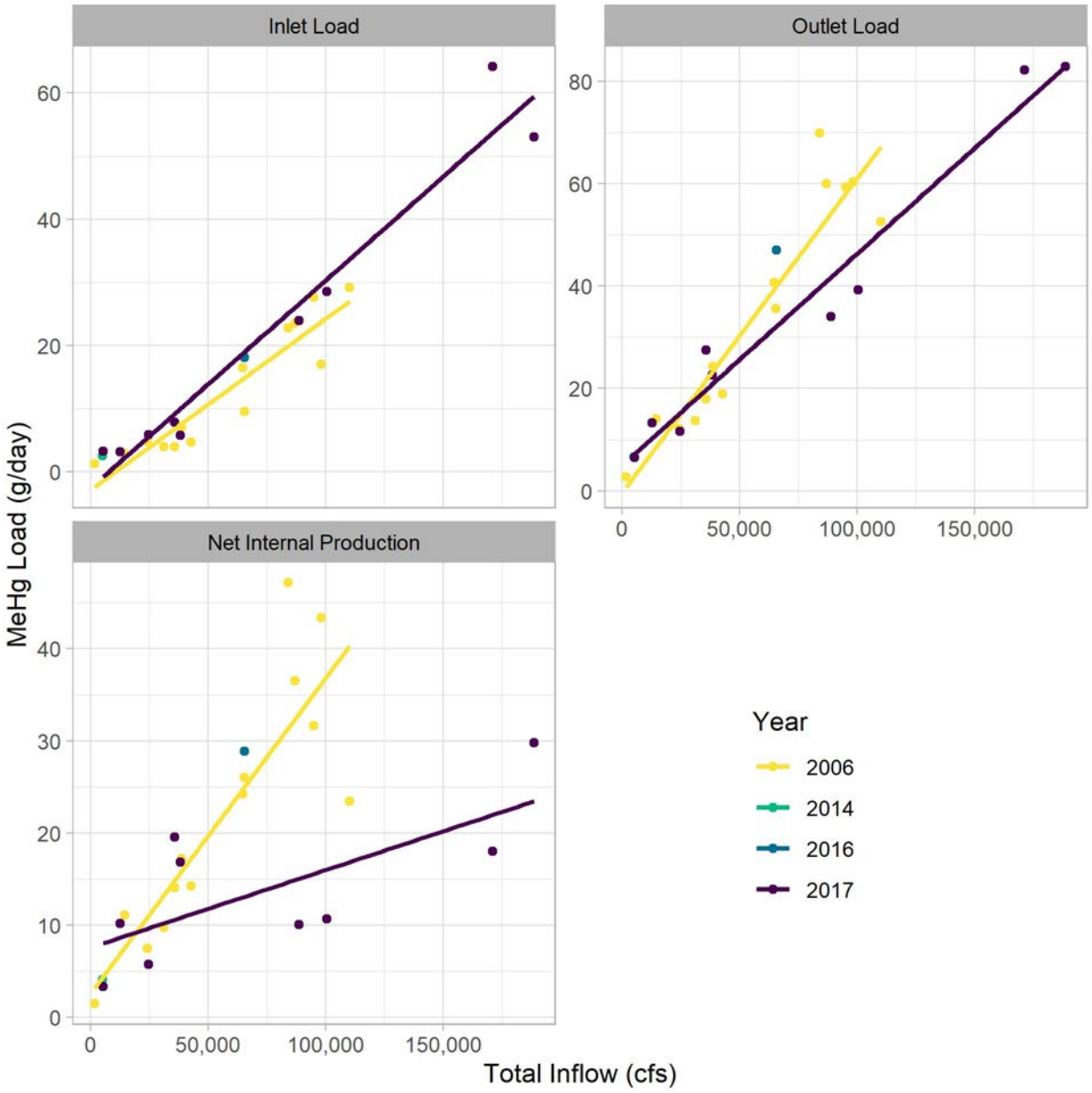

Figure 3-18 Mass Balance of Average Net uMeHg loads (in g/day ± 1 std. dev.) for Tributary Inputs and Loads Leaving the Yolo Bypass at the Stairsteps for WY 2017

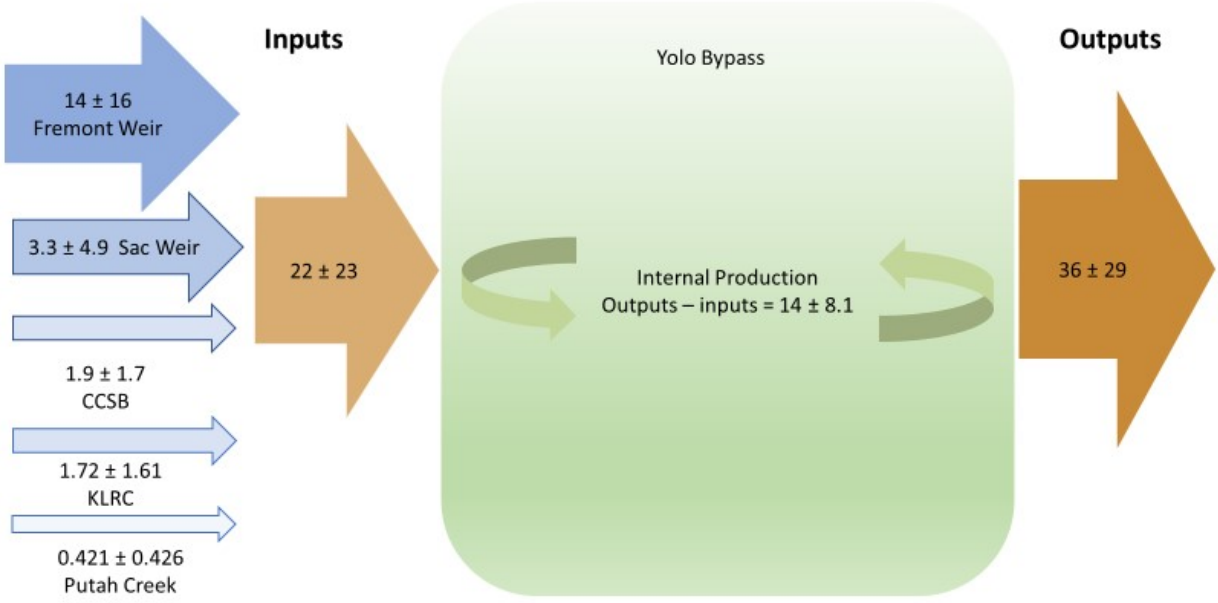

Figure Note: Input calculations included zero flows for Fremont and Sacramento Weirs. Outputs are the sum of discharges from the Toe Drain at Half Lisbon, Liberty Cut and Shag Slough below the stairsteps. High levels of uncertainty reflect the large variability in flows across the sampling events and not the uncertainty associated with load determination for a single location and event.

Upper + Lower Reach

Sampling below Liberty Island provided an overall picture of the loads exiting the full Yolo Bypass and an evaluation of Liberty Island contributions. Of the analytes listed in Table 3-7, Liberty Island, on average was always a net source. This contrasted with net production in the upper reach, which depending on the analyte, could, on average, be either a source or a sink. On average, Liberty Island contributed 16 percent to the uHg loads exported from the full Yolo Bypass and 14 percent of the export load of uMeHg leaving the full Yolo Bypass (Table 3-7). The lack of wetting and drying cycles may help explain the lower levels of uMeHg. Overall, 86% of the MeHg produced in this reach in 2017 was in the filter-passing fraction, which is much different than what occurred in the upper reach and the entire Yolo Bypass. It should be noted that the net loads of all fractions of Hg as well as uMeHg and pMeHg within the Upper Reach had percent differences less than their measurement uncertainty

As shown in Figure 3-19, the Liberty Island reach was consistently a source of fMeHg in all but two sampling events in 2017 (January 31st and March 15th), which were two events with some of the lowest inflows. The largest MeHg contributions from Liberty Island occurred during the large flow events associated with the first flush and mid-February with increased mobilization of particulates enriched with Hg and MeHg (data not shown, see Technical Appendix B). These results imply that the magnitude of the flood event in terms of flow may influence whether the Liberty Island reach is a source or sink of fMeHg and pMeHg with possibly different thresholds for each fraction.

Figure 3-19 Net Loads for the Entire Yolo Bypass Subdivided by Reach for Each Sampling Event

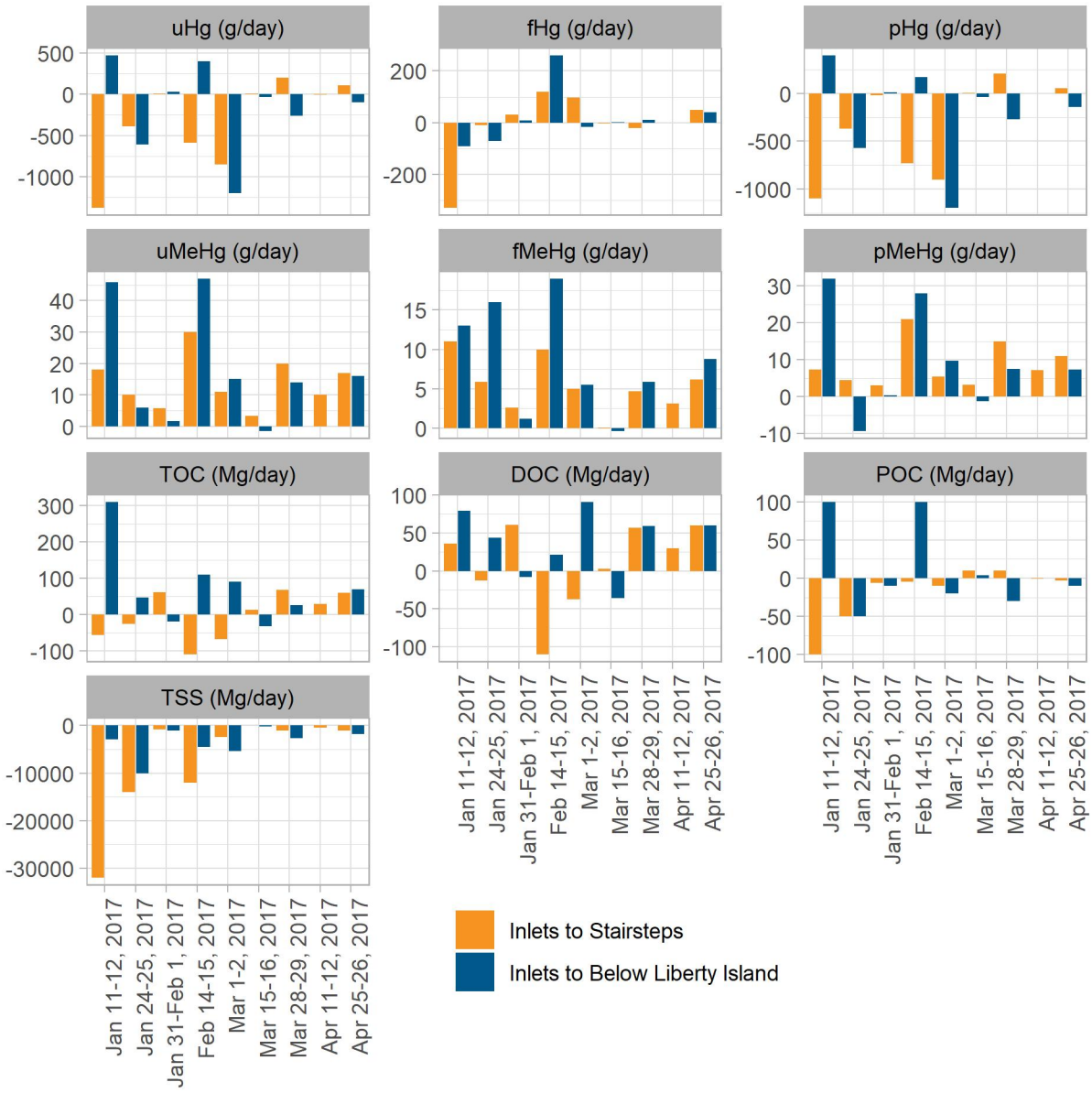

The conceptual model illustrated in Figure 3-20 extends the mass balance model for uMeHg loads to include the lower reach for nine events. There were eight sampling events in WY 2017 which were sampled both below Liberty Island and at the Fremont Weir. Most of this net internal production of uMeHg occurred in the Upper Reach between the inlets and the Stairsteps which supplied 79% of the total amount produced within the Bypass.

Figure 3-20 Mass Balance Model of Average Net uMeHg Loads Entering and Leaving the Entire Yolo Bypass Showing Net Internal Production at the Stairsteps and Liberty Island for Water Year 2017

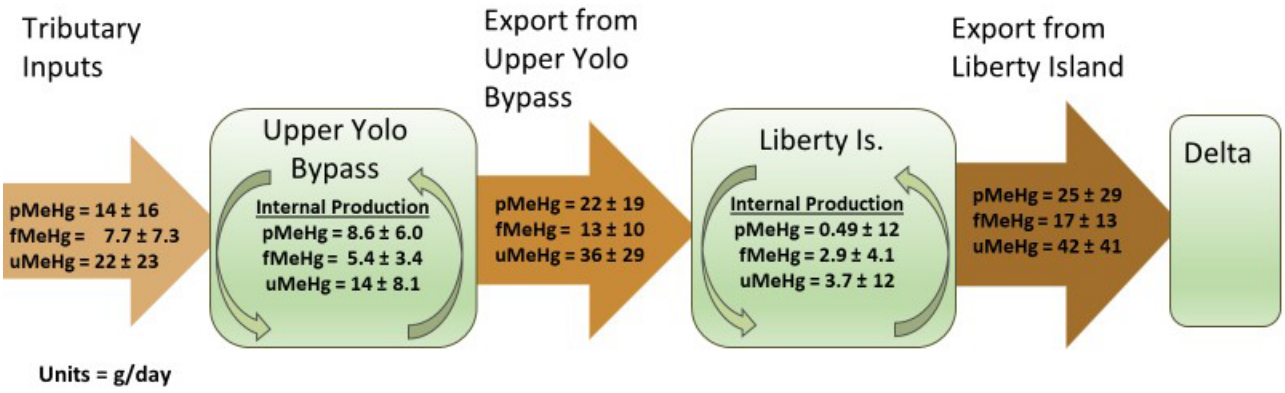

Figure Note: Inputs to the upper Yolo Bypass are the sum of averaged tributary inputs entering the upper reach of the Yolo Bypass. Export from the upper Yolo Bypass (at the Stairsteps) are the sum of average loads from the Toe Drain at Half Lisbon and Liberty Cut and Shag Slough below the Stairsteps. The difference between exports of the upper reach from the lower reach do not equal the calculated net production for Liberty Island for two reasons (1) the upper reach export loads are based on nine sampling events. Export loads exiting below Liberty Island are based on eight sampling events, and (2) there were both positive and negative net uMeHg loads determined for Liberty Island sampling events (see Figure 3-19).

Internal Methylmercury Production in the Upper Reach of the Yolo Bypass

As documented by our mass balance study and by Foe and others (2008), the upper reach of the Yolo Bypass is a net producer of MeHg. Identifying the drivers associated with this internal production is an essential step towards a BMP. To the extent possible, we used our field and laboratory studies to evaluate this data gap. These studies were: (1) the sediment-water exchange flux; (2) the sediment erosion studies (using Gust erosion chamber deployments); and (3) the laboratory and field-based mesocosm vegetation studies. The work focused primarily on the upper reach of the Yolo Bypass.

Sediment as a Source of Mercury

The DMCP defines sediment-water flux to flood water as the source of MeHg in open waters (CVRWQCB, 2011). Previous investigations have also shown this flux to be important (Choe and others, 2004; Heim and others, 2007). The importance of this source was investigated by conducting laboratory studies of sediment-water flux using intact cores to determine the diffusive flux of fMeHg and fHg from several different land use types. The objectives of the sediment-water flux study were to: 1) provide flux rates, for fMeHg for land use types found within the Yolo Bypass; 2) estimate loads of fHg and fMeHg from sediments by land use type and for total area of the Yolo Bypass; 3) estimate the importance of the sediment water exchange in controlling water column concentrations for fHg and fMeHg relative to other process; and 4) provide data useful to setting up and calibrating the D-MCM. Photos showing details of part of the experiment are shown in Figure 3-21. The location of core sample collection to evaluate the sediment-water flux associated with different land uses is shown in Figure 3-22. Details on sample collection, sample processing and data analysis can be found in Technical Appendix C.

Figure 3-21 Photos of A) Intact Sediment Cores Collected from Wild Rice Field in the Yolo Bypass. B) Pore Water Extraction from Sectional Cores Conducted in Glove Box Under Nitrogen

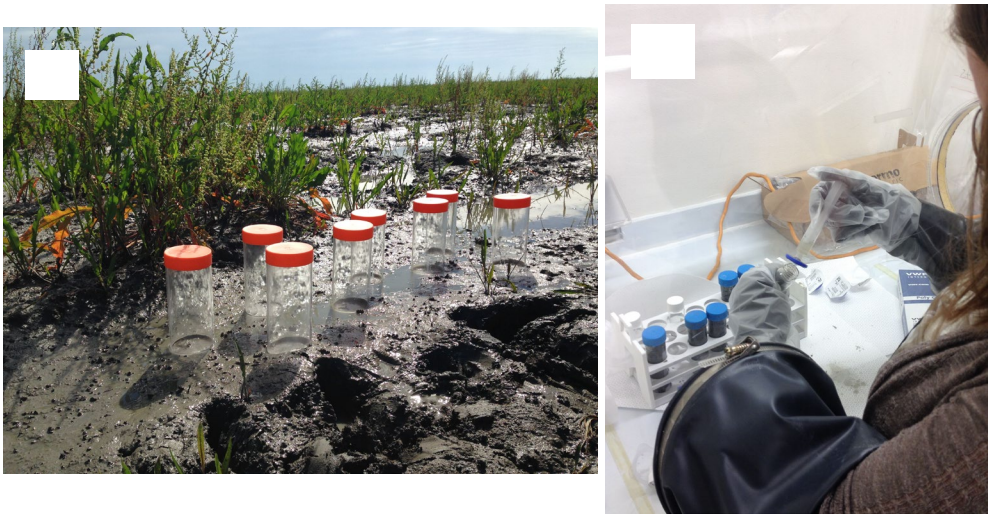

Figure 3-22 Location of Sample Collection Sites for Laboratory Sediment-Water Flux Experiments.

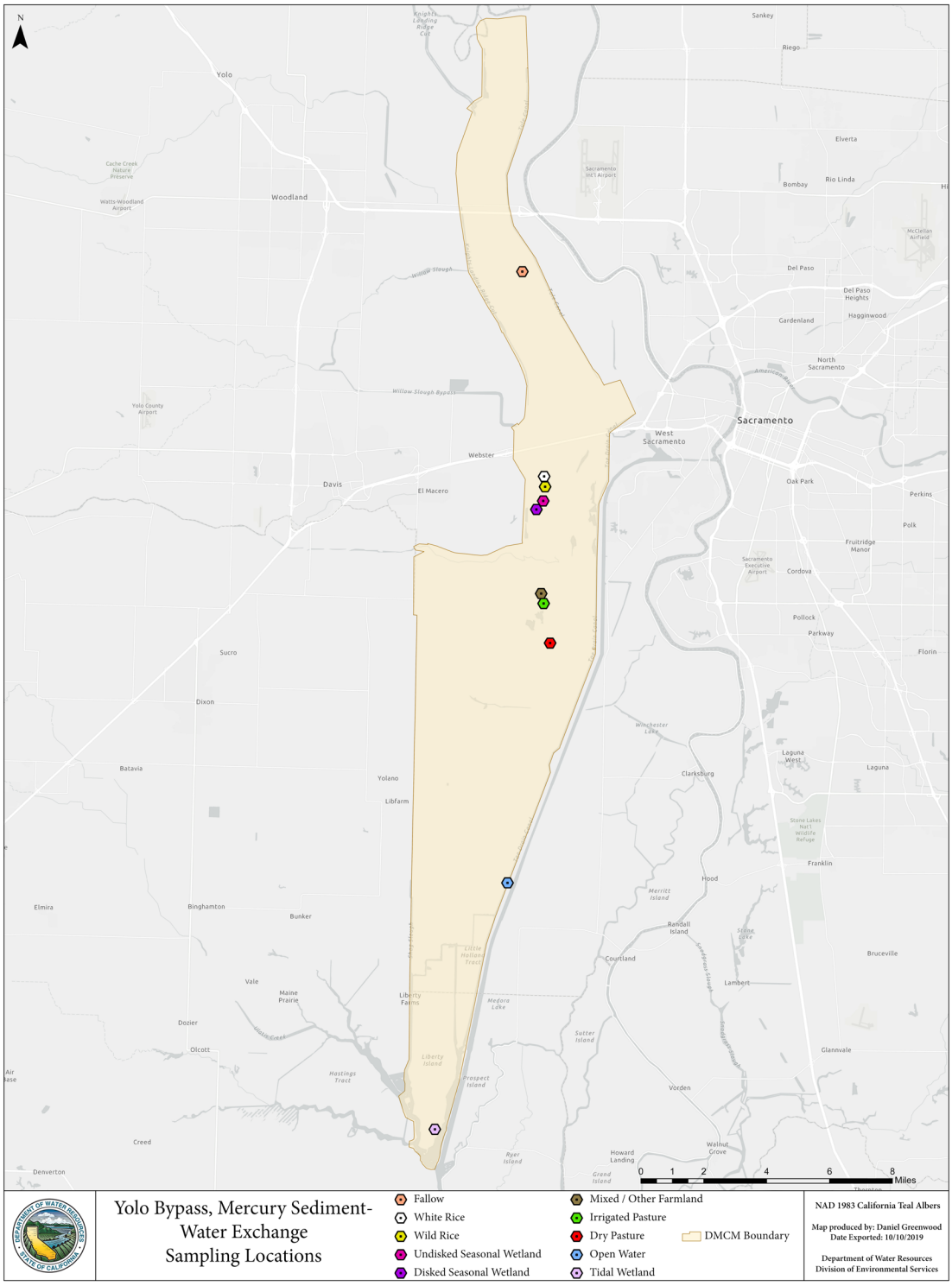

Sediment-water Hg and MeHg Flux

Sediment-water fluxes were determined using two approaches - direct measures of the concentration with time of fHg and fMeHg in overlying water from intact sediment cores and diffusional fluxes estimated from interstitial pore water and overlying water gradients. Results shown in this section reflect direct measurements from incubated cores as this approach captured both advective and diffusional components of Hg sediment-water fluxes thus represented the maximum for introduction of Hg and MeHg from sediments into the Yolo Bypass. Results from both approaches can be found in Technical Appendix C.

Results for fHg and fMeHg were highly variable between land use types (Table 3-8). The largest negative (into sediments) fluxes of fHg and fMeHg were observed in the permanently wetted land uses: -open water and tidal wetland sites. There was generally good agreement in the direction of fHg and fMeHg flux for all land use types with the exception being agricultural land used for white rice cultivation which showed flux into the sediment for fHg and flux out of the sediment for fMeHg. The largest fMeHg fluxes out of the sediments (>20 ng m^{-2} d^{-1}) were observed in seasonal wetland, fallow, and irrigated pasture lands. The range of fMeHg and fHg fluxes observed in this study are similar to those previously reported for open water and wetlands during late winter and spring in the Sacramento Bay-Delta, the Yolo Bypass, and other locations previously studied (see for example Choe and others, 2004, Mason and others, 2006 and Covelli and others 1999).

Table 3-8 **Sediment-Water Exchange Fluxes for fMeHg and fHg Determined Using Intact Core Incubations Collected from the Yolo Bypass with Overlying Water from the Sacramento River.**

Land Use	fMeHg Flux (ng m^{-2} d^{-1})[1]	fHg Flux (ng m^{-2} d^{-1})[1]
Irrigated Pasture	55.3 ± 20.3	114 ± 51.3
Fallow	28.6 ± 13.8	352 ± 140
Undisked Seasonal Wetland	25.8 ± 6.33	159 ± 25.7
Disked Seasonal Wetland	25.7 ± 8.93	156 ± 44.9
Non-irrigated Pasture	12.1 ± 3.9	150 ± 22.1
White Rice	8.91 ± 4.85	-97.4 ± 44.1
Mixed/Other Farmland	3.57 ± 6.76	203 ± 75.8
Wild Rice	2.97 ± 3.50	58.1 ± 29.7
Tidal Wetland	-3.65 ± 2.48	-621 ± 295
Open Water	-10.9 ± 8.95	-218 ± 132

Table Notes: Negative values indicate flux into the sediment. Values are the average ± 1 standard deviation of 4 cores.

Mercury and MeHg in Interstitial Pore Water

Interstitial pore water concentrations of fHg and fMeHg in surficial (0-2 cm) sediment by land use types are shown in Figures 3-23 and 3-24. Surficial pore water concentrations of fHg was highly variable and ranged from 6.53 to 125 ± 41 ng/L. Mean Sacramento River water uHg concentration was 1.75 ± 1.02 ng/L and porewater fHg concentrations were a factor of 3-71 times higher, indicating that there was a positive diffusive flux out of the sediments at all sites. Mean surficial pore water fMeHg concentrations ranged from 0.109 ± 0.037 to 20.3 ± 5.36 ng/L. The lowest fMeHg concentrations were observed in tidal wetlands, fallow, agriculture lands (the exception is wild rice fields) and open water. The highest pore water fMeHg concentrations were observed in seasonal wetlands, wild rice fields, and pasture land.

Porewater fMeHg concentrations were positively correlated with porewater DOC concentrations (data not shown, see Technical Appendix C).

Figure 3-23 Mean Interstitial Pore Water fHg Concentrations in Surficial (0-2 cm) Sediment from Several Land Use Types in the Yolo Bypass

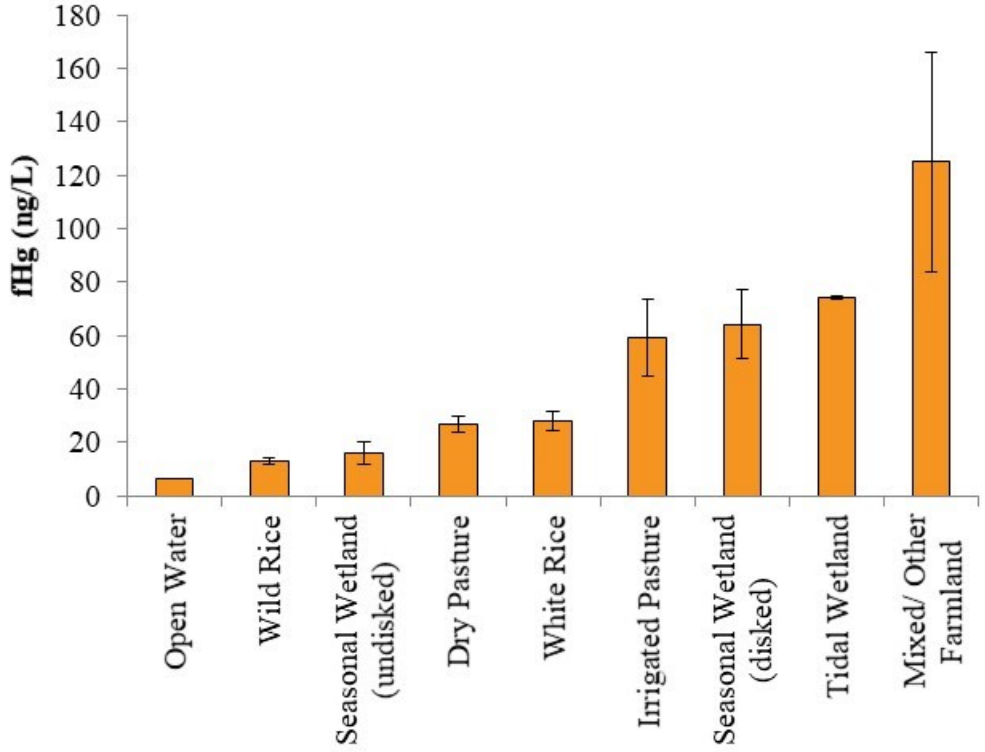

Figure Note: Pore water was isolated from intact sectioned cores under anoxic conditions. Error bars represent the standard deviation of triplicate field replicates

Figure 3-24 Mean Interstitial Pore Water fMeHg Concentrations in Surficial (0-2 cm) Sediment from Several Land Use Types in the Yolo Bypass

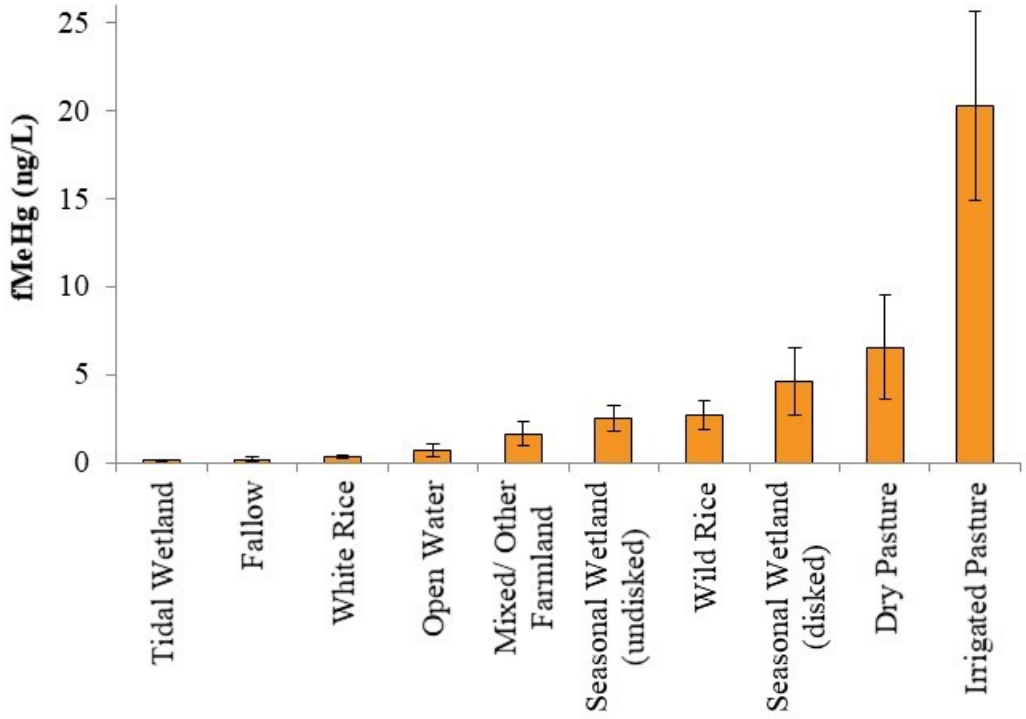

Figure Note: Pore water was isolated from intact sectioned cores under anoxic conditions. Error bars represent the standard deviation of triplicate field replicates

Sediment-water Exchange Loads to the Yolo Bypass

Estimation of fHg and fMeHg loads to the Yolo Bypass from sediment-water exchange for several land use types are given in Figure 3-25. The sediment-water exchange fluxes for the various land use types was scaled up to the land uses in the Yolo Bypass using the acreages in the D-MCM model. There are a number of uncertainties associated with this extrapolation, however, if the land use areas are correct and if the measured sediment water exchanges are representative of field conditions, then the fMeHg sediment-water exchange load to the Yolo Bypass is estimated at 5.04 ± 1.56 g/day. The greatest loading occurred from the two largest land uses in the upper reach of the Yolo Bypass—irrigated pasture and seasonal wetlands. This sediment-water exchange loading agrees remarkably well with the average fMeHg net load of 5.4 g/day determined from our Yolo Bypass mass balance study for the upper reach of the Yolo Bypass (Table 3-7).

Figure 3-25 Estimation of fHg and fMeHg Loads to the Yolo Bypass from Sediment-Water Exchange for Several Land Use Types

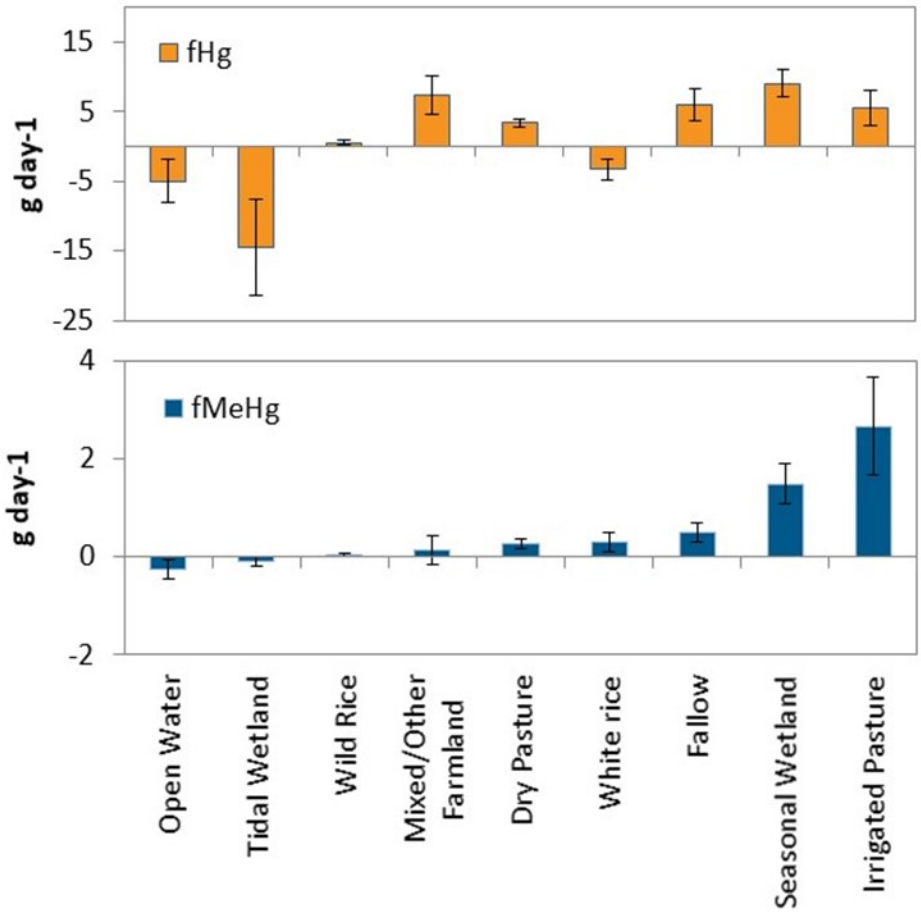

A conceptual model of the contribution of the filter-passing fraction of the sediment-water exchange load to the overall mass balance of uMeHg in the upper reach of the Yolo Bypass is depicted in Figure 3-26. If this sediment-water exchange flux for open water areas of the Yolo Bypass is representative of contributions from inundated Yolo Bypass sediments, then approximately 36% of the net internal production in the upper Yolo Bypass is accounted for via a sediment-water exchange flux of fMeHg. This leaves approximately 9 g/day of internal production of uMeHg unaccounted for. Two potential sources which have not yet been reliably quantified are erosion and resuspension of particles (see next section of this report). Quantification of these sources remain a gap in our knowledge of Hg transport and behavior in the Yolo Bypass. Another interpretation of this modelling effort is that there are other unidentified sources that contribute to the internal production of MeHg in the Yolo Bypass.

Figure 3-26 Contribution of fMeHg from Sediment-water Exchange in Open Water to the Mass Balance of Average uMeHg loads Entering and Leaving the Upper Yolo Bypass (WY 2017) and Unaccounted Masses

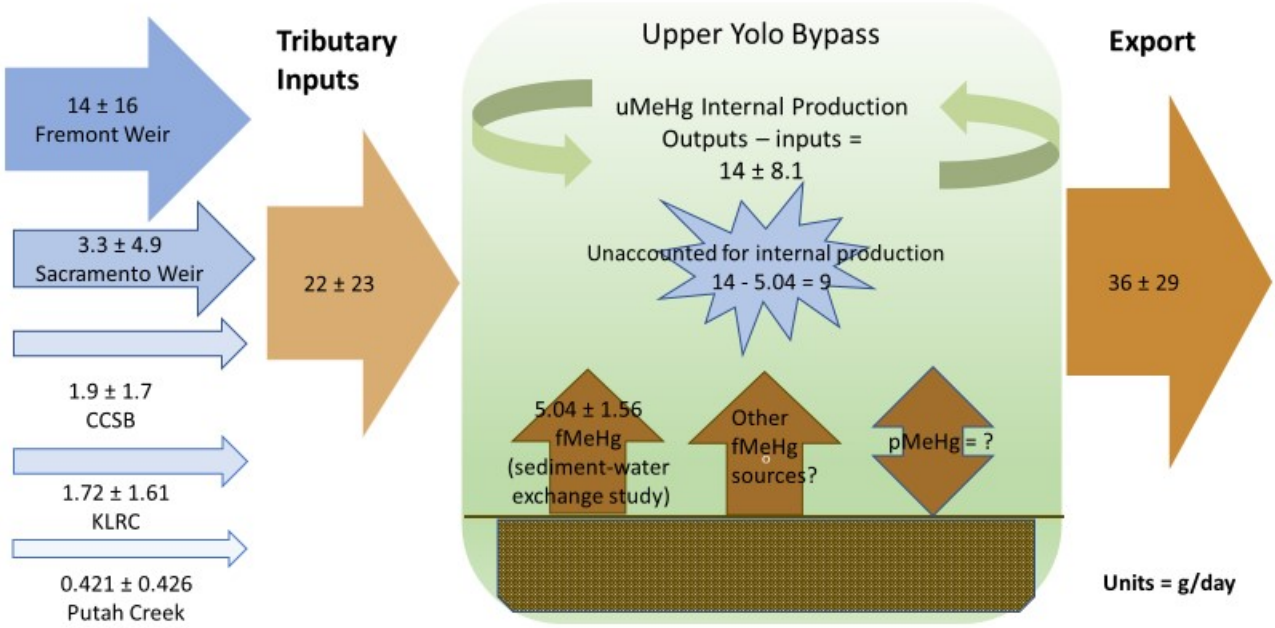

Figure Note: Outputs are the sum of average loads from the Toe Drain at Half Lisbon, Liberty Cut and Shag Slough below the stairsteps. Units are g/day ± 1 standard deviation.

It is important to point out that there are significant uncertainties associated with upscaling the sediment-water flux experiment results to determine MeHg loads for the Yolo Bypass. Uncertainties associated with this upscaling include, 1) accuracy of the base layer GIS map used to scale up for land use types, 2) assumptions that laboratory-based sediment-water exchange measurements with intact cores are representative of field conditions, 3) that short term (~24 hr) laboratory flux measurements are representative of inundation periods of days to weeks, 4) uncertainty in the experimental values, and 5) there is a paucity of sediment-water exchange measurements with which to make the load prediction. Additionally, sediment-water flux was measured over a short time-period whereas this figure assumes that the sediment-water flux remains constant over time. This assumption may not be correct and requires further laboratory experiments. Nevertheless, as a rough screening tool, these extrapolations provide a starting point to quantify sediment water exchange loads as well as useful relative comparisons to identify which land use types are most important in fluxes from the sediment and help to point to where refinement is needed.

Sediment Erosion

Erodibility of surface soils associated with different land use types in the Yolo Bypass was determined using a Gust erosion chamber. The Gust chamber subjects a core of sediment, extracted from the field, to controlled flow speeds arising from rotating flow inside a circular cylinder. The test erodes a very small

layer of surface sediment, typically less than a millimeter thick. The strength of the soil within this layer typically increases with depth and the soil strength versus depth is measured. The two primary results of the test are: 1) critical shear stress required to initiate motion, and 2) a relationship between excess shear stress (actual minus critical) and erosion rate. Gust erosion chamber results were used along with hydrodynamic modeling to predict erosion from different land use types in the D-MCM model. Evaluating erosion by land use type provides insight into the relative contribution of particulates, however, it doesn't provide information on deposition and resuspension of particles. Note that one limitation of the approach taken is that redeposition of the eroded sediments is not simulated. Another limitation is that only two cores were tested per land use. Results from one pair sometimes differed significantly, and there can also be large spatial gradients in erodibility within a given region or land use type.

Each of the major land use types in the D-MCM model were targeted for investigation of sediment erodibility using intact cores (Figure 3-27). Testing was performed in the field immediately after sample collection in the field (Figure 3-28). Erosion from irrigated pasture was tested with both intact vegetation and with the vegetation cropped closely to the soil level. Details associated with operation of the Gust Chamber and experimental results are given in Work and Schoellhamer, (2018) and in Technical Appendix D.

Erosion results for each land use type tested are presented as the initial critical shear stress at which erosion began (τ_{c0}) and the rate at which erosion increases as shear stress increases (Table 3-9). For the land use types sampled, irrigated pasture had the lowest critical shear stress, meaning that it required the smallest flow speed to initiate erosion. But in this case, the rate of increase of the resulting erosion, given higher flow speeds, was small suggesting that the thick vegetation in the unmodified irrigated pasture core resisted erosion. Similarly, the closely cropped core also featured miniscule erosion, likely because the roots helped protect the bed sediment from erosion (See Technical Appendix D). These results led to the recommendation that heavily vegetated areas be treated as unerodable in the D-MCM. The wild rice field sampled exhibited a higher critical shear stress, but also a much higher erosion rate, once the critical shear stress was exceeded. The erosion rate for wild rice was roughly three times greater than that for white rice. Of the land uses tested, the sediment tested from the Toe Drain was the most easily eroded.

Figure 3-27 Location of Sample Collections for the Gust Erosion Chamber Study

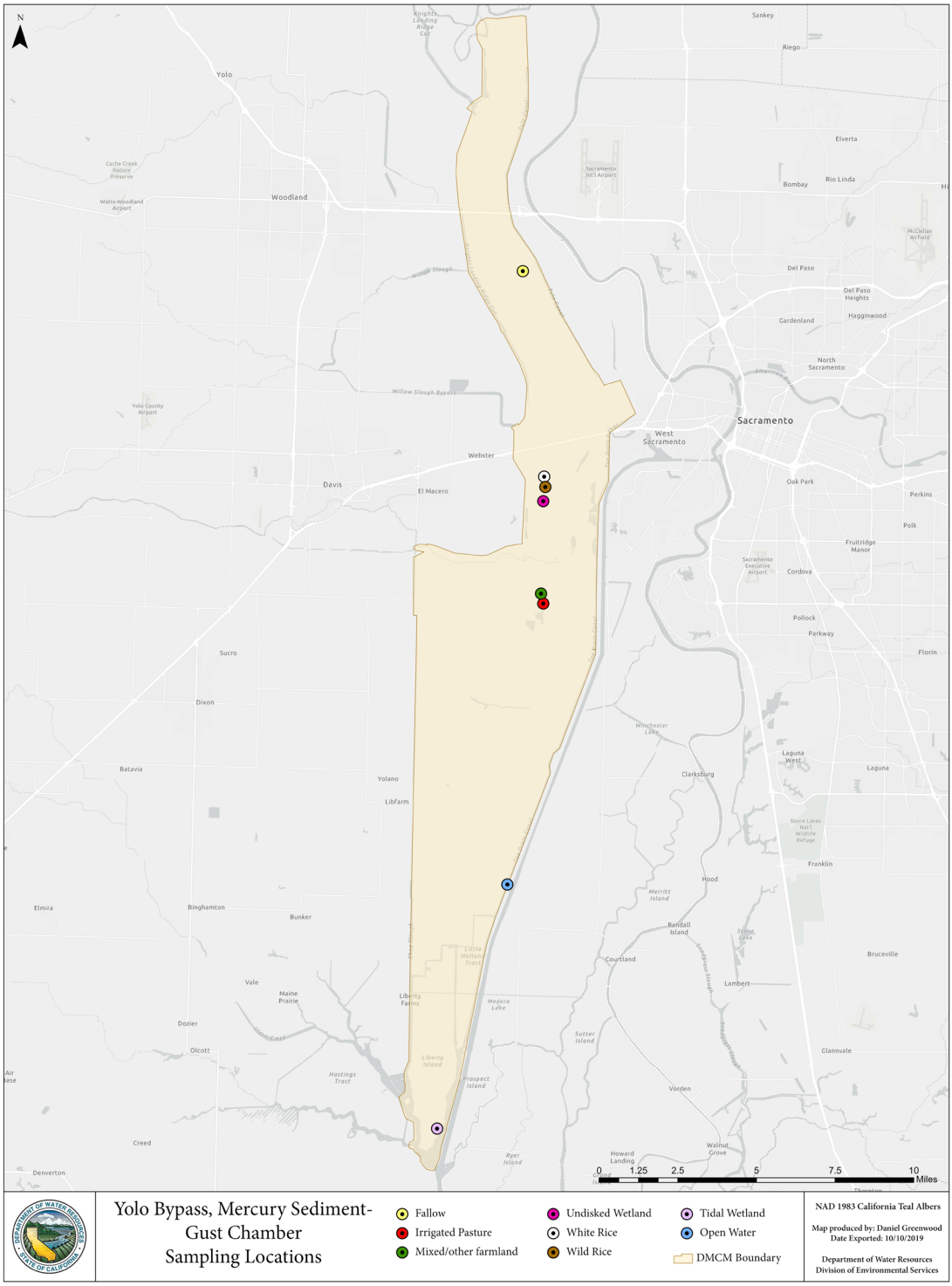

Figure 3-28 Photo of Sediment Erosion Study Experimental Setup in the Field Using Twin Gust Chambers (cylinders suspended above blue tub, lower right)

Table 3-9 **Gust Chamber Measurements of Initial Critical Shear Stress (τ_{c0}) and the Rate of Erosion Increase with Shear Stress ($dm/d\tau_c$) for Several Land Use Types in the Yolo Bypass**

Land use	Initial critical shear stress τ_{c0} (Pascal, Pa)	$dm/d\tau_c$, ($kg/m^2/Pa$)
Toe Drain	0.075	1.27
Wild rice	0.25	0.429
Disked wetland	0.25	0.321
Liberty Island	0.25	0.276
Row crop	0.125	0.207
Undisked wetland	0.1625	0.194
White rice	0.25	0.142
Fallow	0.175	0.0832
Irrigated pasture	0.03	0.0084

Table Note: Land use soils are listed in order of erodibility (highest first).

The Gust erosion chamber studies showed that erosion increased rapidly at the beginning of each shear stress step applied, and then decreased until the next increase in shear stress. This observation indicated depth limited erosion, with little erosion occurring after the initial erosion at each shear stress increase. These results suggest that unless the shear stresses of subsequent floodwaters are higher than antecedent floodwater shear stresses, little erosion occurs until a higher shear stress is encountered. This suggests that

erosion may have the most impact during first flush events, and events where the velocities exceed the velocities of the first flush event. Note that since erosion studies could not quantify deposition or resuspension of particles, these shear stress results do not apply to those situations. Th results of the Gust chamber study support the mass balance study in the Yolo Bypass, which showed a first flush event for a number of analytes, including uHg,

It is reasonable to assume that pMeHg contributions from erosion and resuspension would contribute to the remaining unaccounted production of 9 g/day uMeHg (Figure3-26), however, we lacked a robust approach to translate Gust chamber erosion results into pMeHg values as loads (as documented in DWR, 2015, efforts to use a Bale Chamber to translate Gust Chamber erosion values to pMeHg values were unsuccessful). Therefore, we were unable to add Gust Chamber results to continue to balance the mass in Figure 3-26.

The Role of Vegetation in the Production of Methylmercury in the Yolo Bypass

The lack of mass balance for the internal production of MeHg from sediment-water exchange and the inability to quantify sediment erosion and resuspension (see Figure 3-26) led the technical team to explore other possible internal sources. The role of standing winter vegetation as an internal source was identified as a potential source and a study was initiated to quantify this potential source.

Several lines of evidence suggested that organic matter might be an unaccounted MeHg source contributing to the internal production of MeHg in the upper Yolo Bypass. First, the mass balance study determined that fMeHg loads were the greatest at the start of the flood season, but during the remaining sampling events the particulate fraction became the largest contributor to net MeHg loads (Figure 3-13). As shown in Table 3-5 concentrations of filtered and particulate MeHg increased within the Upper Reach of the Yolo Bypass. Also, the concentration of MeHg per gram of solid rose 229% between the inlet and outlet sampling sites (Table 3-5). These lines of evidence suggest that particulate fractions increased over space and time and filtered fractions increased spatially from north to south. Second, the upper reach transitioned from a net sink to more of a net source of Volatile Suspended Solids (VSS) during the last three months of the flood (Figure 3-15). VSS provides an estimate of the amount of organic material suspended in the water. This would likely result from decomposing plant matter as the flood event progresses. Third, as flood water transited from the Fremont Weir to its exit from the upper Yolo Bypass at the Stairsteps, TSS becomes enriched in organic content as evidenced by the TOC/TSS ratio (Table 3-5). One explanation for this increase in the organic content of the TSS is that the vegetation in the Yolo Bypass is contributing organic particles to the flood waters as it decays over prolonged inundation. Additionally, our Mass Balance study showed that our lowest flow rates occurred in the last third of the extended flood season, therefore, erosion was potentially not a large influence on increases of MeHg on particles. This suggests that as organic material increased, erosion potentially decreased, suggesting that the logical source for this increase in MeHg is decaying plant material.

Due to the large extent of managed vegetated cover present on the Yolo Bypass in the winter, we examined the hypothesis that internal production of MeHg could occur through the inundation and subsequent decay of submerged vegetation. In addition to the data collected in the mass balance study, this hypothesis is supported by previous work in the Yolo Bypass which showed that agricultural rice straw is a labile carbon source that stimulates MeHg production (Marvin-DiPasquale and others, 2014)

and a number of literature studies that support the role vegetation plays in the generation of MeHg (see for example, Hecky and others, 1991, Kelley and others, 1997, Trembley and others 1998, for the role of vegetation in newly inundated reservoirs, Branfireun, 2000, for the role of decomposing plant litter effects on MeHg production, and Lambertsson and Nilsson (2006) who argued that organic matter is the primary driver of MeHg production).

One managed land use that remains vegetated in the winter is pasture, the largest areal land use as quantified in the Yolo Bypass D-MCM land use grid. Unlike rice fields and seasonal wetlands, pasture lands are fully vegetated when the Yolo Bypass floods. Therefore, these vegetated lands may potentially serve as another source of internal MeHg production in the Yolo Bypass. This hypothesis is supported by the significant loss of pasture vegetation after prolonged flooding in the Yolo Bypass (Figure 3-29). (Chris Rocco, Yolo Wildlife Area, Water Manager personal communication).

Figure 3-29 Photos of Sequence of Vegetation Loss in the Yolo Wildlife Area Due to Seasonal Flooding

Figure Note: (A) Non-irrigated Pasture in May 2016 Prior to the Large Flooding Events in the Winter of 2017 (B) Non-irrigated Pasture Prior to Winter Flooding (Fall 2017) (C) Non-irrigated Pasture in March 2017 After Flood Event

In the Yolo Bypass there are two approaches to management of pasture lands—irrigated and non-irrigated. Irrigated pasture is periodically irrigated throughout the spring, summer and fall until winter rains provide water. Depending on the mix of vegetation, these pastures generally have a live, standing crop of vegetative biomass year-round. In contrast, non-irrigated pastures rely on rainfall to provide irrigation water. With the lack of supplemental water throughout the summer and fall growing season, non-irrigated pasture vegetation dies back and remains on the ground until seeds germinate during the following winter rainy season. Our experiments primarily focused on vegetation collected from non-irrigated pasture as this was the dominant management approach in the Yolo Wildlife Area. However, south of the Yolo Wildlife Area, irrigated pastureland dominates (personal communication, Solono County Resource Conservation District).

Experimental Approach

Vegetation senescence experiments were designed to answer questions about the role that dying and decaying vegetation plays in internal MeHg production in the Yolo Bypass during a flood event. The investigations helped to fill data gaps for the Yolo Bypass modelling effort, and to develop information that could be used to help develop Best Management Practices (BMPs) to reduce the production of MeHg and export loads from the upper reach of the Yolo Bypass. A series of studies were initiated to quantify MeHg releases from plants and sediments in pastures. Two pilot studies were first conducted to test and

validate methodologies prior to initiating three larger scale vegetation senescence (hereafter referred to as the VegSens studies) investigations. Two of the larger scale investigations were field-based mesocosm studies (VegSens 2017 and 2019) and the other was a detailed laboratory study (VegSens 2018). Sample locations for all VegSens experiments are shown in Figure 3-30. Photos of mesocosm and laboratory experimental setups are shown in Figures 3-31 to 3-33. Details on sample collection and methodology are given in Technical Appendix E.

Hypotheses

In contrast to the other investigations for this report, which were primarily characterization efforts to provide critical information for the D-MCM, the vegetation senescence experiments were hypothesis driven. As noted above, the pilot studies were designed to demonstrate that vegetation was potentially a source of MeHg during a flood event, and to help validate and determine experimental parameters for the larger scale mesocosm and laboratory studies. Several hypotheses were investigated in the pilot studies:

- Plants are a more significant contributor to methylmercury production (release to overlying water) than sediments alone (without plants).
- Irrigated and non-irrigated pastures release different amounts of MeHg to overlying water
- The duration of the senescence period is important to understanding the timing of the release or production of MeHg from the plant material. A lag period is likely to occur after a flood event before significant release or production is observed.
- Aeration of overlying water affects the release of MeHg to overlying water.

The major hypotheses tested in VegSens 2017, 2018 and 2019 were:

- Grazing the land will lower MeHg releases to overlying flood water
- Disking the land will lower MeHg releases to overlying flood water
- More vegetation results in more MeHg releases to overlying flood water

Figure 3-30 Sampling Locations for Vegetation Senescence Studies

Figure 3-31 VegSens 2017 Mesocosm Experiment. Photos of (A) Mesocosm Chambers with Feed Water and Aeration Lines shown. (B) Disked, Grazed and Ungrazed Treatments (left to right, respectively)

Figure 3-32 VegSens 2019 Mesocosm Experiment. Photos of (A) Ice Chests Serving as Individual Mescosms, (B) Disked, (C) Grazed and (D) Ungrazed Treatments

Figure 3-33 VegSens 2018 Laboratory Experiment

Figure Notes: Photos of: (A) Glass Dish with Test Sediment and Vegetation in Mesh Bag Prior to Experimental Set-up. (B) Close-up of Sediment Within Glass Dish Placed Within a 1 L Beaker. (C) Experimental set-up showing 1 L Beakers Containing Sediment With and Without Vegetation and Aeration Tubing

Pilot Studies

Two pilot studies were conducted in 2015 and in 2016 to provide proof of concept that vegetation was a major driver of MeHg production and to develop sampling and experimental methodology. Sampling techniques with 4-inch diameter core tubes were evaluated as well as the effect of several factors that could influence MeHg releases to the overlying water. These experiments helped to determine the importance of aeration of the overlying water, the optimal duration of an experiment, whether plants were a source of MeHg by comparing treatments with sediment only with treatments with sediment and plants and a comparison of irrigated and non-irrigated fields. Experiments were conducted by adding 1 L of Sacramento river water to treatments and following the change in fMeHg in the overlying water over a several-day incubation period. The increase in fMeHg mass (in ng) in the overlying water as a function of incubation time for the VegSens 2015 pilot study is shown in Figure 3-34. Results for VegSens 2016 can be found in Technical Appendix E.

Several critical observations resulted from the pilot studies which helped guide the development of the mesocosm and more detailed laboratory incubation studies. First, the 2015 pilot experiment showed that sediment with emergent vegetation had significantly higher production of fMeHg than sediments with the vegetation trimmed off ($p < 0.05$, ln transformed, Tukey HSD test). This demonstrated the proof of concept that inundated Yolo Bypass pasture vegetation could serve as a potential fMeHg source. Second, the 2015 pilot studies showed that oxic/anoxic conditions could markedly impact fMeHg production; anoxic conditions produced significantly more fMeHg ($p < 0.05$, ln transformed, Tukey HSD test), however, decomposing vegetation under oxic conditions also produced fMeHg. Because our mass balance study showed that flood waters are mostly oxic, it was important that incubation studies remained oxic to simulate realistic oxygen levels during flood events. Third, the 2016 pilot experiment showed that if water is not exchanged in incubated cores, then DOC levels can increase dramatically after a few days (data not shown). In our Yolo Bypass mass balance study, the DOC levels never exceeded 10 mg/L, therefore, like oxygen, incubation experiments required keeping DOC to levels observed in the flooded Yolo Bypass. Finally, the pilot experiments suggested that an experimental duration between 8-14 days or more should be sufficient to obtain significant changes in MeHg concentrations between treatments.

Figure 3-34 VegSens 2015 Pilot Study. Illustrated is the Increase in fMeHg Mass (ng) in Overlying Water as a Function of Incubation Time for Several Treatments

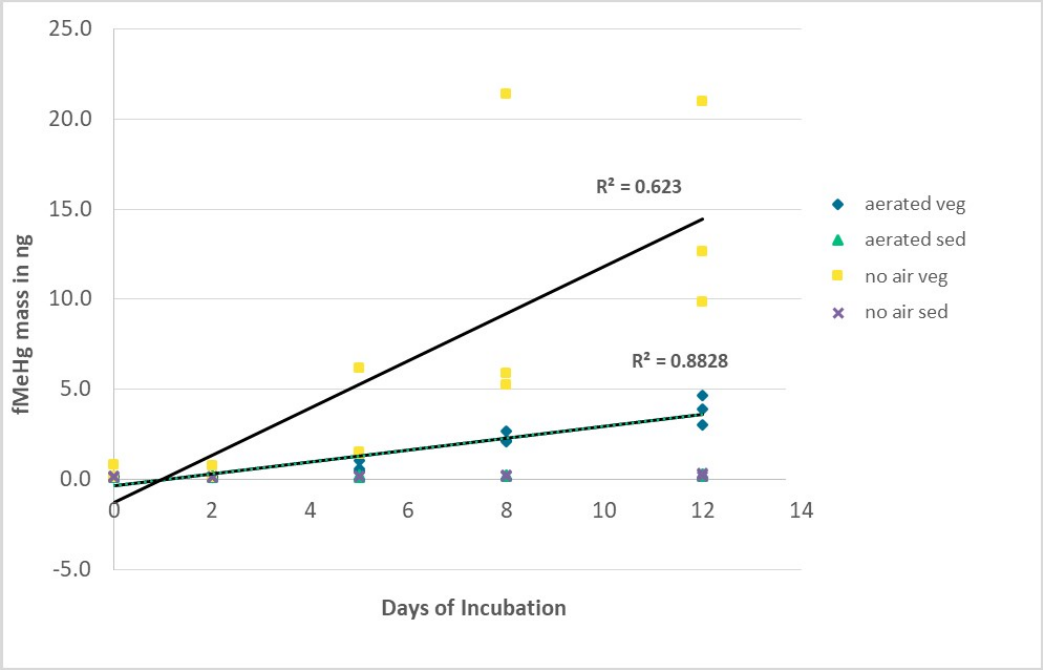

Mesocosm Studies – VegSens 2017 and VegSens 2019

Two field-based mesocosm studies were conducted– VegSens 2017 and VegSens 2019. Surface areas were increased significantly over the pilot experiments by placing soil and vegetation in ice chests resulting in surface areas that were 7 (VegSens 2017) to 43 (VegSens 2019) times greater than that of the pilot experiments. Two new types of sample treatments were added to these investigations, "disked" and "grazed" treatments. Disked samples represent a land use practice used in the Yolo Bypass. Land is mechanically disked to prepare the soil for planting or to turn-under undesirable vegetation. Grazed samples were collected in actively grazed, non-irrigated pasture areas in the Yolo Wildlife area. Ungrazed samples were created by fencing cattle out of the grazed area. Vegetation in the ungrazed and grazed areas were nearly a monoculture of rye grass (Lolium sp.). Specifically, the new hypothesis being tested was:

- The reduced vegetative biomass from disking of pastureland and grazing of cattle on pastureland (two common land management practices in the Yolo Bypass) will reduce MeHg production and lower the fMeHg introduction to overlying water during flood events by removing emergent vegetation available for methylation.

Methods and Experimental Design

Samples for VegSens 2017 were collected at site 3, and soil and plants for the VegSens 2019 study were collected at sites 3 and 4 (Figure 3-30). Biomass estimates at the time of sampling were determined by removing vegetation from three samples of ¼ or ½ m^2 surface areas, drying the vegetation in the laboratory at room temperature, and weighing when dry. VegSens 2017 and 2019 studies were conducted in November 2017 through January 2018 and February through March 2019, respectively. The ungrazed

site in VegSens 2017 (site 4) was constructed by fencing out cattle, whereas the grazed site was immediately adjacent and had cattle grazing on it. Vegetation consisted of a monoculture of dead rye grass. The same ungrazed location was used to collect samples for the VegSens 2019 study. A different location was used for the grazed site and unlike previous samples consisted of living rye grass and other plant species. The VegSens 2019 experiment was designed to improve upon the protocols used in the VegSens 2017 mesocosm experiment. The number of replicates was increased from 3 to 5 and the surface area of the mesocosms was increased 6-fold to more accurately represent and characterize ungrazed conditions.

Four treatments were prepared for VegSens 2017 and VegSens 2019: ungrazed, grazed, disked, and a water only control. The grazed and ungrazed treatments consisted of intact sod with no additional alterations. The disked treatment was meant to simulate disking of a vegetated field and was prepared by mixing the sod into the underlying soil to a depth of approximately 6 inches. The water only controls were ice chests with no sod. Overlying water was changed every 3 to 4 days to limit DOC build-up to < 10 mg/L and make the experiment more reflective of the conditions experienced during floods. fMeHg samples were collected once per week in VegSens 2017 and once every two weeks in VegSens 2019. Measurements were taken over a period of 4 weeks for VegSens 2019 and 5 weeks for VegSens 2017. Overlying water was changed twice a week, on days 3 and 7 of each sample week. The water from days 1 through 3 was discarded to eliminate excessive DOC buildup. The water from days 4 through 7 was used for measurements. Additional details are given in Technical Appendix E. In VegSens 2017, the time interval when MeHg was measured was: 1 Week (12/3/17 to 12/6/17); 2 Weeks (12/10/17 to 12/13/17); 3 Weeks (12/17/17 to 12/20/17); 5 Weeks (12/31/17 to 1/3/18). For VegSens 2019 water was only collected 2/15/2019 to 2/19/2019 and from 3/1/2019 to 3/5/2019.

Results - VegSens 2017

As shown in Figure 3-35 and Table 3-10 disking pasture vegetation into the soil consistently led to lower fMeHg levels than other treatments. By week 5, the grazed and ungrazed treatments both had significantly higher fMeHg concentrations than the disked treatment ($p < 0.025$, $p < 0.001$; respectively, post-hoc Tukey HSD, ln transformed data following significant 2-way ANOVA on ln transformed data). However, there was no significant difference in fMeHg production between grazed and ungrazed treatments ($p = 0.24$, post-hoc Tukey HSD, ln transformed data following significant 2-way ANOVA on ln transformed data).

Particulate methyl mercury (pMeHg) concentrations were determined in all treatments in Week 5. Results shown in Table 3-10 indicated that sediments as well as vegetation contributed to the pMeHg fraction, but that disked treatments produced less pMeHg than the vegetated treatments, however, in this experiment since the overlying water was only gently stirred, it did not represent the larger shear stresses encountered during large storms with current speed up to 5 ft/sec. Therefore, in this experiment, erosion and resuspended sediments was not accounted for.

Figure 3-35 VegSens 2017 Average fMeHg Concentrations for Disked, Grazed and Ungrazed Treatments at 2, 3 and 5 Weeks of Incubation

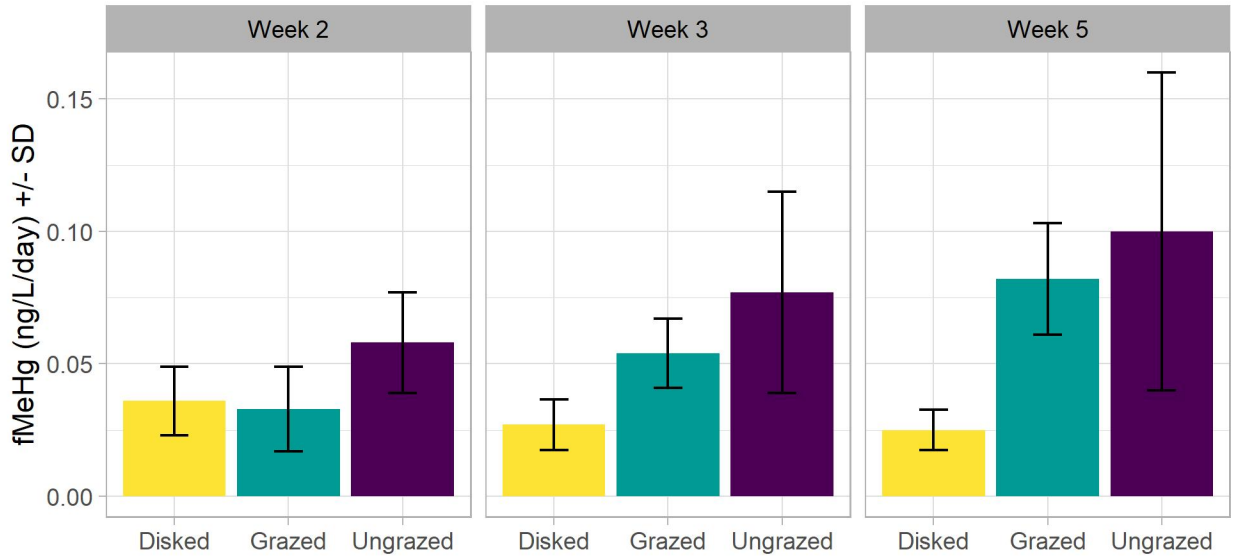

Figure Note: Units = ng/L/day ± 1 standard deviation

Table 3-10 VegSens 2017. Average Flux of fMeHg and pMeHg into Overlying Waters at 5 weeks of Incubation for Three Treatments (Disked, Ungrazed, and Grazed)

	Week 5 Average Flux[1] (ng/L/day)		
	Disked	**Grazed**	**Ungrazed**
fMeHg	0.024 ± 0.008	0.081 ± 0.021	0.101 ± 0.060
pMeHg	0.036 ± 0.022	0.057 ± 0.019	0.050 ± 0.002

[1] The average flux represents the mean ± (1) standard deviation of three replicates collected from a four-day incubation period at the end of the week. Raw data provided in appendix E1-2. pMeHg calculated as the difference between filtered and unfiltered MeHg

Results - VegSens 2019

Like the first mesocosm experiment, the VegSens 2019 mesocosm experiment examined differences in fMeHg production between disked, grazed, and ungrazed treatments, however the number of replicates was increased from 3 to 5 to increase the power to observe differences among treatments. The goal was to verify the disked results observed in the VegSens 2017 experiment and determine if there were also differences between the grazed and ungrazed treatments. Boxplots of fMeHg fluxes for weeks 2 and 4 are shown in Figure 3-36. The control waters (not shown, 5 total) were all below the detection limit of 0.013 ng/L.

Figure 3-36 VegSens 2019. Average fMeHg Concentrations for Disked, Grazed and Ungrazed Treatments at 2 and 4 Weeks of Incubation

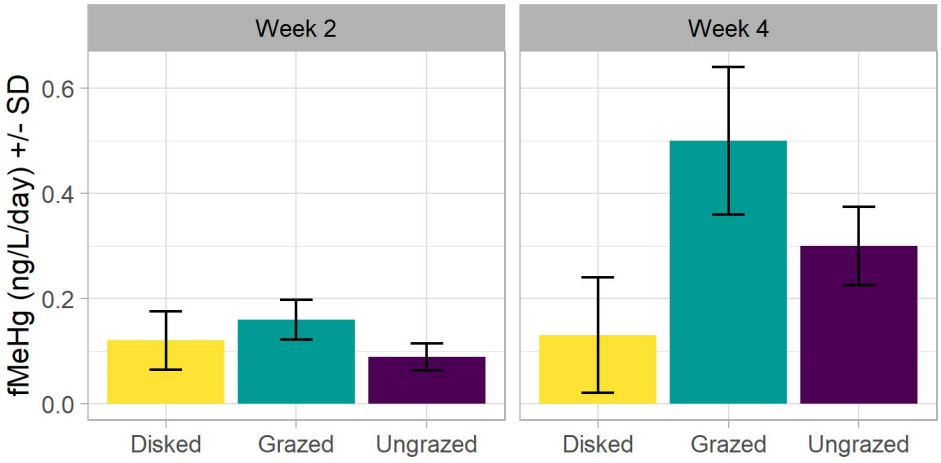

Figure note: Units are ng/L/day ± 1 standard deviation

Increasing the number of replicates did not change the conclusions reached in the VegSens 2017 mesocosm experiment. A 2-way ANOVA analysis on the natural log transformed data indicated a significant interaction effect between sampling events and land management practices ($p < 0.01$); therefore, multiple 1-way ANOVA analyses on natural log transformed data were used. When separated by sampling event, no significant differences were detected in week 2 between treatments. Like the VegSens 2017 results, week 4 fMeHg fluxes in the grazed and ungrazed treatments were both significantly higher than the disked treatment ($p < 0.001$, $p < 0.025$; grazed and ungrazed treatments, respectively). However, like the 2017 experiment, there was no significant difference in fMeHg production between the grazed and ungrazed treatments ($p=0.23$).

One confounding and important finding of the VegSens 2019 mesocosm experiment was the unexpected amount of fMeHg produced from the grazed treatment. The mass of the grazed treatment was approximately 40% of the ungrazed treatment, however, unlike the VegSens 2017 experiment and previous pilot studies, the flux of fMeHg, while not statistically significant, exceeded that observed in the ungrazed treatment. We hypothesize that these results were due to the different vegetation life stages used in the VegSens 2019 experiment. In the VegSens 2017 and pilot experiments, the plant material used was at the same point in its life-cycle, i.e. dead rye grass. However, for the VegSens 2019 experiment a new grazed treatment was used consisting of newly sprouted grass from recent rains. Thus, the grazed treatment consisted of freshly sprouted rye grass, while the ungrazed treatment consisted of dead rye grass. Because the new vegetation produced more fMeHg than old vegetation/biomass of vegetation, it is possible that fresh vegetation enhanced the production of MeHg. This has important land management consequences for the Yolo Bypass. Prior to winter floods, successive rainstorm events can trigger new biomass growth throughout pasture lands and other land uses. Therefore, fMeHg production driven by plant material may be a complicated function between the quantity of standing biomass of successive years of growth and the quantity of new growth prior to inundation by floodwaters.

VegSens 2018 Laboratory Experiment

The VegSens 2018 laboratory experiment was conducted to tightly control the variables associated with pasture lands. The main hypotheses tested in this study were:

- Disking the land will lower fMeHg releases to overlying water
- Grazing the land will lower fMeHg releases to overlying water
- More vegetation results in more fMeHg releases to overlying water

To evaluate the effects of grazing pressure and biomass, different levels of vegetation were added to 1-liter beakers within a given vegetated treatment. Vegetation used in the experiment was a monoculture of rye grass (Lolium sp.) initially collected from a non-irrigated and ungrazed pasture. Manure was included in grazed treatments and as its own isolated treatment to determine if it promoted methylation. A description of the seven treatments (with five replicates/treatment) is given in Table 3-11. Overlying water was changed at pre-determined intervals to ensure that DOC levels did not exceed levels measured in the field. The reader is directed to the Technical Appendix E for greater experimental details.

Table 3-11 **Treatments Tested in the VegSens 2018 Laboratory Study**

Treatment	Description
Control (Water Only)	Municipal tap water containing MeHg below the detection limit was used for all treatments
Sediment Only	Sieved through a 2 mm sized sieve to remove roots and larger organic matter
Ungrazed	Low, medium, and high biomass with vegetative biomasses adjusted to simulate different, a priori, non-irrigated pasture, summer biomass accumulations. Vegetation placed in mesh bags on top of sediment.
Disked Sediment	Low, medium, and high vegetative biomass disked into the sediment. Disked levels of vegetation based on biomass weights measured in ungrazed pasture
Grazed	Low, medium, and high biomass with vegetation and manure levels adjusted to simulate different, a priori, grazing pressures. Vegetation and manure placed in mesh bags on top of sediment
Manure Only	Low, medium, and high manure levels added at the same weight used in the grazed treatments. Manure placed in mesh bags on top of sediment.
Vegetation Only (no sediment)	Low, medium, and high biomass levels added at the same weights used in the ungrazed treatment.

Disking Effects

Disking pasture vegetation into the sediment was a highly effective approach to reduce fMeHg production. Disked treatments undergoing simulated inundation for either 4 or 8 weeks, all had significantly less fluxes in ng/L/day of fMeHg than either the grazed or the ungrazed treatments (Tukey multiple comparison test $p < 0.05$, ln transformed data) (Table 3-12, Figure 3-37). These results clearly demonstrate, that disking of pastureland is very effective at reducing fMeHg releases to overlying water during a flood event.

Table 3-12 **VegSens 2018 Laboratory Study. Results of Tukey Pairwise Multiple Comparisons Tests between Fluxes of fMeHg in ng/L/day of Ungrazed, Grazed and Disked Treatments (ln transformed data)**

		p values for Tukey pairwise multiple comparisons of fMeHg fluxes in ng/L/day		
Treatment Comparison	**Incubation Period**	**High Biomass**	**Medium Biomass**	**Low Biomass**
Ungrazed vs Disked	4 Weeks	0.0002	0.0001	0.0001
Ungrazed vs Disked	8 Weeks	0.0000	0.0002	0.0002
Ungrazed vs Grazed	4 Weeks	0.2312	0.0266	0.0266
Ungrazed vs Grazed	8 Weeks	0.0877	0.0908	0.0908
Grazed vs Disked	4 Weeks	0.0043	0.0248	0.0248
Grazed vs Disked	8 Weeks	0.0002	0.0107	0.0107

Table Note: Dark green cells show treatments significant at the $p < 0.05$ level. Light green shows treatments significant at the $p< 0.1$ level. Cells with no color are not significant at the $p < 0.1$ level.

Figure 3-37 VegSens 2018. Flux of fMeHg at 2, 4 and 8 Weeks of Incubation for Ungrazed Treatments with Low, Medium and High Biomass and Disked Sediment with Low, Medium, and High Levels of Vegetation Disked into the Sediment.

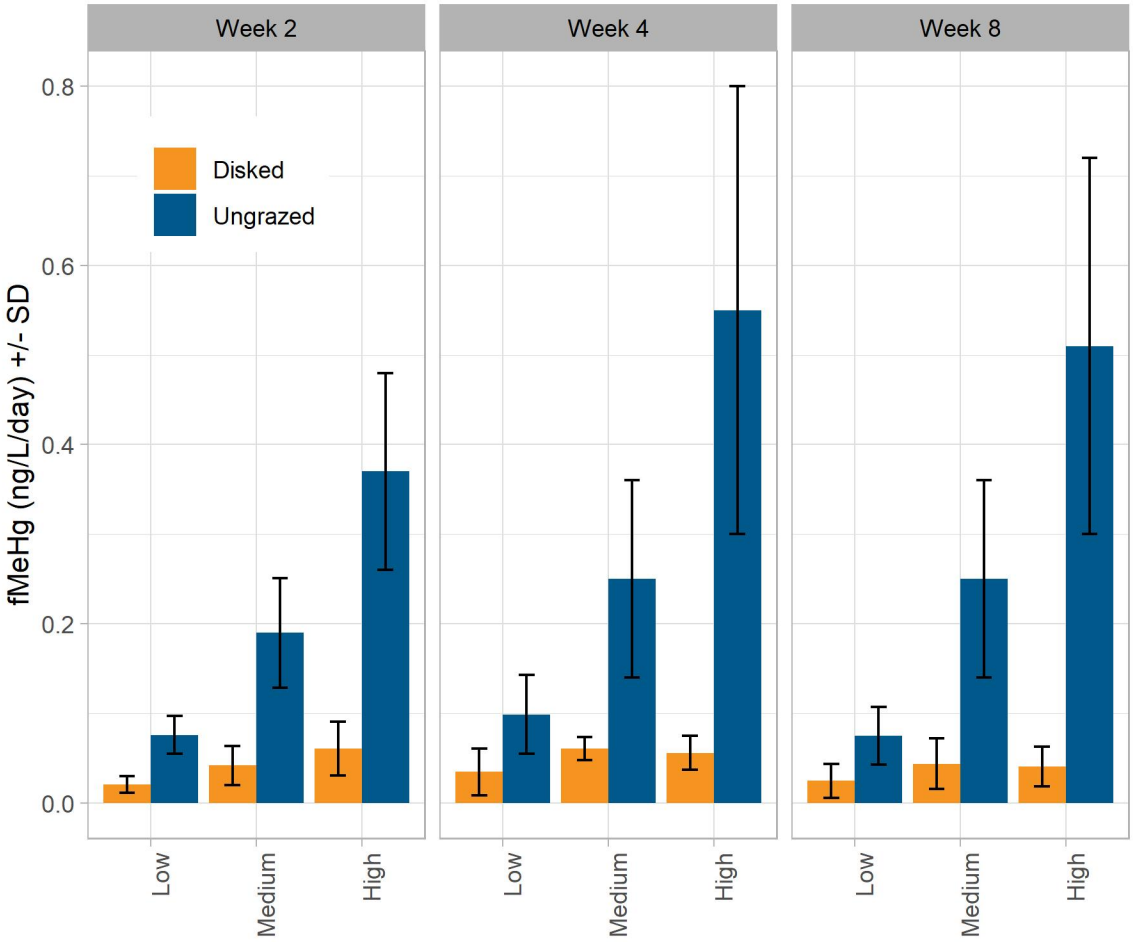

Figure note: units are ng/L/day ± 1 standard deviation; n=5 for each treatment.

Grazing Effects

In several cases, but not all, the grazed treatment had slightly lower rates of release of fMeHg to overlying water compared to the ungrazed treatment (Table 3-12). After 4-weeks of simulated inundation, there were significant differences at $p < 0.05$ in the treatments, with low and medium levels of biomasses (Tukey multiple comparisons, $p < 0.05$, ln transformed data). Comparing the 8-week incubation data, there were no significant differences at $p < 0.05$, but the treatments were significantly different at $p < 0.10$ between grazed and ungrazed treatments at all levels of biomass (Tukey multiple comparison, ln transformed data). These results partially support the hypothesis that grazed pastureland will have lower fMeHg releases to overlying water relative to ungrazed pastureland during a flood event.

Biomass Abundance Effects

The VegSens 2018 laboratory experiment provided several lines of evidence supporting the hypothesis that the greater the mass of vegetation in direct contact with overlying water, the greater the production and release of fMeHg to the overlying water. Biomass quantities added to experimental treatments were

ordered from low to high as disked < grazed< ungrazed. Patterns of MeHg flux were consistent with this treatment order (Table 3-13). Another way of assessing the relationship can be shown by comparing the flux of fMeHg released to overlying water with the mass of vegetation in four treatments: sediment-only, disked, grazed and ungrazed. This relationship is shown in Figure 3-38 for the 8-week incubation data using all three biomass addition levels. In this formulation, the different levels of biomass additions for each treatment can be independently accounted for. A very strong correlation was observed ($r^2 = 0.79$; $p < 0.01$); the higher the mass of vegetation present, the greater the flux of fMeHg, providing clear evidence that the amount of vegetation is very important in influencing the flux of fMeHg into overlying waters during a flood event.

Table 3-13 **VegSens 2018 Laboratory Study**

Treatment	**2 Weeks Incubation (ng/L/day)[1]**			**4 Weeks Incubation (ng/L/day) [1]**			**8 Weeks Incubation (ng/L/day) [1]**		
Biomass Level[2]	Low	Medium	High	Low	Medium	High	Low	Medium	High
Disked	0.021 ± 0.009	0.042 ± 0.022	0.061 ± 0.031	0.035 ± 0.026	0.061 ± 0.013	0.056 ± 0.019	0.024 ± 0.020	0.043 ± 0.028	0.041 ± 0.022
Grazed	0.059 ± 0.014	0.136 ± 0.067	0.122 ± 0.041	0.073 ± 0.025	0.126 ± 0.050	0.364 ± 0.400	0.055 ± 0.018	0.123 ± 0.057	0.230 ± 0.070
Ungrazed	0.076 ± 0.021	0.194 ± 0.061	0.367 ± 0.112	0.100 ± 0.044	0.252 ± 0.113	0.546 ± 0.256	0.076 ± 0.032	0.253 ± 0.107	0.510 ± 0.211
Manure plus sediment	0.014 ± 0.004	0.013 ± 0.003	0.024 ± 0.008	0.036 ± 0.020	0.039 ± 0.015	0.041 ± 0.009	0.027 ± 0.009	0.036 ± 0.015	0.048 ± 0.011
Vegetation Only	0.004 ± 0.001	0.083 ± 0.079	0.149 ± 0.037	0.005 ± 0.002	0.125 ± 0.124	0.223 ± 0.274	0.003 ± 0.009	0.143 ± 0.088	0.372 ± 0.183
Sediment Only[3]	0.007 ± 0.003			0.024 ± 0.016			0.023 ± 0.011		
Control Water[3]	0.008 ± 0.003			0.007 ± 0.006			0.006 ± 0.006		

Table Note: Given are the Mean and Standard Deviation for 5 Replicates of the Flux of fMeHg Into the Water in the Beaker for Seven Treatments at 2, 4 and 8 Weeks of Incubation

[1] Because of water changes twice each week, the fluxes given are based on the increases in concentration observed for a 4-day period at the end of each incubation period. Original data was divided by 4 to provide a concentration on a per day basis. Raw data is provided in Technical Appendix E1, Table E1-6

[2] See Technical Appendix Table E-8 for biomass levels added for the low, medium, and high treatments.

[3] There was no vegetation in the control water and sediment only treatments

.

Figure 3-38 VegSens 2018 Laboratory Study. Relationship Between Mass of Rye Grass Added to Disked, Grazed and Ungrazed Treatments and the Flux of fMeHg into Overlying Water at 8 Weeks of Incubation

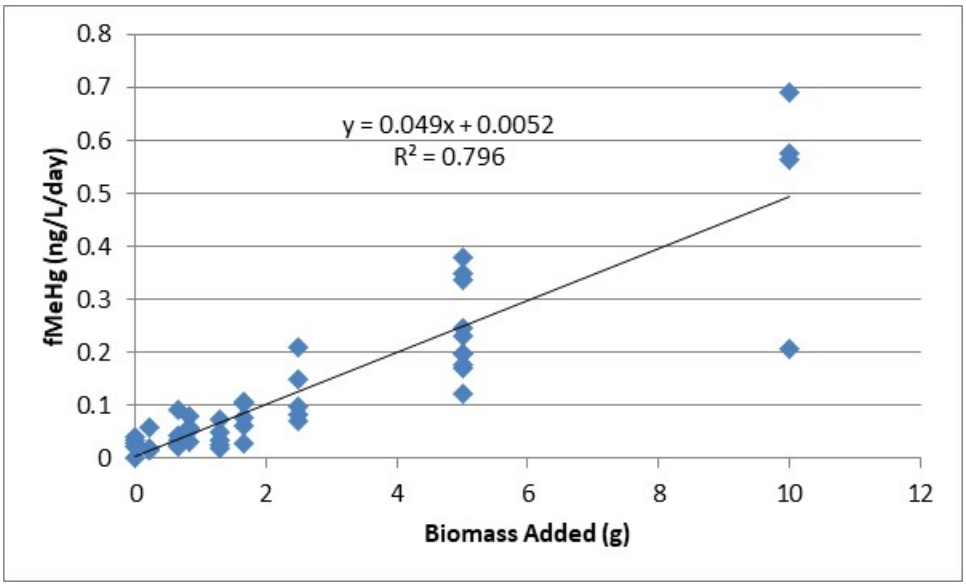

Finally, comparisons between treatments with and without vegetation provides another line of evidence supporting the influence of vegetation on fMeHg production. As shown in Table 3-13, except for control water, the sediment only treatment (with no added biomass) had the lowest fMeHg fluxes of all the treatments. The disked treatment, which had added vegetation mixed into the sediment (but with minimal emergent vegetation), produced slightly higher fMeHg fluxes (max ~2.5 times) than the sediment-only treatment for all incubation periods and biomass loading levels--with one exception, the low biomass diked treatment at 8 weeks of incubation had the same fMeHg flux as the sediment-only treatment. Similarly, comparisons between vegetation alone (with more vegetation added than the disked treatment) and disked showed that fMeHg fluxes in vegetation alone treatments were higher than disked treatments (max ~9 times) and even higher for sediment with no vegetation (max ~21 times), again with one exception--low vegetation alone biomass levels continued to show similar (or lower) fMeHg fluxes as disked and sediment alone treatments. This suite of evidence suggests that the quantity and presence of vegetation plays an important role in determining levels of fMeHg flux.

Investigation of Drivers of fMeHg Release to Overlying Water During a Flood Event

Using the experimental data from the VegSens 2018 laboratory experiments it is possible to assess whether certain land management practices or conditions are drivers of fMeHg production and release to overlying waters during a flood event. Two cases are worth examining: (1) the importance of vegetation relative to sediments as producers of fMeHg; and (2) the importance of manure as a component of a grazed pastureland.

Importance of Vegetation Relative to Sediment as a MeHg Source

Comparing ratios of fMeHg fluxes and statistical evaluations provided additional evidence that pasture vegetation stimulates fMeHg fluxes over sediment. Comparing the fMeHg fluxes between pasture vegetation and sediment alone provides information on the relative importance of vegetation as a driver of fMeHg flux. At weeks 4 and 8, the fMeHg flux increased as vegetation biomass levels increased and with the duration of the incubation. In contrast, sediment fMeHg flux was minor compared to the medium and high biomass levels (Table 3-14). Tukey pairwise statistical tests also support the hypothesis that the vegetation is the primary driver of MeHg production, not sediments (Table 3-15). The ungrazed/disked fMeHg flux ratio is also an indicator of the relative importance of vegetation compared to sediment since in the disked treatment, most of the vegetation is buried within the sediment and relatively little is on top of the sediment. The ungrazed/disked fMeHg flux ratio ranged from 2.9 to 10 across all biomass levels. There was a general trend of increasing ungrazed/disked fMeHg flux ratio with increasing biomass additions and with increasing incubation time. Tukey pairwise statistical tests of ln transformed data also support the hypothesis that the vegetation is the primary driver of MeHg production, not sediments (Table 3-15)

Table 3-14. **VegSens 2018 Laboratory Study. Selected fMeHg Flux Ratios for Different Biomass Levels**

MeHg Flux Ratios	**4 Weeks Incubation (ng/L/day)**			**8 Weeks Incubation (ng/L/day)**		
	Biomass Level[1]			Biomass Level[1]		
	Low	Medium	High	Low	Medium	High
Vegetation Only/Sediment Only	0.20	5.2	9.3	0.13	6.3	17
Ungrazed/ Disked	2.9	4.1	9.8	3.2	5.8	10

Table Note: Ratios calculated from MeHg flux listed in Table 3-10.

[1] See Technical Appendix Table E-8 for biomass levels added for each treatment.

Table 3-15 **VegSens 2018 Laboratory Study. Tukey Pairwise Statistical Tests Comparing the Vegetation Alone and Sediment Alone Treatments and Ungrazed and Disked Treatments at 4 and 8 Weeks of Incubation for Three Levels of Biomass.**

Treatment	**Incubation Period**	**Low Biomass Level[1] (p-value)**	**Medium Biomass Level[1] (p-value)**	**High Biomass Level[1] (p-value)**
Vegetation Alone vs. Sediment Alone	4 Weeks	0.003	0.015	0.505
Vegetation Alone vs. Sediment Alone	8 Weeks	0.003	0.000	0.000
Ungrazed vs. Disked	4 Weeks	0.0001	0.0001	0.0002
Ungrazed vs. Disked	8 Weeks	0.0002	0.0002	0.0000

[1] See Table E-8 for biomass levels added for each treatment

These results also raise the question of the role of sediment-water flux over extended periods of inundation. These experiments suggest that, over time, the contribution of sediment-water flux may be eclipsed by fMeHg flux from pasture vegetation. Vegetation Senescence and sediment-water flux experiments were not designed to evaluate this question, so this remains an area for further investigation.

Importance of Manure in the Generation of MeHg

At 4 and 8 weeks of incubation there was no significant differences between sediment only treatments with manure added and treatments consisting only of sediment (ln transformed data, Tukey multiple comparisons, $p > 0.05$, weeks 4 or 8) (Table 3-16). These results suggest that the presence of manure has no or minimal effect on MeHg production.

Table 3-16 **VegSens 2018 Laboratory Study. Summary of Tukey Pairwise Statistical Test Comparing Sediment Alone and Sediment Plus Manure Treatments at 4 and 8 Weeks of Incubation for Three Biomass Levels**

	Low Biomass[1] (p-value)	Medium Biomass[1] (p-value)	High Biomass[1] (p-value)
4 Weeks Incubation	0.677	0.596	0.882
8 Weeks Incubation	0.933	0.583	0.126

[1] See Technical Appendix Table E-8 for biomass levels added for each treatment

Pasture Vegetation as an Internal Source of MeHg to Flood Waters in the Yolo Bypass

Changes in rye grass MeHg mass were examined in situ and in VegSens 2018 and 2019 using non-irrigated pasture vegetation placed in mesh bags. For the 2018 laboratory study, dead rye grass, collected in the fall of WY 2017, provided the initial MeHg concentrations for pre-flood in-situ vegetation and for initial vegetative concentrations of bagged vegetation used in the VegSens 2018 laboratory study. Vegetation for VegSens 2019 mass calculations was collected at the same time and location as the sod samples collected for the VegSens 2019 experiment.

Concentrations and mass of MeHg of inundated rye grass increased in the laboratory over time. As shown in Table 3-17, MeHg concentrations in the vegetation increased 7 to 16-fold. The mass of MeHg associated with plant material increased between 5.7 and 12-fold. In parallel, vegetation decay was observed. Weight loss was 22 and 26 % for VegSens 2018 and 2019 experiments, respectively. This is consistent with visual observations. Before and after photos of a rye grass field, following the 4-month flood of WY 2017, showed most of the rye grass had either decomposed or been physically removed by floodwaters (Figure 3-29). These results clearly indicate that MeHg is produced in vegetation during a flood event, and that MeHg is slowly released as the plant decomposes when submerged.

Table 3-17 **Concentrations and Masses of MeHg In Bagged Rye Grass Suspended in the VegSens 2018 And 2019 Mesocosms**

Study	Initial MeHg Conc. (ng/g)	Final MeHg Conc. (ng/g)	Final/Initial Conc.	Initial MeHg Mass (ng)	Final MeHg Mass (ng)	Final/Initial Mass	% Weight loss (1-2 months)
VegSens 2019 (@ 4 weeks)	3.4 ± 0.3	56.8 ± 11.9	16.7	6.8 ± 0.7	83.4 ± 15.4	12.3	26.3 ± 4.11
VegSens 2018 (@ 8 weeks)	3.4 ± 0.3	25.1 ± 2.0	7.3	34.1 ± 3.3	194 ± 14.9	5.7	22.6 ± 5.1

Table notes: (1) 2.0 g of vegetation was used in VegSens 2019 (n=3), 10 g of vegetation was used in VegSens 2018 (n=5). The samples for determining starting concentrations for both experiments had n=5) The starting mass of MeHg in the plants was calculated by multiplying the concentration of MeHg in the plant material (n=5) by the biomass of the plant in the experiment (either 2 or 10g of tissue depending on the experiment). The final mass of MeHg in the tissue was determined by multiplying the weight remaining in the mesh bag after decomposition by the concentration of MeHg in the tissue. See Technical Appendix E for details.

The significance of this internal MeHg vegetation source from pastures into flood waters of the Yolo Bypass can be demonstrated by comparing it with the average net internal increase in the mass of uMeHg found in the Yolo Bypass Mass Balance studies and with the level of MeHg reduction required by the DMCP for the Yolo Bypass.

Based on pasture land biomass estimates (data not shown, see Technical Appendix E), concentrations of MeHg in decaying rye grass were scaled up to the areal coverage of pastureland in the Yolo Bypass (Table 3-18). As delineated in the land-use base map used by the Yolo Bypass D-MCM, pastureland covers an area of 70.6 km2. Using this approach, on average, the mass of MeHg associated with rye grass pasture over the course of a 120-day flood event was 1710 ± 560 g or 14.3 ± 4.6 g/day. This compares favorably with the uMeHg internal load values calculated in the Mass Balance study of 14 ± 8.1 g/day. Note that the Mass Balance study integrates all uMeHg contributions, not just pasture vegetation and that comparisons of field estimates of loads to those from a small number of laboratory experimental studies should be used with caution. There are a number of assumptions and inherent biases associated with scaling up these experimental studies, however, as a proof of concept, this exercise suggests a new and plausible source of internal Yolo Bypass MeHg production, not originally considered in the DMCP, requiring further investigation.

Table 3-18 **Estimate of Total MeHg Mass in 70.6 km^2 of Pastureland and its Flux to Overlying Water During the Flood Event of 2017**

Study	Initial MeHg Conc. (ng/g)	Final MeHg Conc. (ng/g)	Initial MeHg mass in 70.6 km^2 of pasture (g)	Final MeHg Mass in 70.6 km^2 of pasture (g)	Initial MeHg Flux for 120 days g/day	Final MeHg Flux for 120 days g/day
VegSens 2019 (@4 weeks)	3.4 ± 0.3	56.8 ± 11.9	188	2360	1.56	19.7
VegSens 2018 (@ 8 weeks)	3.4 ± 0.3	25.1 ± 2.0	187	1040	1.56	8.68
Field Collections after 2017 Flood (dry pasture)	1.9 ± 2.2	37.4 ± 3.6	105	1560	0.87	13.0
Field Collections after 2017 Flood (irrigated pasture)	1.9 ± 2.2	45.4 ± 36.2		1890		15.7
Average	2.9 ± 0.9	41.2 ± 5.9	160 ± 48	1710 ± 560	1.3 ± 0.4	14.3 ± 4.6

Table note: The determination of the production of MeHg in pastureland vegetation in the Yolo Bypass and its flux to overlying water during the flood event of 2017 is based on the VegSense 2018 and 2019 mesocosm experiments as well as post-flood field collections. The mass of MeHg in the pastures was calculated by multiplying the concentration of MeHg in the plants by the biomass of plants in all the pastures (see Technical Appendix E for biomass values). The flux was calculated by dividing the mass of MeHg in the pastures by 120 days (the approximate length of the 2017 flood).

The DMCP requires Yolo Bypass MeHg load reductions of 88 g/year from open water sources and 833 g/year collectively from all sources (CVRWQCB. 2011). Our estimate of 1710 ± 560 g of MeHg produced from senescing vegetation suggests there is enough MeHg in vegetation in pasturelands, that if its release from vegetation during a flood event could be mitigated (through land management practices), it would result in a major reduction, if not all of the DMCP goal of 833 g/year.

Conclusions

Mass Balance of MeHg in the Yolo Bypass

Depicted in Figure 3-39 is the mass balance of MeHg in the Yolo Bypass for WY 2017 determined from the Yolo Bypass mass balance study (Technical Appendix B). The internal production includes input fluxes for sediment-water exchange and vegetation senescence. Introduction of MeHg from erosion was difficult to estimate. We lacked a robust approach to translate Gust chamber erosion results into pMeHg values as loads. Therefore, we were unable to add Gust Chamber results to continue to balance the mass in Figure 3-39. It is reasonable to assume that pMeHg contributions from erosion and resuspension would contribute to the remaining unaccounted production, however, in terms of the largest land use in the Yolo Bypass D_MCM model, pasture erosion associated with Gust Chamber studies appeared negligible.

The average export flux of uMeHg from the upper Yolo Bypass (36 ± 29 g/day) exceed average tributary input fluxes (22 ± 23 g/day), indicating that there is an internal production within the upper Yolo Bypass of 14 ± 8.1 g/day, increasing the export concentration of uMeHg from the tributaries by 61%.

Figure 3-39 Mass Balance of MeHg in the Yolo Bypass for WY 2017

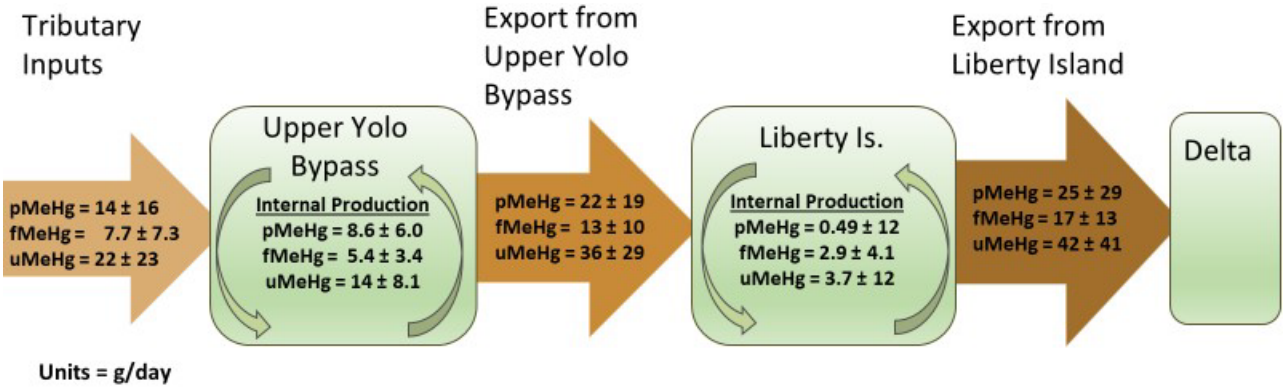

Figure Notes: (1) Given are average loads in g/day ± 1 standard deviation, (2) Internal production fluxes were determined by averaging the net difference (output –input) determined for each individual sampling event. Thus, the average flux for the internal production does not simply represent the difference between the average output flux minus the average input flux. In the case of Liberty Island, the difference between exports of the upper reach from the lower reach do not equal the calculated net production for two reasons a) the upper reach export loads are based on nine sampling events. Export loads exiting below Liberty Island are based on eight sampling events, and b) based on the sampling event, net uMeHg loads for Liberty Island were both positive and negative (see Figure 3-19), (4) The Liberty Island contribution to the total export is based on the difference between loads isolated at Ryer Island and Yolo Bypass output loads as calculated above the stairsteps.

The observation that the upper Yolo Bypass is a net internal source of uMeHg and that net loads of uMeHg increased with increasing inflow confirms previous observations made by Foe and others (2008) during an extended Yolo Bypass flooding event during the winter of 2005-06. The 2005-2006 study also covered the reach between the inlets and the Stairsteps and focused solely on uMeHg. One major difference between the current work and the 2005-2006 study was the magnitude of the load increase with increase in flow. The upper Yolo Bypass appeared to produce more uMeHg during the 2005-2006 study than during the 2017 flood event at comparable flows. This disparity in load observations in different flood events may be related to differences in the sampling programs (see Technical Appendix B for details), but it also strongly suggests that mercury behavior, fate and transport can differ markedly between years in which the Bypass floods.

A major advancement in the mass balance for MeHg in this current study over the previous mass balance study by Foe and others (2008) was to investigate the contribution of Liberty Island as a source/sink of MeHg entering the Delta. The total uMeHg export flux to the Delta, with the Liberty Island contribution, is 42 ± 41 g/day. The average internal production of uMeHg for Liberty Island, determined from individual sampling events was 3.7 ± 12 g/day, which adds approximately 10% to the uMeHg flux from the upper Yolo Bypass. This estimate of internal production is lower than one would predict from the net flux difference between the average export flux minus the average import flux (42 g/day – 36 g/day = 6 g/day; which corresponds to an increase of 14% to the uMeHg load from the upper Yolo Bypass). One possible explanation for the high uncertainty associated with the average internal production not agreeing more precisely with the net difference between the import and export at Liberty Island is that on several sampling events, Liberty Island was a net sink for uMeHg. Estimates of the internal production of uMeHg within Liberty Island suggest that on average Liberty island may be a small contributor of uMeHg (3.7 ± 12 g/day), although the uncertainty, as represented by the standard deviation, in establishing the Liberty Island average internal production flux is three times the estimated average.

Another major advancement in the mass balance for MeHg in this current study over the previous mass balance study by Foe and others (2008) was the partitioning of the uMeHg into particulate and filter-passing fractions (Figure 3-39). In general, pMeHg made up most of the uMeHg, ranging between 60 and 64% of the average uMeHg for all load determinations, with the exception of Liberty Island, where the average internal production of pMeHg made up only 13% of the uMeHg fraction.

It is important to highlight that this Yolo Bypass mass balance for MeHg has significant uncertainty associated with the load estimates for the three MeHg fractions determined (i.e. uMeHg, fMeHg, and pMeHg), but that the uncertainty associated with these averages is due to the large changes in flows across the 9 sampling events. As shown by r^2 values, there were highly significant relationships between load and flow (Figure 3-16 and Technical Appendix B). Flow explained ~ 50% and 83% of the net uMeHg loads for the upper reach and entire Yolo Bypass respectively. These results illustrate the influence of flow on load calculations and explains the high variability associated with average loads. This uncertainty, as a result of large changes in flow, impedes our ability to close with certainty the mass balance. The closure can be no better than the uncertainty associated with the individual loads estimated for the individual MeHg fractions. Nevertheless, given this caveat, the mass balance shows reasonable closure, suggesting that the major loads have been identified. It is entirely possible that other smaller loads have not been identified.

In addition, other sources potentially contributed to uncertainty, including; 1) the paucity of data (there were only 9 grab sample events); 2) the difficulty of collecting samples across the entire hydrograph; 3) the ability to scale up laboratory and field-based mesocosm and sediment-water exchange studies to the entire Yolo Bypass; 4) the heterogeneity of land use types in the Yolo Bypass; 5) the ability to monitor a process over the time scale of a flood event; and 6) the inherently large variability of MeHg as well as Hg and TSS loads during a flood event of this magnitude and duration with extremely large fluctuations in flow. Additional and more detailed discussions of why there is so much uncertainty is given in the next section on Data Gaps and Next Steps and in the individual chapters in the technical appendices.

First Flush Event Mass Balance

Depicted in Figure 3-40 is the mass balance of MeHg determined for the upper Yolo Bypass from the initial sampling event for WY 2017 (1/11-12/2017), which we are characterizing as a "first flush" event. The first flush event showed significant load enhancements over the average loads observed for the entire flood event. There was also another high flow event on February 14th, surpassing the hydrologic flow on January 11th, in which MeHg loads again rose up, suggesting that a "first flush" type event can occur more than once during a seasonal flood if hydrologic flow reaches elevated levels. The uMeHg tributary load into the upper Yolo Bypass during the first flush event (64 g/day) was about triple the average uMeHg load determined for all sampling events (22 ± 23 g/day). Similarly, the export uMeHg load from the upper Yolo Bypass during the first flush event (82 g/day) was about 2 times the average uMeHg export load determined for all sampling events (36 ± 29 g/day). The first flush event for Liberty Island was dominated by the pMeHg fraction, accounting for approximately 70% of the total load exported from the combined upper Yolo Bypass and Liberty Island areas.

The concentrations of MeHg during the first flush event in the upper Yolo Bypass were also elevated over the average concentration for all 9 events. For example, the concentrations of uMeHg, fMeHg and pMeHg during the first flush event from the Fremont Weir sampling site, which represented the majority

of the fresh water flow (73%), were 0.146, 0.044 and 0.10 ng/L, respectively and the average values for the 8 sampling events from the Fremont Weir sampling site (including the first flush event) were 0.090 ± 0.028, 0.034 ± 0.007 and 0.056 ± 0.022 ng/L, for uMeHg, fMeHg and pMeHg, respectively. The process driving the increase in concentration with increasing flow has not been elucidated. Because MeHg concentrations in the Fremont Weir site were also enhanced during the first flush event, it is clear that increasing MeHg loads with increasing flow reflect both the enhanced delivery of water and an increase in MeHg concentration associated with the increased hydrologic load. The exception perhaps being the internal production of MeHg.

Figure 3-40 Methylmercury Mass Balance for the First Flush Event on January 11, 2017 in the Upper Yolo Bypass.

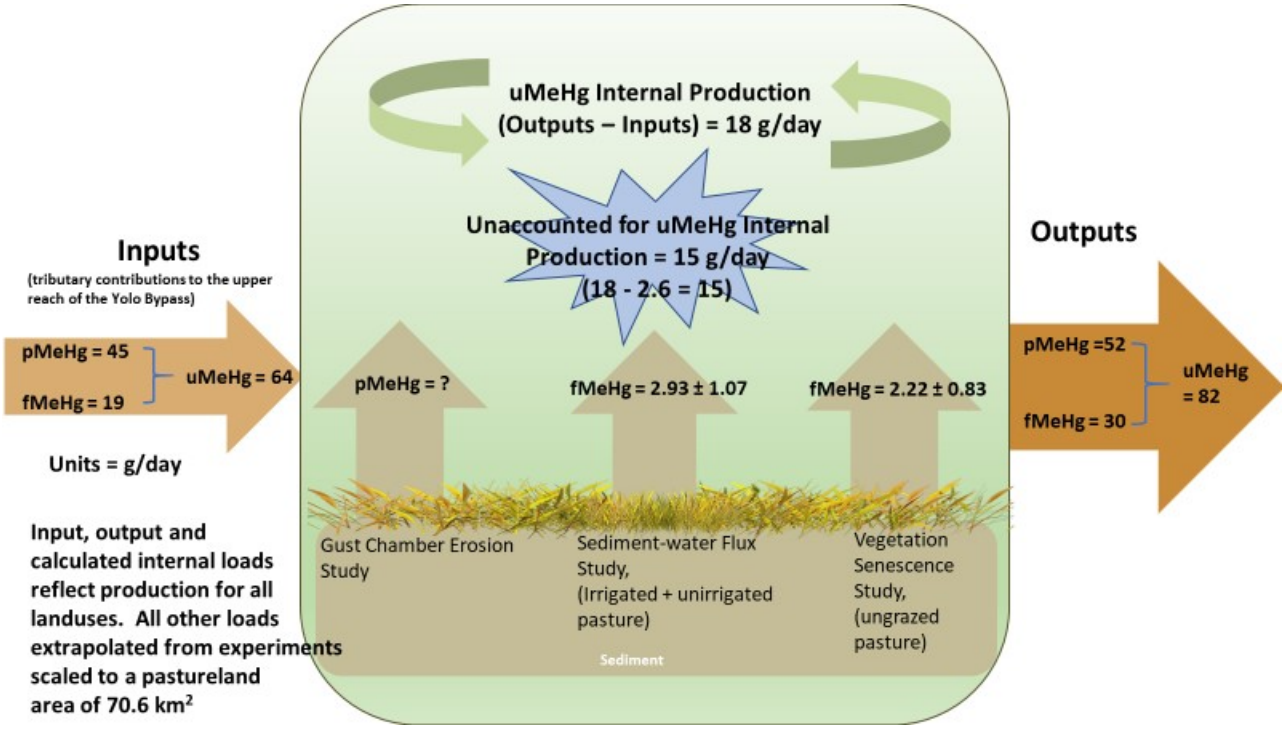

Figure Note: The data for the sediment-water exchange flux and the vegetation senescence flux were scaled to a pastureland area of 70.6 km². The flux of 2.6 g/day represents an average flux obtained from the sediment-water flux study and the Vegetation Senescence study. Inputs were calculated as the sum of tributary input loads collected on January 11, 2017. Output loads represent the sum of the loads calculated from the Toe Drain at Half-Lisbon, Liberty Cut and Shag Slough below the Stairsteps on January 12, 2017.

The net internal production of uMeHg in the upper Yolo Bypass during the first flush event, based on the export load minus the input load of 18 g/day, is similar to or perhaps slightly greater than the average net internal production determined for the entire flood event in 2017 (14 ± 8.1 g/day). The source of the internal production of MeHg during the first flush event is not clear. In pasture lands, sediment-water exchange and vegetation senescence studies both produced estimates of fMeHg fluxes to the overlying water of about 2.6 g/day, leaving about 15 g/day of internal production for the entire Yolo Bypass unaccounted for. As the vegetation was only recently flooded, it is assumed that the breakdown of the vegetation has not yet been significant and that release of MeHg contained within the plant tissue is minimal. It is possible that pMeHg from erosion accounts for a majority of the unaccounted-for internal

production. The Gust Chamber erosion studies conducted in pastureland land showed minimal erosion, but this was not necessarily the case for other landuses (see Table 3-9), however it was difficult to reliably convert Gust Chamber erosion values into definitive flux values for erosion contributions, therefore, in the conceptual model this term was not estimated. Additionally, there may be fMeHg processes that we did not capture in our laboratory work that would require further investigation.

The partitioning of the uMeHg into filter-passing and particulate fractions during the first flush event were similar to that observed for all sampled flood events in WY 2017. For example, the tributary input load during the first flush event was 70% in the particulate fraction, while the average pMeHg tributary input for the 2017 flood event was 64% pMeHg. Similarly, the export pMeHg during the first flush event was 63% of the uMeHg load, while the average pMeHg for the export from the upper Yolo Bypass during the 2017 flood event was 61% pMeHg.

Flooded Pastureland Vegetation as an Internal Source of MeHg to the Yolo Bypass

The mesocosm studies suggest that during periods of extended flooding, vegetation, and not sediment, may be the principal driver behind the net loads leaving the upper reach of the Yolo Bypass. Depicted in Figure 3-41 is a timeline of the increase in methylmercury in pasture vegetation during a seasonal cycle in the Yolo Bypass in which a flood event occurs. In the spring, the pastureland has new vegetation that is actively growing. By fall to early winter the pastures reach peak vegetation biomass. In the winter, a flood event covers the vegetation and it begins to slowly decompose. During the flood event, there is a significant conversion of the inorganic Hg to MeHg within the vegetation after 4 to 8 weeks of incubation, such that after several months of flooding, the levels of MeHg in plant tissues have increased more than 10-fold. By early to late spring, after the flood event has ended, the vegetation has almost completely decomposed, leaving mostly barren pastureland. Concomitantly, all the MeHg that was contained in the plant tissues has been released to the overlying water, both as dissolved and particulate MeHg. It is also recognized that some portion of the plant MeHg likely undergoes de-methylation during the decomposition process and that a significant portion is exported or removed to sediments as pMeHg.

Figure 3-41 Seasonal Cycle of Pastureland Biomass and Associated Methylmercury Content in the Yolo Bypass During a Season in Which a Flood Event Occurs

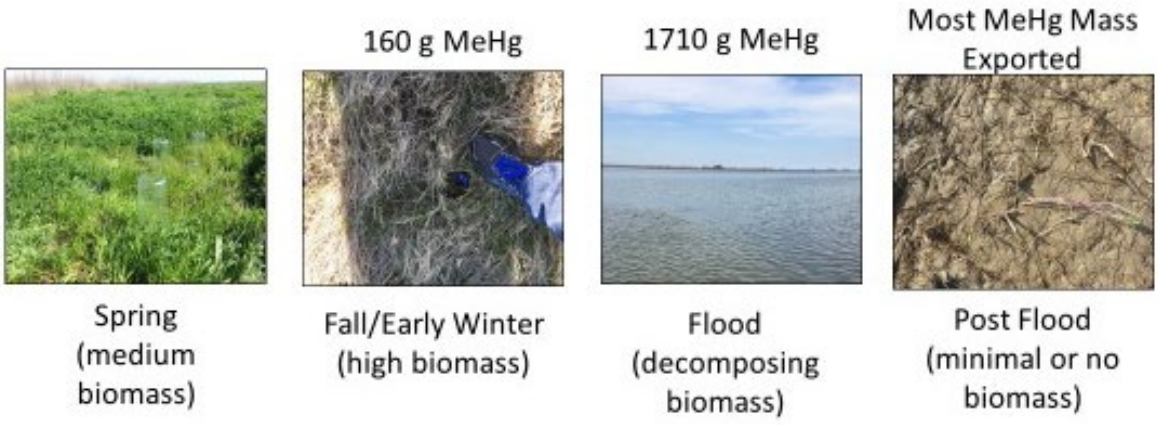

Figure Note: The site depicted is a non-irrigated pastureland which is where all the samples for the mesocosm studies were obtained. See Table 3-18 for calculations of MeHg mass.

A distinction should also be made between fresh and senescent vegetation in producing MeHg. The fresh vegetation in VegSens 2019 produced a higher flux of fMeHg to overlying water than the dry vegetation even though the fresh vegetation biomass was only 40% of the dried vegetation. This example illustrates the compounding difficulty of understanding the effects of grazing, disking, and vegetation age/condition on MeHg production and the flux of fMeHg to overlying waters. New vegetation starts growing as soon as the ground is wetted by rain, usually in October or November. If the biomass of the new vegetation is significant at the start of the flooding event there would ultimately be a larger mass of MeHg available for introduction into flood waters in the Yolo Bypass than if the vegetation that was flooded originated from older vegetation that was dead and dried out during the previous summer. Additionally, irrigated pasture remains green and alive throughout the winter.

The relative significance of decaying vegetation on flooded pastureland as an internal source of MeHg to flood waters in the upper Yolo Bypass is illustrated in a conceptual mass balance model in Figure 3-42. The 2017 and 2019 Vegetation Senescence studies determined a fMeHg flux of 1.4 ± 0.8 g/day and an estimated pMeHg flux of 2.2 ± 1.3 g/day (lower left portion of Figure 3-36; see Technical Appendix E for details) based on the disked mesocosm treatments. Combining these two fluxes provides a sediment-water exchange flux for uMeHg of 3.6 ± 2.1 g/day, which represents only 26% of the internal production. The emergent vegetation mesocosm treatment (lower right-hand portion of (Figure 3-42) includes both the fMeHg introduction from sediment-water exchange and the release of fMeHg from decaying vegetation, which combined introduce 4.4 ± 3.0 g/day of fMeHg to the overlying water (see Technical Appendix E for details). The estimated pMeHg contribution from this treatment (blue arrows and boxes) add another 7.0 ± 4.8 g/day, for an overall load of uMeHg to overlying water from flooded pastureland vegetation of 11.4 ± 7.8 g/day. By difference, the contribution of uMeHg to overlying flood water from senescent vegetation only (lower middle portion of Figure 3-42) is estimated at 7.8 ± 1.8 g/day; 3.0 ± 0.7 as fMeHg (orange arrows and boxes) and 4.8 ± 1.1 as pMeHg (blue arrows and boxes).

The emergent vegetation alone accounts for 56% of the internal production determined by the Yolo Bypass mass balance study. Adding in the sediment-water exchange to the vegetation senescence contribution and 83% of the internally produced MeHg in the Yolo Bypass can be accounted for by

introduction from flooded pastureland. Within the uncertainty of the load calculations, the internal production from sediment-water flux and vegetation senescence effectively balances the internal production of uMeHg determined from the mass balance study. Our work could not adequately quantify the pMeHg contributions of erosion, deposition and resuspension of solids, and only estimate the pMeHg contributions from sediment-water exchange and vegetation senescence. Therefore, in this conceptual model, the importance of pMeHg in the Yolo Bypass is not currently understood or constrained.

Figure 3-42 Conceptual Model of the Importance of Pastureland Vegetation in the Internal Production of MeHg in the Upper Yolo Bypass

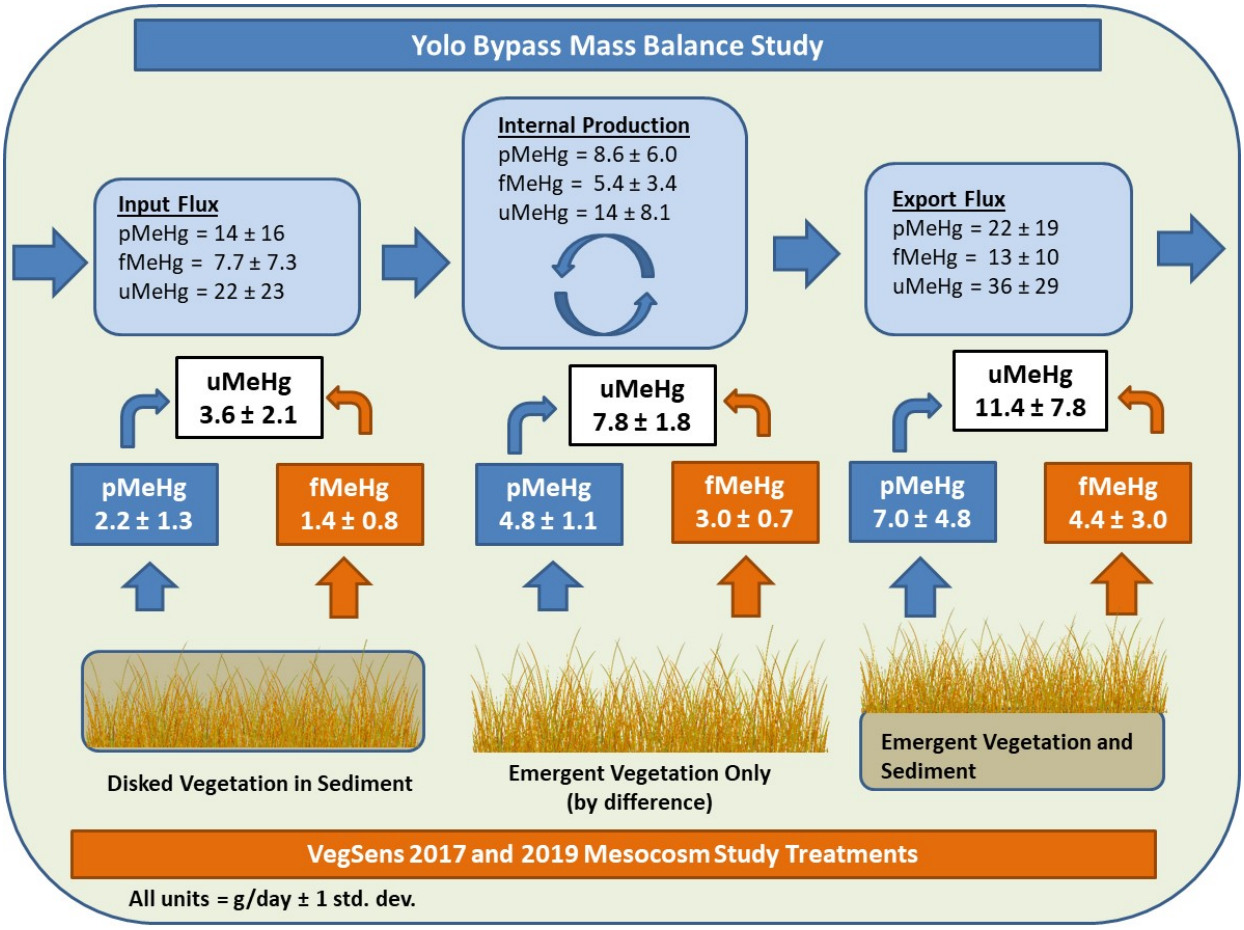

Figure note: The upper portion of Figure 3-42 repeats the mass balance of MeHg in the upper Yolo Bypass determined from the mass balance study described in Figure 3-39. The lower portion of Figure 3-42 shows the loads of MeHg introduced to overlying water determined during the VegSens 2017 and 2019 mesocosm studies. The introduction of fMeHg to overlying water from pastureland with emergent vegetation is shown in the lower right-hand portion of Figure 3-42 (orange arrows and boxes) and includes both the sediment-water exchange and introduction from decaying vegetation. The introduction of fMeHg to overlying water from sediment-water exchange processes (lower left portion of Figure 3-42; orange arrows and boxes) was estimated based on the disked vegetation mesocosm treatments. The introduction of fMeHg to overlying water from senescent emergent vegetation alone was estimated as the difference between the emergent vegetation and disked vegetation treatments (lower middle portion of Figure 3-42; orange arrows and boxes). An estimate of the pMeHg input to overlying water from the mesocosm treatments was estimated based on the ratio of pMeHg/fMeHg of 1.6 determined during the Yolo Bypass mass balance study (blue arrows and boxes)

Data Gaps and Next Steps-Field Studies

- The mass balance study for WY 2017 was based on just 9 manual sampling events. This paucity of data does not permit coverage of the hydrograph with the detail necessary to capture time dependent flux details. More high frequency sampling is needed, focusing on capturing peaks in the hydrograph as well as rising and falling flows. Use of automated sampling stations at key inlet and export points would fill this data gap and reduce uncertainty.
- Major biogeochemical processes often control the behavior, fate and transport of minor constituents, like mercury and methyl mercury in aquatic systems. Identifying clear linkages between mercury and methylmercury and a major biogeochemical process(es) will help with the development of best management practices to minimize the production of methylmercury within the Yolo Bypass and its export to the Delta. One investigation of particular relevance is the role that organic matter plays in methylmercury production and transport in the Yolo Bypass.
- Current sediment-water exchange flux measurements were conducted on short duration (1-2 days) investigations. We do not know how sediment-water exchange fluxes of mercury and methylmercury change over time, from initial flooding through month-long periods of inundation. Data are needed on the sediment-water flux throughout the flood event to more accurately capture this important flux.
- Given the areal size of the Yolo Bypass additional measurements of sediment-water exchange, pore water and solid phase concentrations for the land use types studied would decrease current uncertainties in mercury loads from the sediment. Studies should be conducted on vegetated and non-vegetated examples of each land use type.
- Gust Chamber erosion studies had limitations due to sample size and site heterogeneity. Future erosion research should increase sampling size, replication and spatial coverage to reduce uncertainty associated with the heterogeneity of the large geographical area of the Yolo Bypass.
- The Gust Chamber results describe only erosion processes, but deposition processes can be important in a floodway, both for its effect on subsequent erosional events and for mercury budgets.
- It is not known what the primary source(s) are for the (inorganic) mercury that accumulates in pasture vegetation. A likely source is the large mercury burden that currently exists in pastureland sediments. What role current exogenous sources of mercury from tributaries contribute to mercury levels in vegetation is not clear. Of particular interest is discharges from Cache Creek Settling Basin and whether the form of mercury released is readily available for uptake by vegetation and methylation. In addition, there are other possible sources as well, including atmospheric mercury deposition. Identifying the most important sources may help to guide development of a BMP for reducing methylmercury production during a flood event.
- Previous work has shown incomplete mixing of Yolo Bypass tributary water masses during flooding events (Sommer and others, 2007), therefore, understanding the effects on methylation from source waters originating from the western and eastern side of the fully flooded Yolo Bypass may also be an important piece to understanding methylation dynamics in the Yolo Bypass
- Pasture vegetation showed significant increases in methylmercury content during simulated flood events in the upper Yolo Bypass. Current vegetation senescence studies, as sources for methylmercury production in the Yolo Bypass, focused primarily on rye grass contributions. This work should be expanded to include quantification of methylmercury production during a flood event from other types of vegetation, irrigated and non-irrigated pastures, fresh and old vegetation, and

more accurate measurements of vegetation biomass in the Yolo Bypass. This will help reduce the uncertainty associated with the determination of the flux for this process and help identify the drivers to focus BMPs.

- Vegetation senescence studies primarily focused on methylmercury in the filter-passing fraction. Further studies are needed to understand vegetation contributions to particulate methylmercury introduction during a flood event.
- Vegetation senescence studies showed the importance of vegetation quality (i.e. whether the organic matter is readily metabolizable) and biomass quantity as possible drivers of mercury methylation in vegetation. A major question to resolve is whether vegetation quality or simply the biomass of vegetation present limits methylmercury production. Answering this question will help to develop targeted BMP's for limiting methylmercury production.
- The field and mesocosm studies all showed that disking of fields significantly reduces the input of methylmercury to overlying water during a flood event. What is not clear is whether disking pasture areas is a viable alternative for pasture management in the Yolo Bypass. A first step toward answering this question is to explore the feasibility of using disking in pasture lands through discussions with land-owners and the Resource Conservation Districts, followed by verifying disking results through field experiments.
- While not conclusive, it appears that grazing of cattle reduces vegetation biomass and the introduction of methylmercury to overlying waters during a flood event. Additional small-scale grazing studies need to be conducted to confirm the significance of its potential reduction. If grazing can be shown to significantly reduce methylmercury reduction during a flood event, then it should be evaluated as a viable alternative for pasture management in the Yolo Bypass.
- Approaches to reduce vegetative biomass in pasturelands by means other than disking and grazing should be explored. For example, evaluating the reduction of vegetative biomass using fall flood-up practices, like those already used in rice fields and seasonal wetlands.
- The Liberty Island reach, like the upper Yolo Bypass, was also a net producer and exporter of methylmercury to the Delta. Therefore, it is important to include the Liberty Island reach in any future studies involving determinations of loads of mercury or methylmercury to the Delta.

Limitations and Complications to Conducting Large-Scale Field Studies in the Yolo Bypass

In our workplan/technical memo, larger field trials were originally proposed to examine the questions ultimately pursued through laboratory and mesocosm experiments. The roadblocks necessitating a return to a mesocosm and laboratory experimental approach remain, and any future field studies seeking to evaluate control mechanisms will need to spend resources to overcome them. For example, we had proposed using the experimental ponds in the Yolo Wildlife Area to conduct large-scale experiments, to overcome limitations often associated with heterogeneity issues often encountered in small-scale field experiments. However, any work in the experimental ponds would have required the expense of rehabilitating the ponds back to their original state as a useable system. This will include dredging the ponds of fill and grading the sites to allow the head pressures created by the system to flow at velocities observed in the flooded Yolo Bypass. To evaluate grazing pressure, this will require the cooperation of

ranchers to closely control cow's movement onto only designated experimental sites. Re-creating vegetative biomass observed in the Yolo Bypass within the experimental ponds will require successive seasons of agricultural management to build up biomass to ambient conditions before experiments can be conducted.

One significant and unavoidable issue to conducting large-scale field manipulations in the Yolo Bypass is the water source. The water source for the experimental ponds is the Toe Drain which consists of ground water and recirculated agricultural drain water which intermittently has high MeHg concentrations (Moss Landing Marine Laboratory, unpublished data). Toe Drain water quality is very different from the low MeHg concentrations found in the dominant flood waters in the Yolo Bypass. Pilot tests may be needed to see how a land use reacts under inundation from different source waters. This approach has value beyond the use of the experimental ponds as Cache Creek Settling Basin waters have much higher concentrations of Hg and MeHg than flood waters originating from overtopping of the Fremont Weir.

Finally, there are site access limitations, and moreover safety concerns, with sample collections in the Yolo Bypass during full flood periods. Tuning the Yolo Bypass Dynamic Mercury Cycling Model (D-MCM) could have benefitted from data in areas within the fully flooded Yolo Bypass, rather than its peripheries.

References

Branfireun M. 2000. *The Role of Decomposing Plant Litter in Methylmercury Cycling in A Boreal Poor Fen.* Department of Geography. Master of Science. McGill University, Montreal, 2000.

Choe K-Y, Gill GA, Lehman RD, Seunghee H, Heim WA, and Coale KH. 2004. "Sediment-Water Exchange of Total Mercury and Monomethyl Mercury in the San Francisco Bay-Delta." Limnology and Oceanography, Volume 49, Issue 5, Pages 1512-1527. https://doi.org/10.4319/lo.2004.49.5.1512.

Covelli S, Faganeli J, Horvat M, Brambati A. 1999. "Porewater Distribution and Benthic Flux Measurements of Mercury and Methylmercury in the Gulf of Trieste (Northern Adriatic Sea)." Estuarine, Coastal and Shelf Science. Volume 48, Issue 4, Pages 415-428.

CVRWQCB. 2011. Amendments to the Water Quality Control Plan for the Sacramento River and San-Joaquin Basins for the Control of Methylmercury and Total Mercury in the Sacrament-San Joaquin River Delta Estuary (Attachment 1 to Resolution NO. R5-2010-0043. Viewed online at: https://www.waterboards.ca.gov/centralvalley/water_issues/tmdl/central_valley_projects/delta_hg/2011_1020_deltahg_bpa.pdf. Accessed: Aug. 22, 2019. Last updated: June 13, 2019.

Department of Water Resources 2015. Open Water Workgroup Progress Report. Delta Mercury Control Program. Prepared by the Open Water Workgroup and the Open Water Technical Group. Submitted to the Central Valley Regional Water Quality Control Board, Region 5, October 20, 2015. 203 pages. Available at: https://www.waterboards.ca.gov/centralvalley/water_issues/tmdl/central_valley_projects/delta_hg/control_studies/deltahg_oct2015pr_openwater.pdf. Accessed January 20, 2020.

EPA. 1995. Method 1669: Sampling Ambient Water for Trace Metal as EPA Water Quality Criteria Levels. United States Environmental Protection Agency. Office of Water (4303). EPA 821-R-034, April 1995. 42 pages.

Foe C, Louie S, and Bosworth D. Task 2. Methyl Mercury Concentrations and Loads in the Central Valley and Freshwater Delta, August 2008. In Transport, Cycling, and Fate of Mercury and Monomethyl Mercury in the San Francisco Delta and Tributaries: An Integrated Mass Balance Assessment Approach. CALFED Mercury Project Final Report, September 15, 2008. Available at: http://islandora.mlml.calstate.edu/islandora/object/islandora%3A08af4458-e767-4484-9bae-b0608b47852b. Accessed July 24, 2020.

Hecky RE, Ramsey DJ, Bodaly RA, Strange NE. 1991. Increased Methylmercury Contamination in Fish in Newly Formed Freshwater Reservoirs. In: Suzuki T, Imura N, Clarkson TW (Eds.). Advances in Mercury Toxicology. Plenum, New York, Pages 33-52.

Heim W A, Coale KH, Stephenson M, Choe Key-Young, Gill, GA, and Foe C. 2007. "Spatial and Habitat-Based Variations in Total and Methyl Mercury Concentrations in Surficial Sediments in the San Francisco Bay-Delta." Environmental Science and Technology Volume 41, Issue 10, pages 3501-3507. https://doi.org/10.1021/es0626483.

Kelly CA, Rudd JWM, Bodaly RA, Roulet NP, St.Louis V, Heyes A. 1997. "Increases in Fluxes of Greenhouse Gases and Methyl Mercury Following Flooding of an Experimental Reservoir." Environmental Science and Technology, Volume 3, Pages 1334-1344.

Lambertsson L, Nilsson M. 2006. "Organic material: The Primary Control on Mercury Methylation and Ambient Methylmercury Concentrations in Estuarine Sediments." Environmental Science and. Technology, Volume 38, Pages 1487–1495.

Mason RP, Kim E-H, Cornwell J, Heyes D. 2006. "An Examination of the Factors Influencing the Flux of Mercury, Methylmercury and Other Constituents from Estuarine Sediment." Marine Chemistry, Volume 102, Issues 1–2, Pages 96-110.

Marvin-DiPasquale, M, Windham-Myers L, Agee J, Kakouros E, Kieu LH, Fleck JA, Alpers CN, Stricker CA. 2014. "Methylmercury Production in Sediment from Agricultural and Non-Agricultural Wetlands in the Yolo Bypass, California, USA." Science of the Total Environment. Volume 484, Pages 300–307.

Sommer TR, Harrell WC, Swift TJ. 2007. "Extreme Hydrologic Banding in a Large-River Floodplain, California, USA." Hydrobiologia, Volume 598, Pages 409-415

Suddeth Grimm R, Lund JR. 2016. "Multi-Purpose Optimization for Reconciliation Ecology on an Engineered Floodplain: Yolo Bypass, CA." San Francisco Estuary and Watershed Science, Volume 14, Issue 1, Article 5, 23 Pages

Tremblay A, Cloutier L, Lucotte M. 1998. "Total Mercury and Methylmercury Fluxes Via Emerging Insects in Recently Flooded Hydroelectric Reservoirs and a Natural Lake." Science of the Total Environment, Volume 219, Pages 209-221.